PROPERTY OF: U.S. Department of Interior
OFFICE OF SURFACE MINING
Eastern Technical Center Library
Pittsburgh, Pa. 15220

INVESTIGATION OF BLAST-INDUCED UNDERGROUND VIBRATIONS FROM SURFACE MINING

by

Michael K. Phang
Professor, Civil Engineering
The University of Alabama

Thomas A. Simpson
Associate Professor, Mineral Engineering
The University of Alabama

and

Robert C. Brown
Professor, Civil Engineering
The University of Alabama

This research was conducted with grants from the Office of Surface Mining and the Bureau of Mines, Department of the Interior, under contract numbers G5105008 and G5115011, as authorized by Title III of PL95-87, The Surface Mining and Reclamation Act of 1977. The views, opinions, and conclusions expressed in this document are those of the authors and do not necessarily state or reflect the official policies or recommendations of the Department of the Interior of the United States.

December 1983

TABLE OF CONTENTS

	Page
INTRODUCTION	1
Background	1
Objectives	2
Scope of Work	2
Previous Work	3
Acknowledgments	5
DESCRIPTION OF THE TEST SITE AND MINING OPERATIONS	8
General Effects of Geology	8
Physiography and Geology	8
Electric Logging	16
Site Preparation and Blasting Sequence	22
INSTRUMENTATION AND VIBRATION MEASUREMENT	26
Selection of Measurement System	26
Instrumentation Recording and Blasting Program - First Phase	35
Recording Vibrations Underground in the Mine	37
Recording Vibrations at the Surface	42
Other Vibration Recording Instruments	42
Summary of First Phase	46
Instrumentation Recording and Blasting Program - Final Phase	51
DATA REDUCTION AND PROCESSING	60
Data Presentation and Analysis	61
Statistical Analysis	62
Borehole Meter and Other Responses	67
COMPUTER SIMULATION PROGRAM FOR DYNAMIC ANALYSIS	74
Comparison Between Field Results and Computer Simulation	87
STRESSES CALCULATED AT THE MINE ROOF	91
SUMMARY: OBSERVATIONS AND CONCLUSIONS	93
RECOMMENDATIONS	96
REFERENCES	97
APPENDICES	101
Appendix I-A	103
Appendix I-B	160
Appendix I-C	188
Appendix I-D	229
Appendix I-E	350
Appendix II-A	356
Appendix II-B	376
Appendix II-C	380
Appendix II-D	385
Appendix II-E	397
Appendix II-F	401

ILLUSTRATIONS

Figure		Page
1.	Index map showing location of project	9
2.	Plan view of Shannon Mine showing lines of section along the bottom of the slope (Section A-A') and along the slope profile (B-B')	10
3.	Plan view of instrumented intersection showing fracture and cleat orientation	12
4.	Geologic section along the Shannon mine slope showing generalized lithologic sequence	13
5.	Columnar section showing lithologic sequence (looking northwesterly, section A-A', see Fig. 2)	14
6.	Coal section in rib of south pillar of instrumented control section in Shannon mine	15
7.	View of geophysical recording unit during electric logging of D.D.H. 20	17
8.	Sonic and bulk density log of D.D.H. 20 showing lithologic interpretation	18
9.	Extracting core from core barrel (D.D.H. 20)	19
10.	Typical seam thickness log	21
11.	Typical coal quality log	23
12.	Part of test site cleared in preparation for drilling blastholes	24
13.	Drilling and measuring blasthole depth at site	24
14.	Layout of blastholes, underground instrumentation, and shooting sequence for first phase	25
15.	Loading blastholes with explosives	27
16.	Model VS-1600 W. F. Sprengnether Engineering Seismograph placed for recording vibrations on the mine floor	27
17.	Location of surface instruments in relation to blasting area	29

Figure		Page

18. Emplacement of 4-inch diameter PVC casing in borehole prior to installation of vertical borehole seismometer and two-way telephone line 30

19. Installing a Model 1462, Bison Instrument, vertical borehole meter in the 4-inch diameter open borehole 31

20. Lowering the Mark Engineering borehole seismometer into position for recording 32

21. Cracks in mine roof prior to blasting. 32

22. Post-blast photograph showing scaling and pre-existing fractures in mine roof 33

23. Typical surface effects around borehole after blasting 34

24. Seismometer (transducer) installed on mine roof. 34

25. Sprengnether Engineering Seismograph, VS-1200, with S-1400 seismometer (transducer) on left. 36

26. Velocity sensitivity curves for the VS-1200 seismograph. . . . 39

27. Typical tracing of underground velocity record 40

28. Seismic triggered seismograph, Model ST-4, Dallas Instruments, Inc. installed on mine floor. 41

29. Typical tracing of surface velocity record 43

30. Mark Borehole Seismometer, Model L-10-3D SWC 44

31. Velocity sensitivity curves for the VS-1100 seismograph. . . . 45

32. Irad Gage direct recording convergence meter, DMC-2, with time chart installed in mine 47

33. Irad Gage H-300 load cell, P-350 strain indicator and torque wrench. 48

34. Load cell installation on mine roof. 49

35. Operating the Vishay P-350A strain indicator 49

36. Diagram showing pattern of drill holes for final phase blasting 52

37. Schematic diagram showing instrumentation for final phase blasting sequence. 54

Figure		Page

38. Recording of arrival time and peak particle velocity at station 8, shot 5 55

39. Tube mounted strain gage for measurement of pressures in coal pillar. 56

40. Complete set of instruments for combined recording of pressure and peak particle velocity. 56

41. Recording of strain and peak particle velocity at station 6, shot 5. 57

42. Drilling hole in pillar to install tube-mounted stress detector 58

43. Inserting stress detector in pillar 58

44. Instrument array for recording stress and vibration measurements in mine pillar 59

45. HP-86 computer system with two flexible disc drives used in analyzing vibration data 59

46. Linear regression curve for the surface with scaling factor of 1/2 69

47. Linear regression curve for the underground mine roof with scaling factor of 1/3. 70

48. Linear regression curve for the underground mine floor with scaling factor of 1/3. 71

49. Two-dimensional plane view showing location of shot point(S), Station 3 (B), and Station 5 (C). 72

50. Corrected results of particle acceleration, velocity, and displacement for Shot 8 at Station 3. 75

51. Maximum response spectrum for Shot 8 at Station 3 76

52. Fast Fourier Transform for Shot 6 at Station 3. 77

53. Fast Fourier Transform for Shot 6 at Station 1. 78

54. Fast Fourier Transform for Shot 6 at Station 2. 79

55. Fast Fourier Transform for Shot 6 at Station 5. 80

56. Finite element mesh generated for this study. 82

Figure | Page

57. Input load-time function. 84

58. Stress versus depth for different loadings. 86

59. Stresses on underground mine roof versus depth for different charge weights. 89

60. Stress-time domain curve. 92

LIST OF TABLES

Table		Page
1.	Physical Properties of Core Samples from D.D.H. 20	20
2.	Blast Hole Information - First Phase	28
3.	Sensitivities for Gain Switch Settings	38
4.	Data for Final Phase Blasting Sequence	53
5.	Vibration Data - Surface	63
6.	Vibration Data - Underground Mine Roof	64
7.	Vibration Data - Underground Mine Floor	66
8.	Linear Regression Data for Surface	68
9.	Linear Regression Data for Mine Roof	68
10.	Linear Regression Data for Mine Floor	68
11.	Vibration Data - Station 3 After Correction	73
12.	Energy Ratios for Station 3 and Station 5	81
13.	Stress Versus Depth for Different Loadings	85
14.	Data for Linear Regression Equation	88
15.	Calculated Pressures/Forces by Different Workers	90
16.	Summary of Observed and Calculated Stresses in the Mine Roof	94

INVESTIGATION OF BLAST-INDUCED UNDERGROUND VIBRATIONS FROM SURFACE MINING

by Michael K. Phang, Thomas A. Simpson, and Robert C. Brown

INTRODUCTION

Background

The use of explosives to fragment rock generates ground vibrations which may have a detrimental effect on contiguous underground coal mine openings. Increased surface blasting by a burgeoning number of surface coal mines and quarries has caused considerable concern among underground mine operators. Ground vibration effects generated from surface mine blasting are also causing public concern. In response to this concern, the U.S. Bureau of Mines (Stagg and Engler, 1980) has measured and analyzed ground vibrations and their effects on underground and surface structures.

Some of the complaints registered against the mining industry are claims of substantial material damage from vibrations generated by the blasting; others are nuisance complaints of minor damage or annoyance. In general, allegations of damage from surface blasting have been sufficiently numerous to constitute a major problem for mine operators engaged in blasting operations. They have recognized the need for more technological data to evaluate the vibration problems associated with blasting. Both the operators and the general public need adequate safeguards based upon factual data to protect their specific interests. The coal mine industry needs reliable information from which to change blasting operations to reduce the number and severity of major damage claims and eliminate the growing number of nuisance complaints. The problem is of major concern not only to coal mine operators and nearby property owners, but also to federal, state and local governments. At the same time, environmental control agencies responsible for blasting and explosives use require reasonable and appropriate guidelines to protect the miners' lives.

An understanding of vibration characteristics and of how underground structures respond to ground vibrations will help define limits which will enable operators to confine blasting to levels which will minimize adverse effects. The characteristics of vibrations are strongly affected by the degree of explosive confinement afforded by the overburden, stemming, and geologic conditions. The imposed load distribution and the induced deformation created in the underground mine by surface blasting is a major factor affecting the stability of the underground mine. Extensive government regulation on blasting operations has created a need for uniform instrumentation and measurement techniques, whereby more realistic and practical design procedures can be employed.

In 1976, coal production in Alabama was approximately 22 million tons, of which approximately 7 million tons were from underground mines. It is estimated that production will increase to 25 million tons from underground mining by 1989. Some of the increased production will come from mines adjacent to, or intersecting, on-going surface mining activities. This

will require the establishment of safety criteria to minimize the vibration effects on the underground coal mine openings caused by surface blasting. The safety criteria will be the allowable guidelines for acceptable operating and surface mine blasting procedures. The guidelines will permit the underground and surface mining activities to be carried on simultaneously without disrupting their operations.

Objectives

The initial objective of this study is to evaluate an instrumentation and field monitoring program designed to record and monitor surface blasting effects on underground coal mine openings. The overall objective of this research is to study potential mine roof damage criteria and develop guidelines for surface mine blasting procedures overlying underground coal mine operations from which a safe and economical operating limit can be established.

Potential damage criteria and guidelines can be developed by quantifying the relationship between identifying the nature and degree of underground vibrations and damage produced in a mine on the underground structure. To predict the characteristics of underground vibrations occurring from a surface blast it is necessary to establish, through the use of measuring devices, the propagation relations of underground vibrations originating from surface blasting. Hence, it is essential that the vibration measuring equipment currently in use be evaluated and that specifications for new instrumentation and a monitoring program be developed. Part of this study will provide an approach to the design of an instrumentation and field monitoring program for use in investigating the damage criteria of surface blasting on underground coal mine openings.

Scope of Work

Ground vibrations from surface blasting are an undesirable side product of the use of explosives to fragment rock for mining and quarrying excavations. The wave of vibrations from a blast propagates in all directions. In monitoring the vibration waves, the frequency, range or amplitude, and duration of the waves must be measured. Recording the peak amplitudes and frequency is the generally acceptable procedure for studying ground vibrations. Care must be taken in selecting the proper instrumentation for the different vibrations encountered in mining, construction, and quarry blasting.

The vibration of a particular point in the ground can be described as a time-varying displacement from which velocity and acceleration can be calculated. Vibration levels measured by seismographs are expressed in inch/inch for displacement, inch/inch/second for velocity, or inch/inch/second squared for acceleration.

In addition to recording the ground particle velocity as measured by the seismograph, fractures in the roof of the mine should be recorded by photography or mapping of such fractures before blasting to observe any changes in the nature and size of the fractures. The behavior of these fractures, therefore, can be visually monitored before and after blasting.

To determine the effects of surface blasting on underground openings, critical areas of fractures must be identified to choose the best instrumentation site and the most effective instruments for field monitoring. A preliminary survey around a mine opening, as well as a historical and geological knowledge of the area, form the foundation for choosing the site.

In the study of any underground opening for evaluating blasting effects, a few basic observations must be made:

1. Information regarding the regional geology of the mining area for surface mine design as well as for underground mine studies.

2. Maximum ground particle velocity at surface and underground resulting from blasting in order to evaluate the seismicity of the site.

3. Imposed stress and induced deformation resulting from external forces applied to the underground openings, including their direction and magnitude in order to evaluate the rock behavior of the mine roof.

4. Physical properties (dynamic and static) of the rock and coal in the vicinity of the underground openings by investigating core samples from selected mine locations.

5. The geometry of the openings.

These data are then used for evaluating surface blasting effects on underground openings and developing potential damage criteria and guidelines for safe and economical mine operations.

Previous Work

Many investigations have been conducted, both in the United States and other countries, on the effects of ground vibrations from blasting on residential and other surface structures. The blasts studied ranged from laboratory experiments to full-scale nuclear explosions. The subjects have included efficiency of explosive products, blasting techniques, behavior of ground and structural materials, energy propagation, and damage from vibrations. One of the first such studies reported in the United States was made in 1927 by Rockwell (1927). Using displacement seismographs and falling-pin gages, he was the first to use instruments to measure ground vibrations. Rockwell concluded that quarry blasting would not produce damage to residential structures if they were more than 200 to 300 feet away from the quarry operation. He also stressed the need for obtaining accurate quantitative measurements of the vibrations produced by blasting.

The first major effort to establish potential damage criteria for residential structures due to quarry blasting was made by the Bureau of Mines during the period of 1930 to 1940 (Thoenen and Windes, 1942). As a part of this research project, displacement seismographs and calibration tables were designed to study the effects of ground vibration from blasting. The result of this study showed that acceleration, calculated from displacement measurements, was the criterion most closely associated

with damage to residential structures. In a later study, Crandall (1949), proposed a damage criterion which was based on particle velocity calculated from displacement and acceleration measurements. Langefors, Kihlstrom, and Westerberg (1958) studied the tests of vibrations from blasting and also proposed damage criterion based on particle velocity.

The Bureau of Mines in 1958 reopened their vibration study. The investigation was conducted because of a pressing need for additional blasting vibration information, the availability of more reliable instrumentation for seismic measurements, and the accessibility of applicable seismic information from other related disciplines were available. As a result of this program, transducers were then developed by the Bureau of Mines to measure acceleration, displacement, and velocity directly. However, peak particle velocity remained as one of the recommended damage criteria.

The vibrations were measured and collected by Wall (1967) at various locations such as ceiling panels, foundation walls, and at the surface of the ground near the structure, using the peak particle velocity determined from the vector sum of all three ground vibration components. The Bureau of Mines reported the results on seismograph calibration, instrumentation design requirements, soil coupling of gages, and damage criteria based on velocity. These studies were later used by industry to revise and update design and production of velocity seismographs (Nichols et. al., 1971). However, there were still questions regarding the effects of surface placement of transducers, the frequency range that should be measured, velocity seismograph calibration, and velocity measurement procedures.

Other published studies give a summary of instrumentation and damage criteria and list frequency and scaled-distance ranges for vibrations from coal mining, stone quarrying and construction activity. A study by Siskind, Stagg, Kopp, and Dowding (in press) deals with demonstrating new measurement analysis techniques of velocity exposure level and response spectra for surface mine blasting.

Investigations of rock behavior have been conducted by the Bureau of Mines for many years. A variety of instruments have been designed and developed to measure field and laboratory rock deformation and stress. In 1961, Reed and Mann built some practical tools for measuring rock deformations. A report was published by the Bureau of Mines (Merrill et al., 1961) dealing with the measurement of the deformation of a borehole in rock subjected to a change in applied stress. A gage designed to measure the borehole deformation was constructed and reported by Obert, Merrill, and Morgan (1972). Tincelin and Sinou (1964) used similar instruments to monitor deterioration of mine roofs near production blasts. A later study by Waddle (1965) evaluated the instrumentation for rock mechanics and proposed its application to other engineering problems. A report (Merrill, 1967) described the construction and calibration of the three- component borehole deformation gage and strain indicator.

An earlier publication by Campbell and Dodd (1968) gives an overview of design considerations for an underground power plant subjected to

stresses from earthquake shaking. A recent study by Hayatdavoudi and Brown (1979) describes the instrumentation design for underground measurements and reported results on potential damage criteria based on peak particle velocity and stress. This investigation indicated that the dynamic stresses developed underground as a result of blasting operations were related to the ground particle velocity, because the stress criterion was based on converted velocity values. Past research by Beus and Chan (1980) has shown that the in-situ ground stress is a major factor affecting shaft stability. This research proposed that some field determination of the three-dimensional in-situ stresses at shaft sites must be made to properly assess the magnitude and orientation of the stresses.

A comprehensive review by Jensen and Munson (1979) provides general guidelines for this research. This study deals with potential damage to underground coal mine openings from surface blasting. The report by Jensen and Munson included an instrumentation and field monitoring program for measuring underground vibration from surface blasting. They maintain the design of an underground mine is generally based on a consideration of static loads many times greater than any expected dynamic stresses. If conditions are such that static stresses are nearly equal to the strength of supporting rock, added dynamic stresses from blast vibrations could cause collapse. Instrumentation and monitoring procedures used in this study are similar to those used by Jensen and Munson.

Acknowledgments

There were many individuals and a number of companies who contributed greatly to the successful completion of this project, and the investigators wish to acknowledge them and recognize the work and materials that they provided toward this project. Without their contribution, the project would never have been completed.

To the students, undergraduates and graduates, we owe a profound debt of gratitude for their indulgence and patience with us during meetings. We are indebted to Rown-Chen Fan, an M.S. candidate in Civil Engineering, who prepared his thesis on the instrumentation and assisted in the installation of the instruments used to measure the blast vibrations on the surface and in the subsurface. Yung-Kwaun Jow, an M.S. candidate in Mineral Engineering, prepared his thesis on the complexities of the vibrations generated from blasting. His study necessitated many hours at a computer. David Tavatli, a Ph.D. candidate in Civil Engineering, spent untold hours researching data on detonation pressure and borehole pressure. His work carried on into the complex domain of finite element analysis, along with Jow's effort, provided much of the major results reported on in this project.

We were assisted in this project by other students who very ably helped us to install instruments in the mine, underground and on the surface, and who also assisted in the preparation of maps, diagrams, and tables. The assistance of Barbara Friedman and Swee Fong, Civil Engineering undergraduate students, are gratefully acknowledged. Also, we should name Pablo Vasquez, William J. Nemeth, and Supachai Tantekom, all Civil Engineeering graduate students, who worked on the project during some period of the project activity. We also would like to mention Russell

McLean, James Cooper, John Richardson, and Sitakanta Mohanty, all Mineral Engineering graduate students, who were employed on the project at various times.

All of these students provided valuable and capable assistance in bringing this project to a successful culmination.

The investigators wish particularly to cite the many individuals who worked for several companies and gave freely of time, equipment, and supplies.

We are especially grateful to Clarence Blair, President of Black Diamond Coal Company, who donated the facilities of their Shannon Mine for our use in carrying out the field phases of the project. Others from Black Diamond, namely Robert Towry, mining engineer; Arnold Dagnan, surveyor; Harold Oglesby, surveyor helper; Paul Province, mine foreman; and Denny Pugh, Sr., mine maintenance supervisor, gave generously of their time and advice when needed. Robert Carr, geologist, provided diamond drill hole logs and assisted in geologic interpretations. Not only did the Black Diamond Company provide these personnel, but they also allowed use of their bulldozer for the clearing of drilling sites and other items of equipment sorely needed to get the job done. All of this effort constituted a considerable item in the mine's operating budget. We shall always be grateful to them for this assistance and the spirit of cooperation that prevailed.

The Nickel Plate Mining Company, Albert Bowen and Nicky Osborn, co-owners, donated the drilling of twelve 5-inch diameter blastholes ranging in depth from 40 to 60 feet. They also provided the explosives and accessories to shoot these holes. It should be mentioned that John McGill, reclamation supervisor, and Billy C. Kennedy, director of planning and explosives expert, provided invaluable assistance in seeing that this phase of the project was properly executed and completed.

A division of Boren Companies, Apache Machine & Supply Company, owned by Russell F. Boren, generously donated the drilling of sixteen 6-3/4-inch diameter blastholes ranging in depth from 40-60 feet. H. E. "Hal" Middleton, Jr., supervisor, and T. E. "Tom" Bruner, drilling superintendent, were on the site to supervise and direct the drilling of these blastholes. To them and their company we owe a grateful note of thanks.

To Charles Ingram of Gulf Oil Chemicals Company, Explosives Department, we are grateful for the donation of over 3-1/2 tons of explosives material to shoot for the second field phase of our project. We also acknowledge Ray Gant, technical sales representative of this company, for his invaluable field assistance.

We wish also to acknowledge the kind generosity of Dennis Gamble, President of Gamble Blasting Consultants, who provided technical assistance and frequent advice during the study.

Although VME, Louisville, Kentucky was contracted to provide digitized data and calculate energy spectrum for the different shots, personnel of the organization, particularly Bernt Larsson provided valuable constructive criticism and gave unselfishly of their time; for this assistance, we are grateful to them.

Finally, to all of our colleagues, particularly Dr. Duk-Won Park, Department of Mineral Engineering who initially guided one of the graduate student's research thesis, and friends in the mining industry with whom we discussed the various phases of the project, we extend our grateful thanks. We especially would like to remark about the tremendous interest and spirit of cooperation that prevailed while working with the people in the mining industry.

DESCRIPTION OF THE TEST SITE AND MINING OPERATIONS

General Effects of Geology

Geologic structure and mineralogical make-up cause a difference in wave propagation. If the rocks at the site are essentially horizontal and stratified and consist chiefly of massive rock units with horizontal isotropy and uniform cover, little difference in wave propagation would be expected with direction. Conversely, if there are structural discontinuities such as jointing, folding, and faulting anisotropy or any other type of lineation, such as a mineralogical and/or grain oriented fabric, propagation may differ with direction.

The thickness of soil and depth and degree of weathering have a direct effect on the amplitude and frequency of displacement recordings. Also, the intensity of vibration in loose soil and weathered overburden material is greater than in hard, unweathered bedrock media. For equal explosive charges and distances, gages installed on rock outcrops indicate lower amplitudes and higher frequencies than gages installed on the overburden. Because soil and overburden rock thicknesses vary from mine to mine and within some mines, brief, simple tests were conducted to determine whether or not similar effects were present in the particle velocity recordings.

Physiography and Geology

This research was done at the Shannon Mine of the Black Diamond Coal Company in the Appalachian Ridge and Valley physiographic province in east-central Alabama, Jefferson County. The mine is approximately four miles northwest of Abernant, Tuscaloosa County, and the mine portal is in the SW1/4, Section 3, T20, R6W, as shown in Figure 1. The mined area comprises approximately 180 acres underlying parts of Sections 3 and 10 of T20S, R6W.

The terrain is composed of hills and vales of low to moderate relief attaining a maximum elevation of 625 feet above mean sea level (msl) and a minimum relief of 480 feet above msl.

The surface drainage pattern is dendritic and consists chiefly of several small intermittent streams that flow in a northerly direction on the northwestern side of the property and several small intermittent streams which flow in a southerly direction on the southeastern side of the property. A series of northeasterly trending small strip mine lakes and strip mine spoil banks border the northwestern property boundary, and an old strip mine lake cuts across the southwestern corner of the property.

The Shannon Mine and adjacent surface and underground mines occur in the extreme southwestern part of the Blue Creek Basin of the Warrior Coal Field of Alabama. Figure 2 is a plan view of the site showing a part of the underground mine.

Map Location

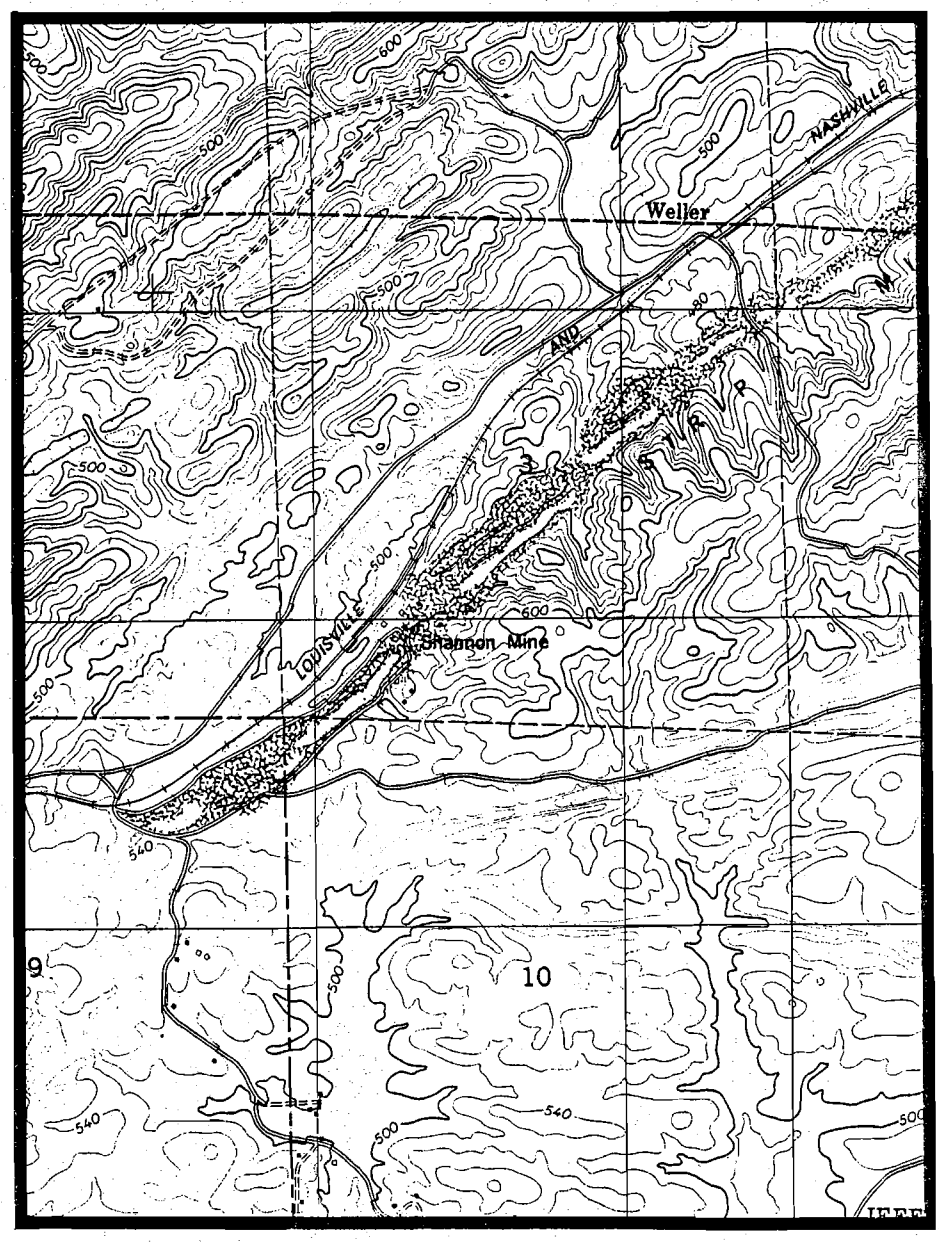

MILES

0.0 0.5 1.0

Figure 1. Index map showing location of project.

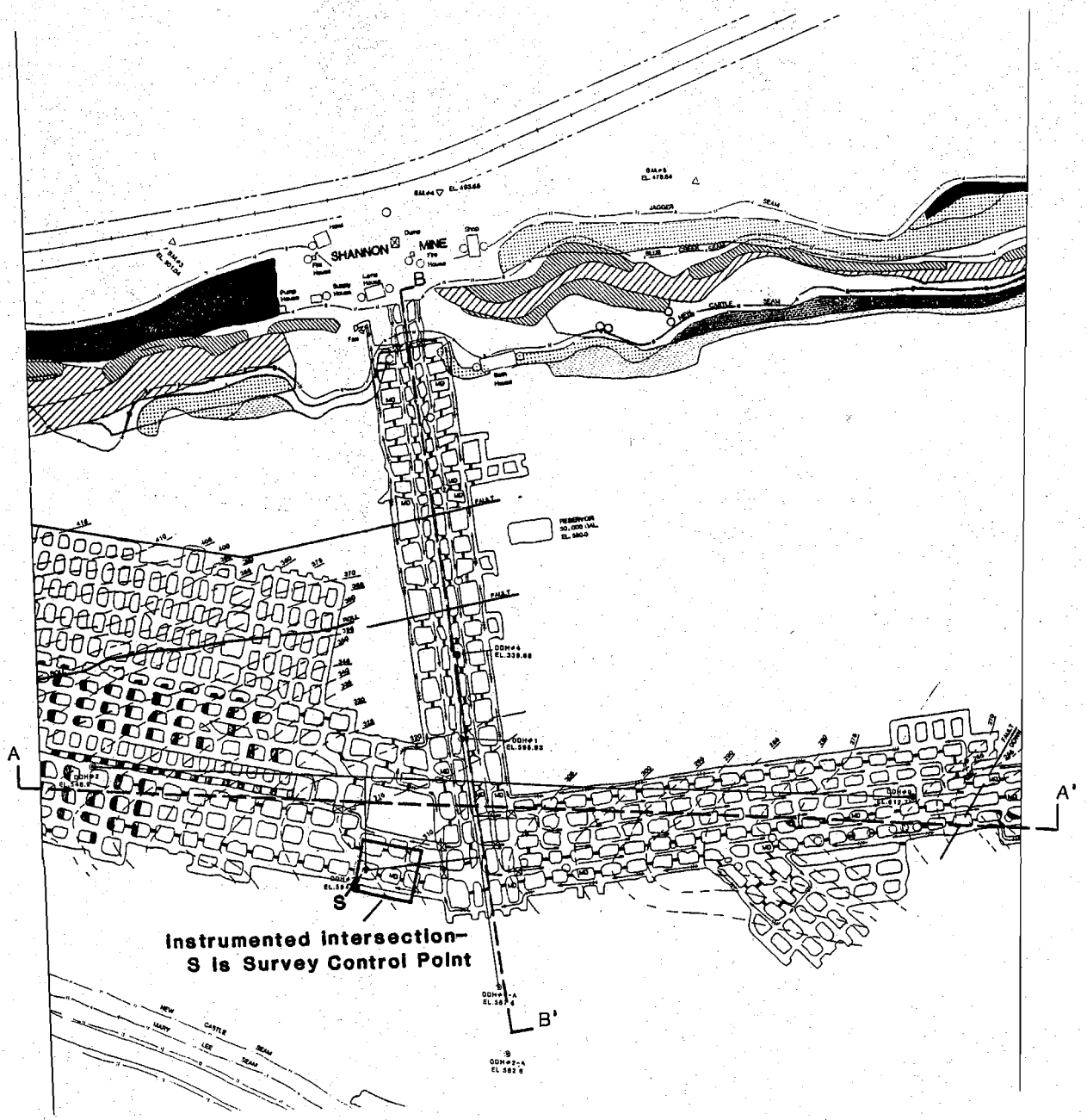

Figure 2. Plan view of Shannon mine showing lines of section along the bottom of the slope (section A-A') and along the slope profile (B-B').

The basin is an asymmetrical syncline that has a northeasterly trending axial trace and plunges to the northeast. The Shannon Mine occurs at the southwestern extremity of the syncline close to the structural point of termination. The strata along the northwestern flank of the major structure has a relatively shallow dip to the southwest, which averages about 17°SW. Along the southeastern flank, the strata dip is much steeper, dipping as much as 80° NW.

The Blue Creek Basin is underlain by an alternating sequence of shale, sandstone, conglomerate, and coal seams of the Pottsville Formation of Pennsylvanian age. The rock units vary in grain size, color, and thickness. The lithologies range from mudstones and siltstones to sandstones and occasional pebble conglomerates. The thickness of different rock units range from laminae to thin-bedded to thick-bedded units that are mere partings of fractions of an inch in thickness for shales and shaly sandstones to sandstone units that are as much as 20 feet in thickness. The thicker sandstone units are well cemented and extremely tough and tenacious.

The coalbeds underlying the area are those represented by the Mary Lee group. The coalbeds presently being mined in the area from the oldest to youngest are the Jagger, Blue Creek, and Newcastle, with the Blue Creek being the most important. The basin is only about one mile wide at the mining site and the depth of cover ranges from 0 at the outcrop to about 500 feet at the bottom of the Shannon slope.

Faulting is common throughout the basin and the faults cut across the basin in oblique angles chiefly as normal faults with displacements ranging from only a few inches to as much as 100 feet. There are probably more faults that are not visible in the surface and subsurface. Movement parallel to and along bedding planes occurred during the folding process and evidence of this can be readily observed on some of the exposed rock surfaces.

Jointing is common and the density and frequency varies according to local structural irregularities. The coal is generally well cleated with butt and face cleats oriented generally in a northwesterly and northeasterly direction (Figure 3).

The Shannon Mine is a slope mine and the incline has an average slope of 10 degrees opened on the Blue Creek coal seam. The distance down the slope from the portal to the bottom is about 1800 feet. Figure 4 is a slope profile (B-B') showing the generalized geologic section and Figure 5 shows a columnar section looking northwesterly.

The Blue Creek coalbed ranges from about 6 feet to 12 feet in thickness and a typical cross-section of the coal seam is shown in Figure 6 which was measured on the rib of the south pillar at the instrumented intersection.

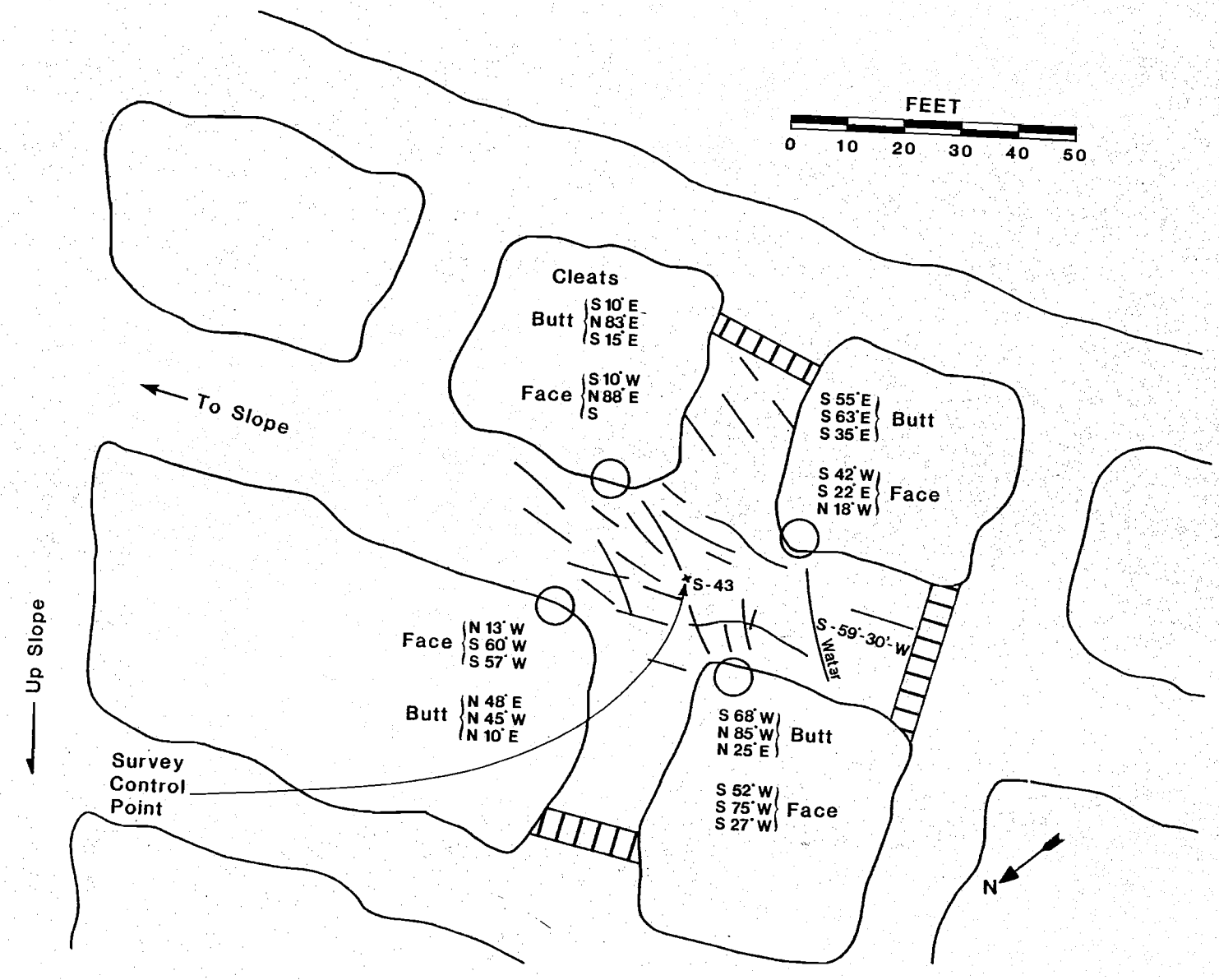

Figure 3. Plan view of instrumented intersection showing fracture and cleat orientation.

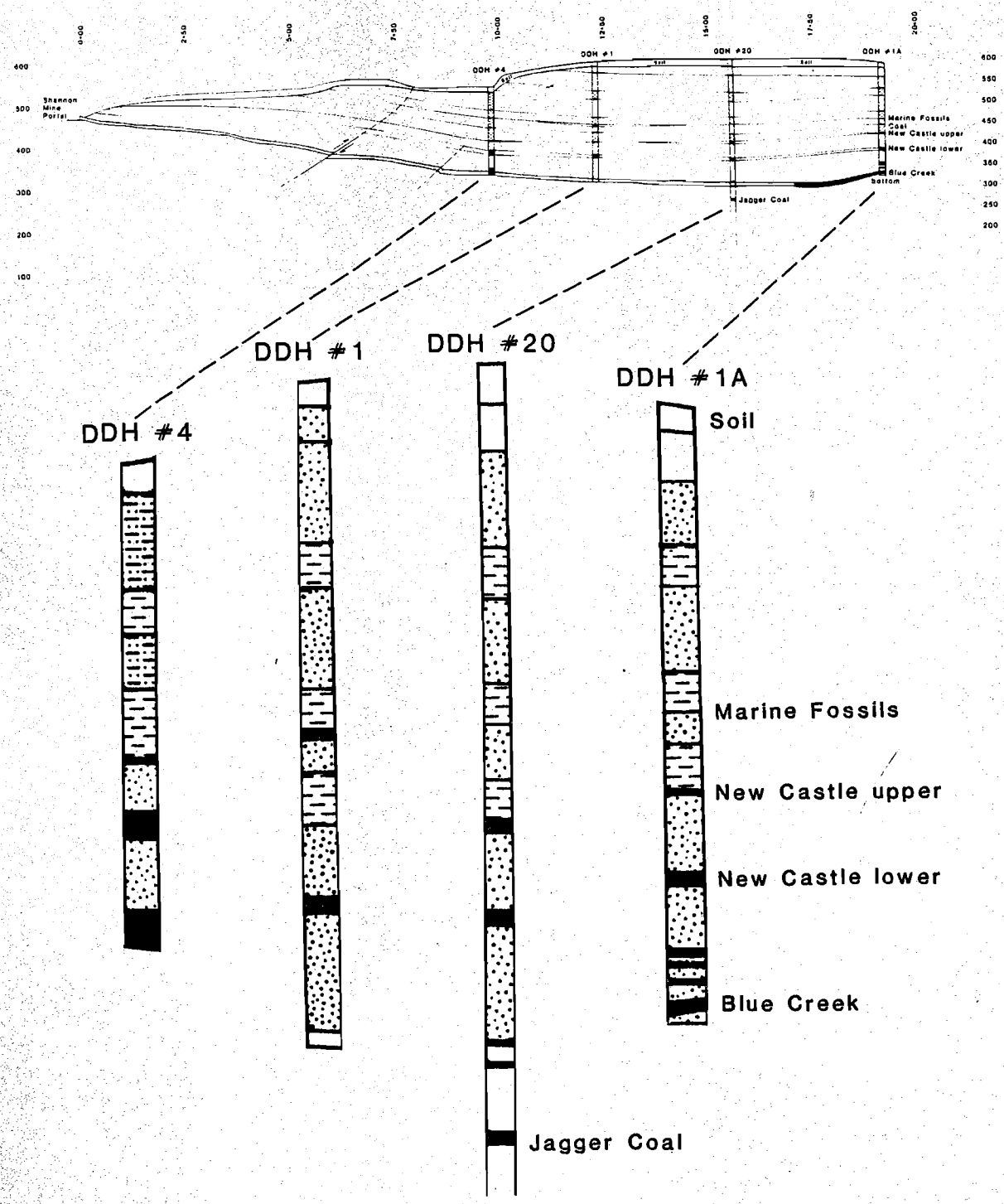

Figure 4. Geologic section along the Shannon mine slope showing generalized lithologic sequence.

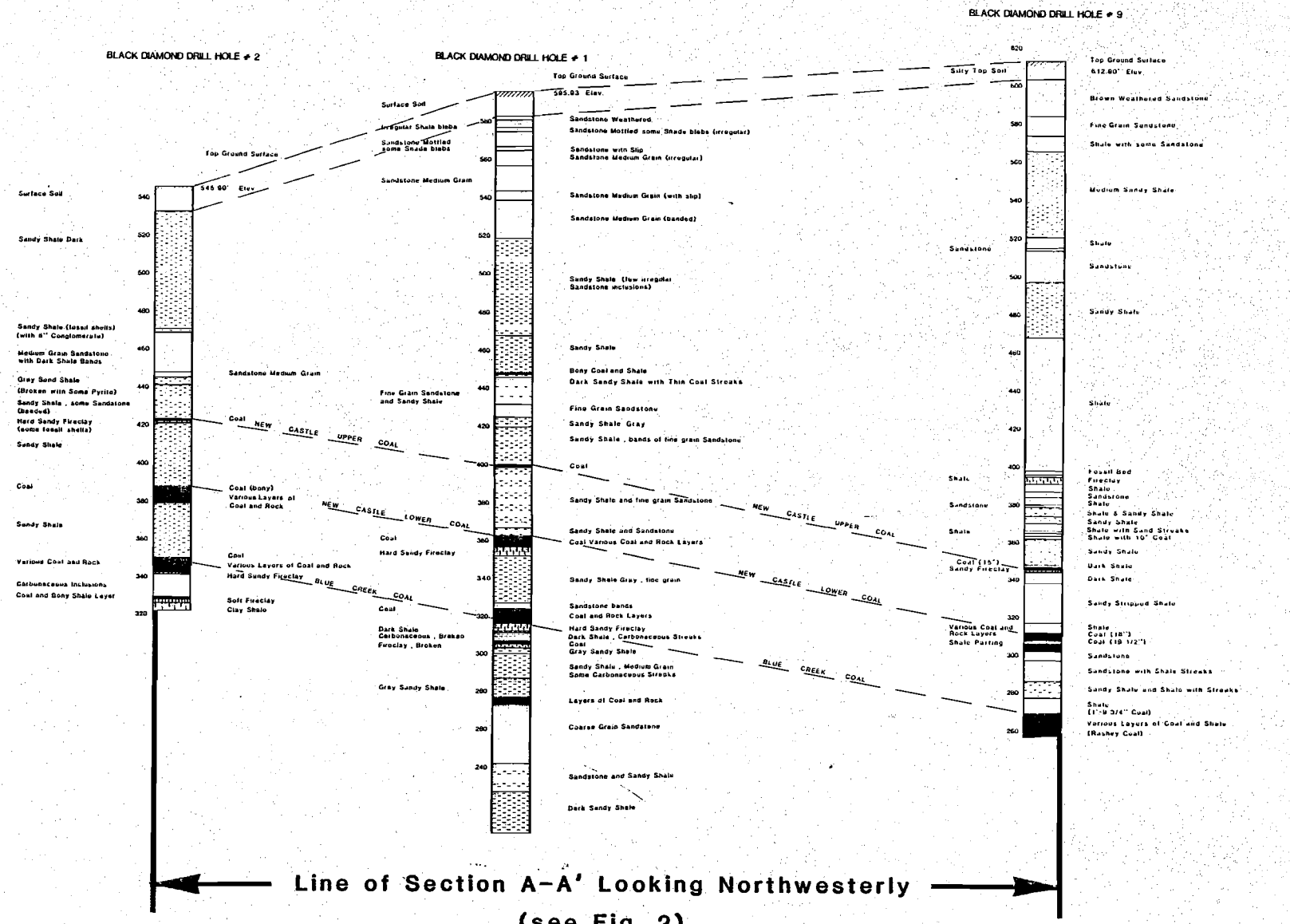

Figure 5. Columnar section showing lithologic sequence.

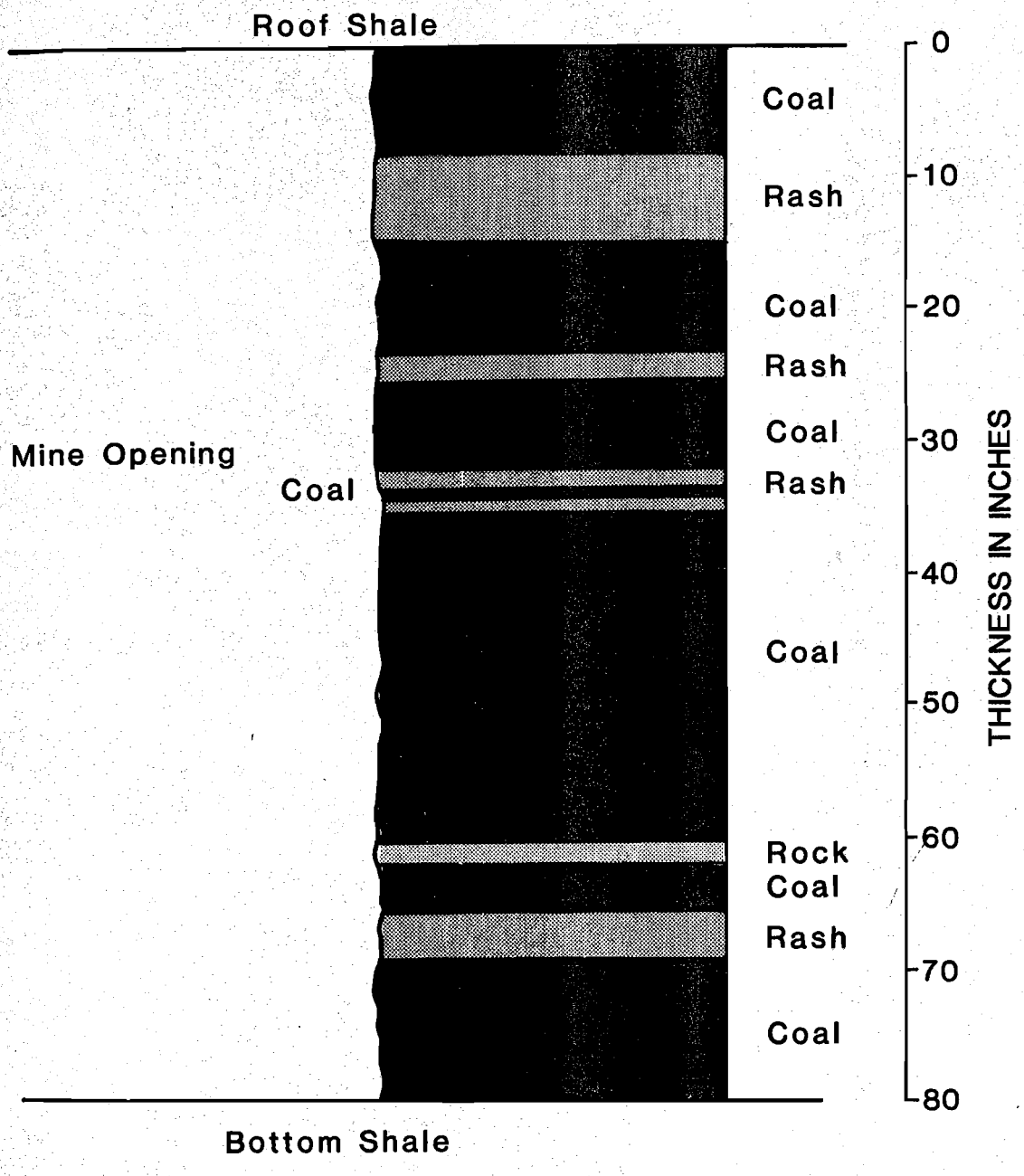

Figure 6. Coal section in rib of south pillar of instrumented control section in Shannon mine.

Electric Logging

Electric logs were run in borehole DDH 20 at the site to substantiate the interpretation of the drilling log and provide additional subsurface data (Figure 7). The borehole was drilled 40 feet southeast of the survey control point and 342 feet deep penetrating a pillar in the Blue Creek coal seam and down to the underlying Jagger coal seam (Figure 8). Core samples were collected and selected samples of the core were tested in the laboratory for various physical strengths and properties (Figure 9). These data were compared with the geophysical logs for verification and correlation. The laboratory test results are given in Table 1.

Four electric logs were obtained from the run, including: (1) coal lithology log; (2) seam thickness log; (3) coal quality log; and (4) multi-channel sonic log.

The coal lithology log consists of a gamma ray and density log together and these are usually sufficient for basic coal lithology identification -- shale, sandstone, mudstone, marine bands, and coal. The caliper of the hole is usually included in this log and identification can be somewhat difficult if the response of the caliper is poor. However, the borehole diameter of D.D.H. 20 was 2-7/8 inches and the depth comparatively shallow with no caving; therefore, the tool response was not affected.

The gamma ray response relates to the natural radioactivity. Generally, the source of this activity is potassium or more specifically the associated isotope K40. Potassium is present in most shales in the form of a mica mineral. Hence, the measurement is usually an evaluation of shale content. Readings less than the value of an established shale line means an increasing presence of sandstone.

The tool actually measures electron density which is related to bulk density. In the case of rock volume, examination by a density tool depends upon source-to-detector spacing. Because lithology does not require high resolution, it is advantageous to use the long-density spacing tool. Density measurements are usually diagnostic in their own right, but usually it is necessary to study them in conjunction with a gamma ray log.

The seam thickness log is another type of log run using the caliper log in conjunction with what is called a bed-resolution density log. Both logs are run on expanded scales of about 20 to 1 for the best and most reliable thickness determination.

Again, due to the small hole diameter and formation competency, the caliper log shows consistent and persistent walls with no caving. Under these favorable conditions, the midway points at the top contacts and bottom contacts of the beds allow the use of the midpoint as the point to use for seam thickness measurements. An example of a seam thickness log is shown in Figure 10.

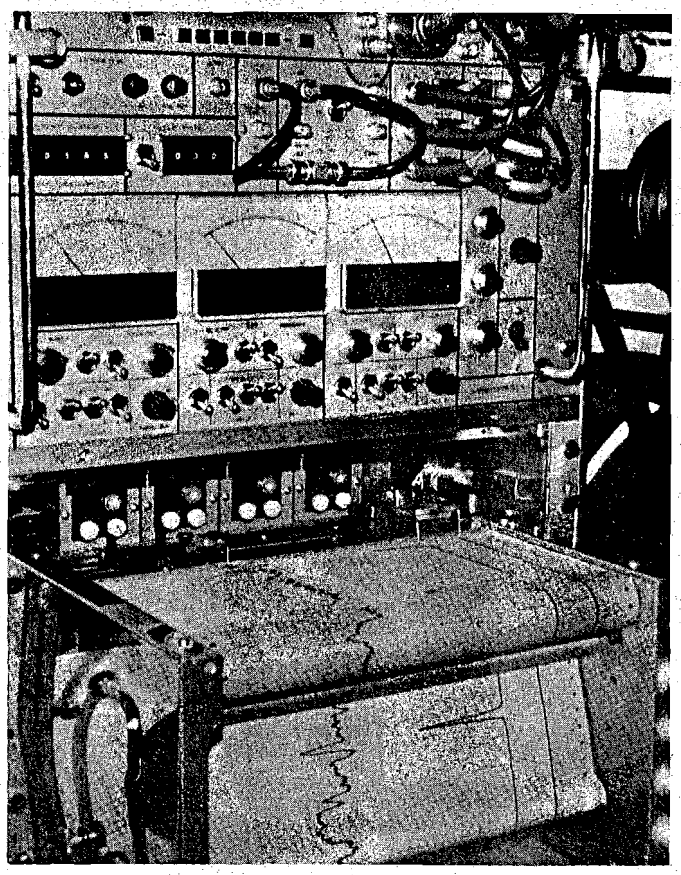

Figure 7. View of geophysical recording unit during electric logging of D.D.H. 20.

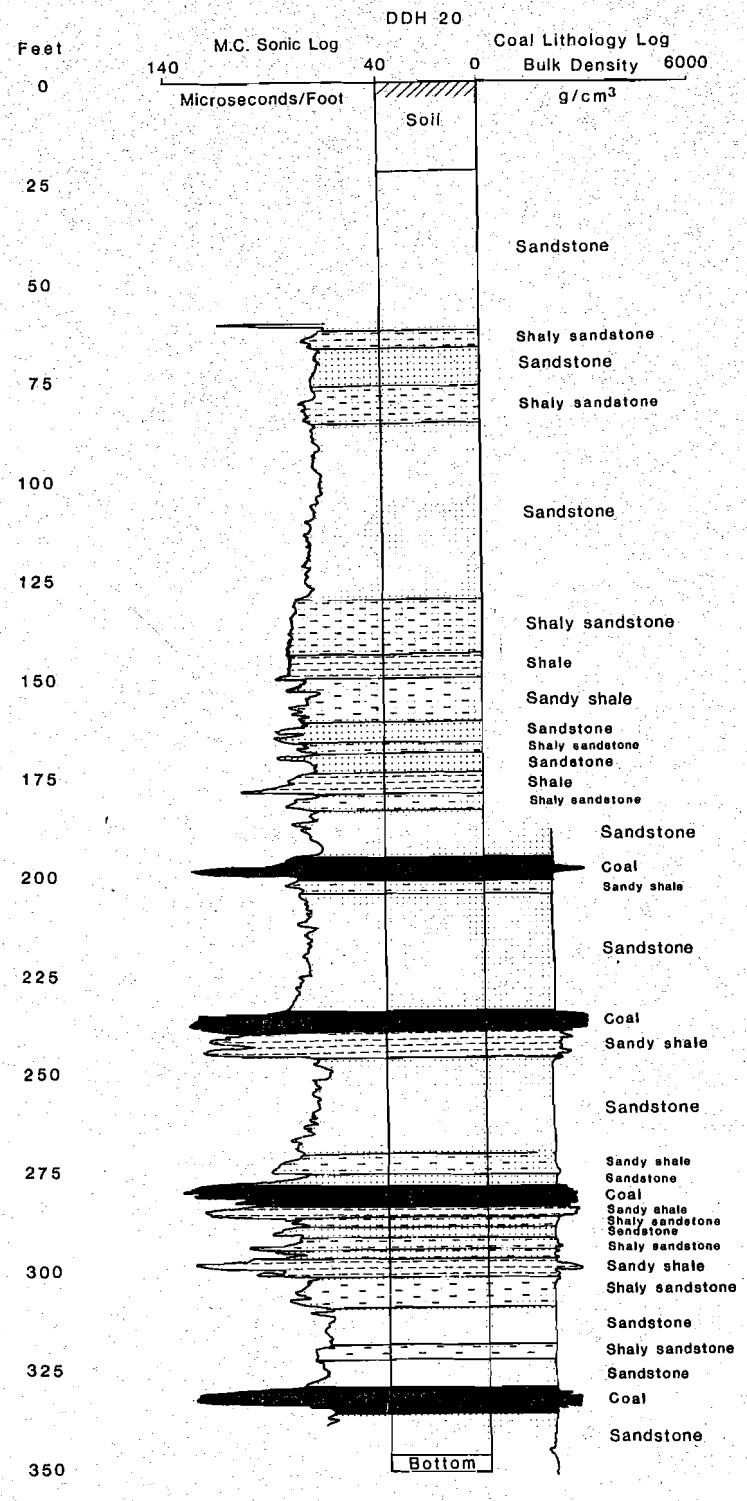

Figure 8. Sonic and bulk density log of D.D.H. 20 showing lithologic interpretation.

Figure 9. Extracting core from core barrel (D.D.H. 20).

Table 1. Physical Properties of Core Samples from D.D.H. 20

Core Sample	Depth (a) (ft)	Specific Gravity	Dynamic Test: V_S (ft/sec.) Shear Wave Velocity	Dynamic Test: V_P (ft/sec.) Compression Wave Velocity	E (psi)	Ultimate Strength (psi)	Poisson's Ratio
1	41.80	2.84	5264.17	10495.00	1.07×10^6	30,000	.33
2	78.10	2.50	5447.67	9001.95	-------	27,000	.28
3	106.30	2.71	3935.46	13071.89	2.85×10^6	47,500	.45
4	153.20	2.67	6713.90	13935.58	3.20×10^6	53,000	.35
5	175.50	2.54	4115.10	9884.98	1.78×10^6	36,500	.40
6	192.10	2.67	6526.10	12845.85	3.00×10^6	43,500	.33
7	218.70	2.67	6554.70	12104.62	2.57×10^6	16,500	.29
8	264.10	2.67	6042.80	10710.47	3.20×10^6	34,000	.27

(a) Depth from surface

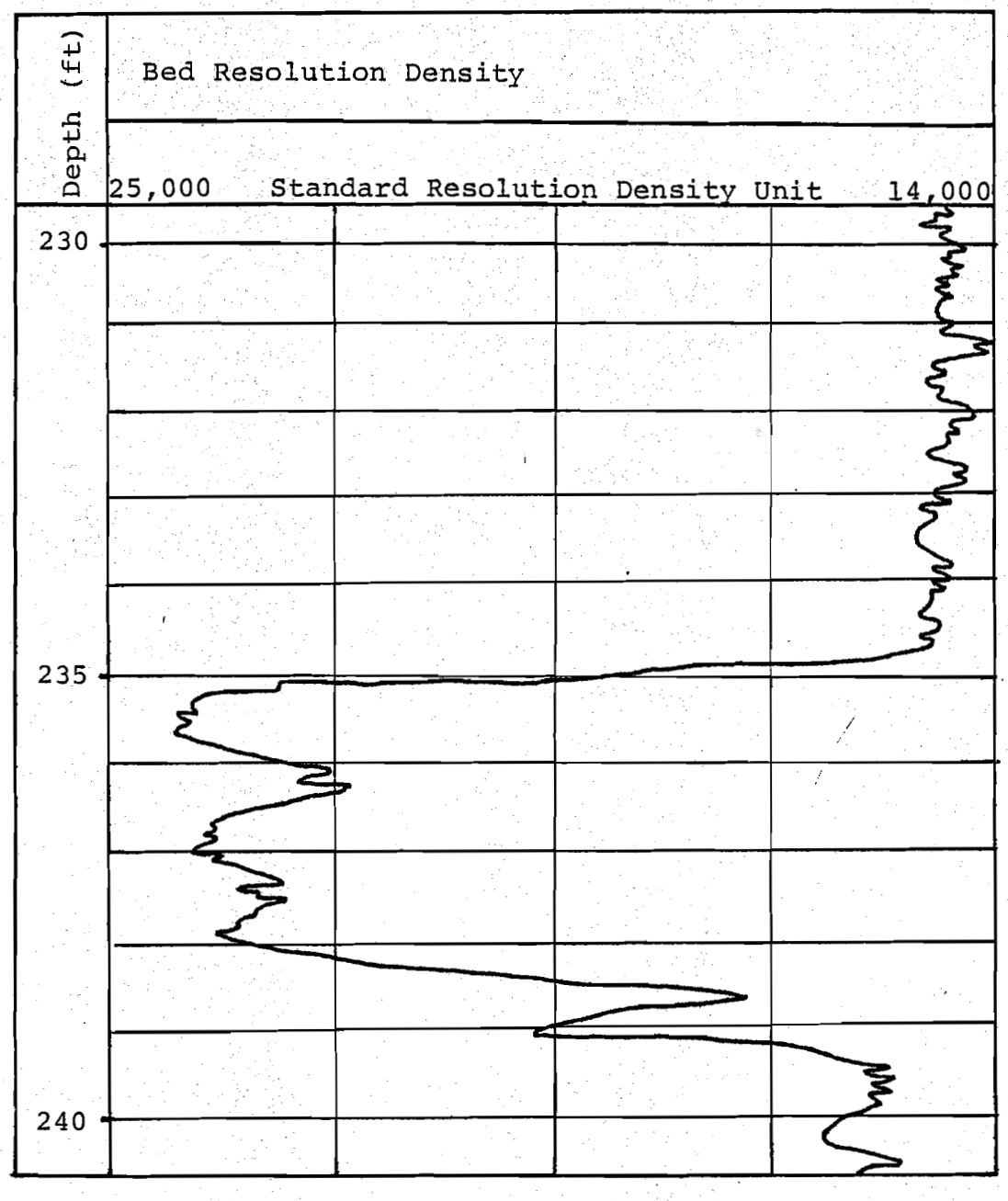

Figure 10. Typical seam thickness log.

The coal quality log is used in combination with the gamma ray log and long spacing density log. This combination of tools when correctly read and interpreted provides additional checks on coal thickness and general coal quality as related to ash content. Generally, there is a mineral relationship between the ash content of a coal sample and the bulk density of a coal sample for a given type of coal. Provided the coal type is known, the measurement of density will give an evaluation of ash content.

Because coal quality was not considered an important parameter in this study, no major attempts were made to classify the coal quality. It should be pointed out, however, that in a splurge of major coal exploration activity needed to determine the economic feasibility of coal reserves and coal quality for washing purposes, the coal quality log would be a necessity in the overall mine design. The coal quality log from the gamma ray log is shown in Figure 11.

A multi-channel sonic log was also run to aid in providing data on the physical character of the overburden rock types.

The caliper log can be useful when washed or caved areas are encountered during the logging operation, but the most useful tools are the combined gamma ray and density logs. Low gamma ray logs and high density indicate harder rock zones.

The function of rock strength reflected by various moduli of elasticity is a function which combines the effect of rock density and the effect of compressive stress. The sonic log measures a form of compressive stress. Therefore, the combination of this measurement with an appropriate density determination does give a useful indicator of rock strength.

The geophysical data derived from the wireline logging techniques of borehole D.D.H. 20 provided evidence to support other techniques used in this research.

Site Preparation and Blasting Sequence

The surface of the test site was cleared and prepared for drilling and blasting operations (Figure 12). Blast holes were drilled using a 5-inch diameter drill. The holes were approximately 60 feet deep and penetrated the first predominant sandstone layer below the weathered zone.

Figure 13 shows a drill rig in operation and research team measuring the depth of blast holes after drilling. The arrangement of blast holes was in a cross pattern with respect to the control point and the holes were drilled on approximately 25-foot centers. Figure 14 shows the location of blasting holes, underground instrument location, and sequence for the first phase of shooting.

For the first and final phases of shooting the blast holes were loaded with different charge weights of explosives at about the same depth from the drill-hole collar. Prilled ammonium nitrate (ANFO) and fuel oil were used as the explosive charge. Each hole was loaded with ANFO and stemming

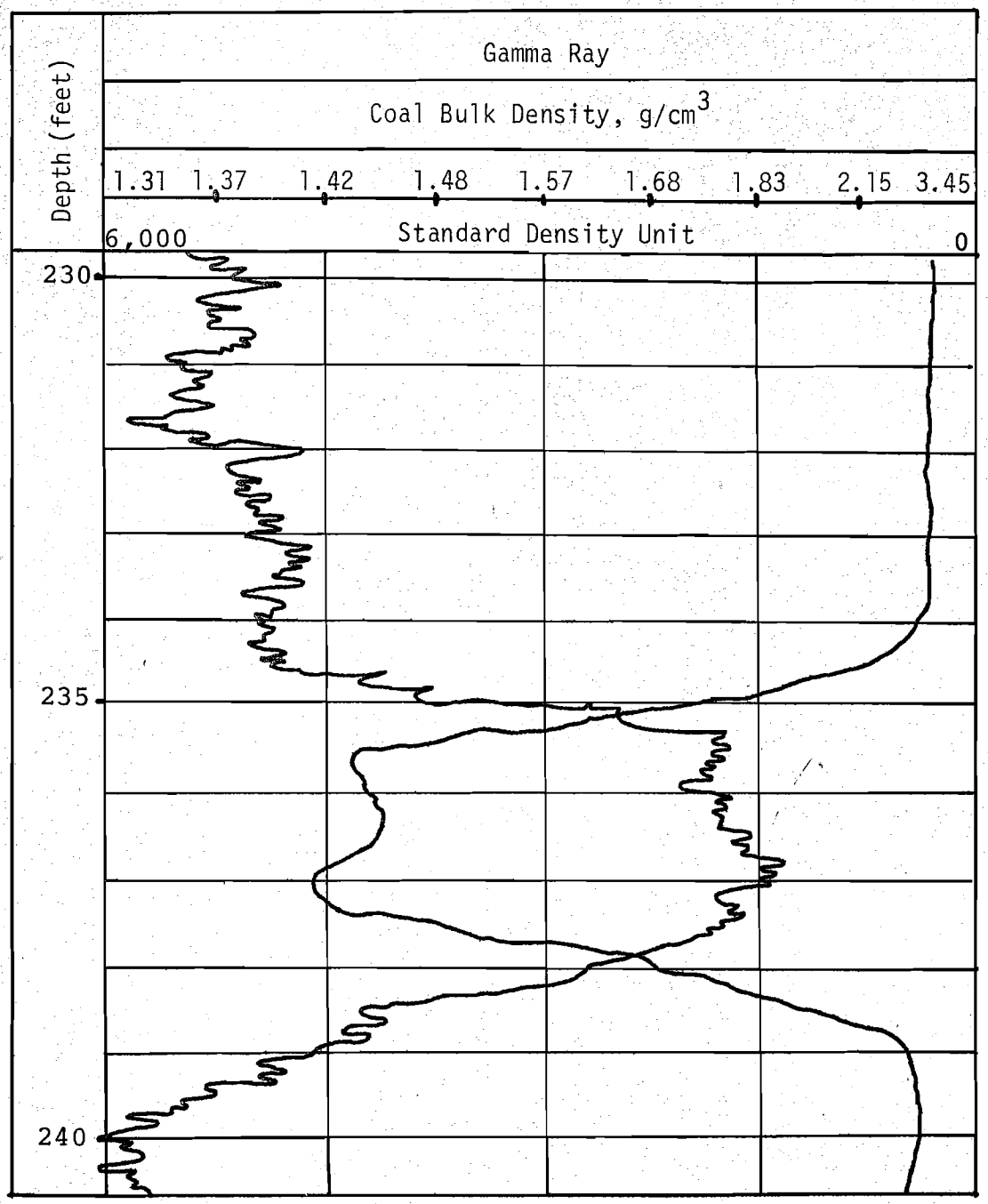

Figure 11. Typical coal quality log.

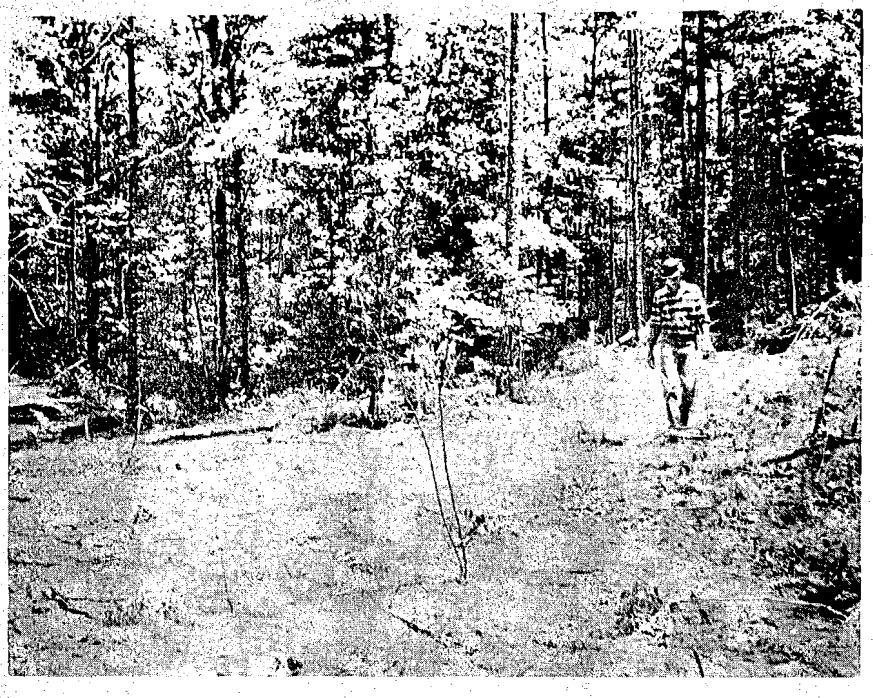

Figure 12. Part of test site cleared in preparation for drilling blastholes.

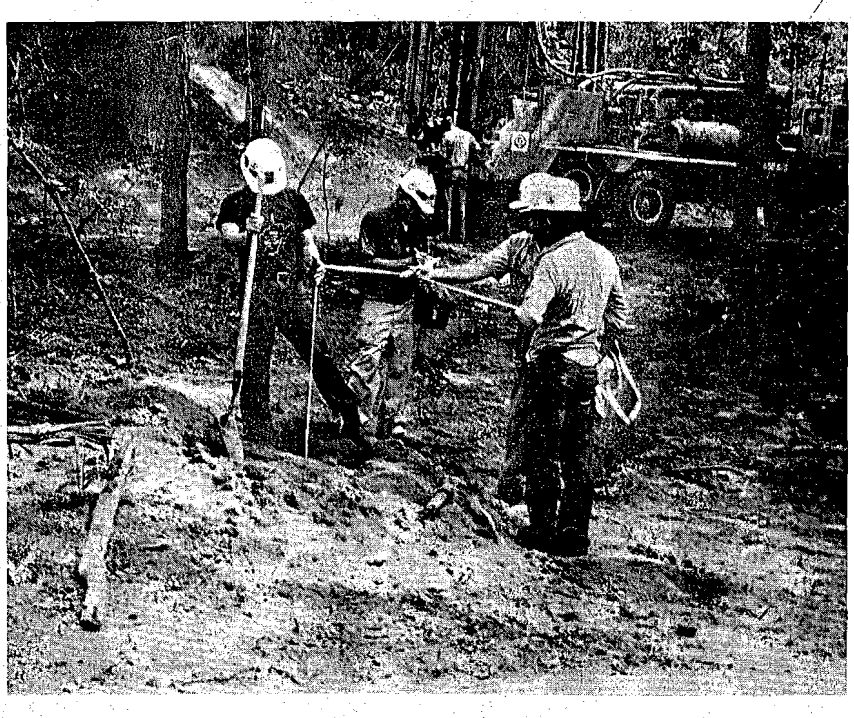

Figure 13. Drilling and measuring blasthole depth at site.

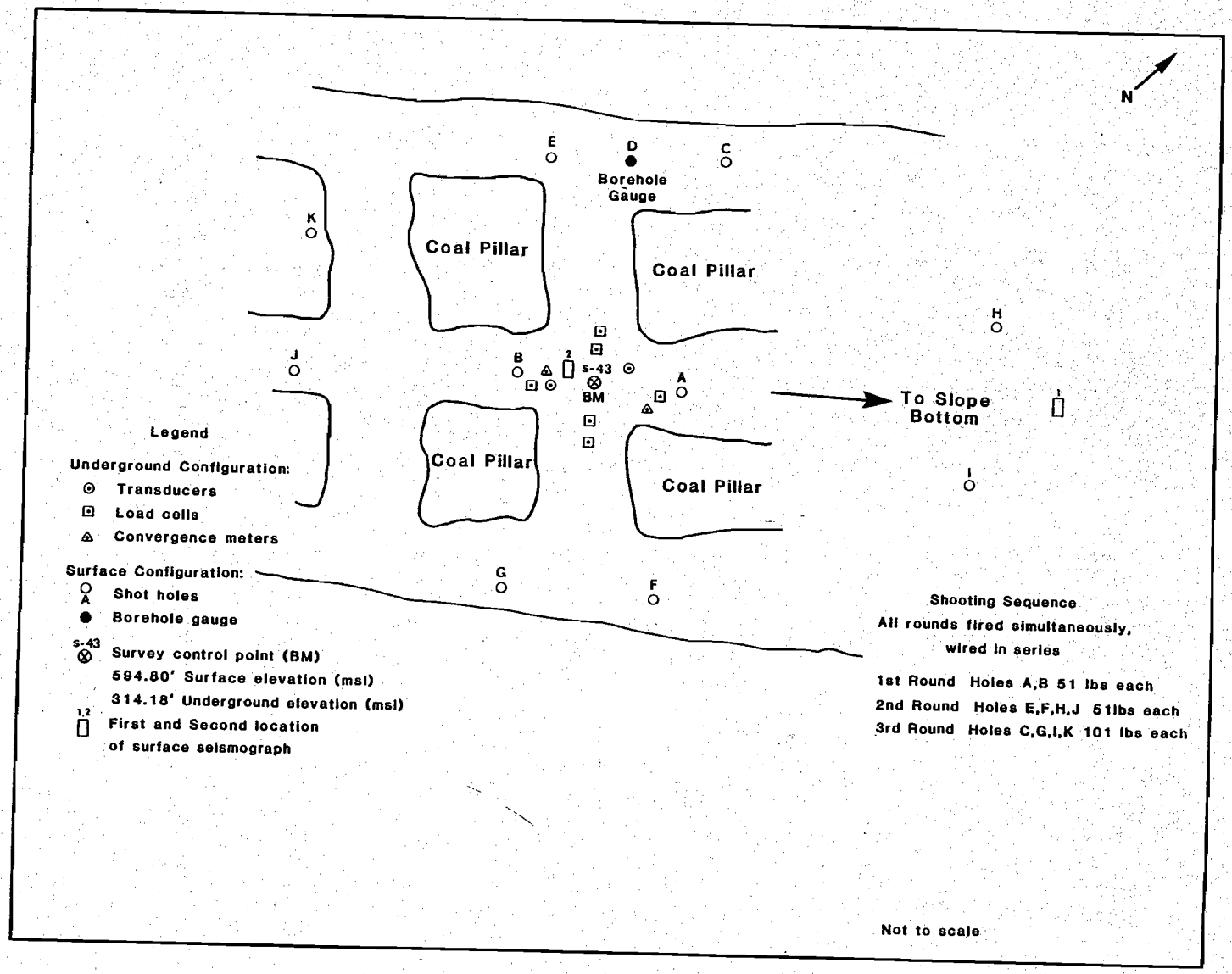

Figure 14. Layout of blastholes, underground instrumentation and shooting sequence for first phase.

which consisted of the borehole cuttings at the site (Figure 15). The blast holes were then sequentially fired. Table 2 gives the blasthole data for each shot sequence for the first phase of blasting.

Two seismographs (model VS-1100 and model VS-1600) were placed on the coal mine floor. The VS-1600 seismograph is designed for automatic and unattached field recording (Figure 16).

Two other seismographs (model VS-1100 and model VS-1600) were placed on the surface to analyze the blasting vibrations by conventional statistical analysis. Station 1 was relocated to station 2 on the final phase blast (Figure 17). This was necessary to consider the possible effects of faulting or other geological structural features that exist at the site.

Additional instruments for measuring the blast vibration were installed in a 4-inch diameter open vertical borehole. The borehole was drilled to accomodate two borehole gages and a two-way telephone line Figure 18). A model 1462 Bison Instrument vertical borehole sensor was installed and a model L-10-3D-SWC Mark Engineering Borehole Seismometer was installed (Figures 19 and 20). The Bison instrument was placed at about 50 feet below the collar of the hole and the latter at about 150 feet below the borehole collar. These instruments were used to measure the ground vibration in the rock units to study attenuation characteristics.

At the same time, pre- and post-blast observations were made by spraying paint on the roof surface of the rock prior to blasting. This was to observe any possible rock fractures caused by surface blasting or further displacement of pre-existing fractures in the mine roof (Figure 21). Some scaling of the mine roof rock was observed after blasting (Figure 22). The blast holes were loaded with different charge weights of explosives at about the same depth from the collar and the holes were sequentially fired. Figure 23 shows the typical surface effects after blasting at one of the holes.

INSTRUMENTATION AND VIBRATION MEASUREMENT

The instrumentation and field monitoring program was designed to consider both short-term and long-term effects of surface blasting on underground coal mine openings. The study was designed to collect and document blasting vibrations, assess mine roof damage, and blast design data. In order to collect the desired data for the program, it was necessary to select the proper instruments to provide the required data.

Selection of Measurement System

A wide range of instrumentation and support services are available on the market. Most offer many choices to the operator responsible for choosing a type of monitoring program. In selecting the correct

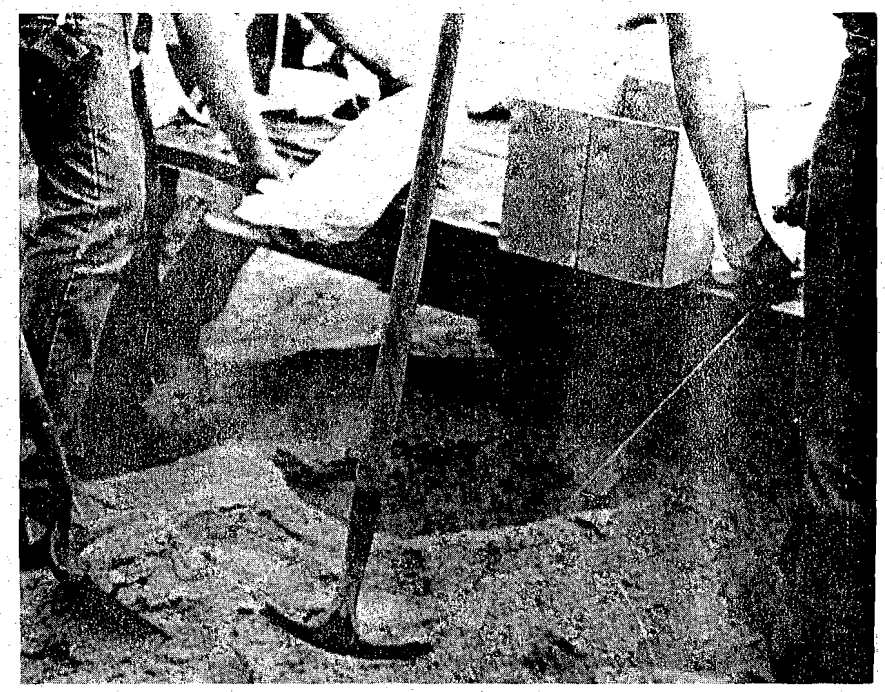

Figure 15. Loading blastholes with explosives.

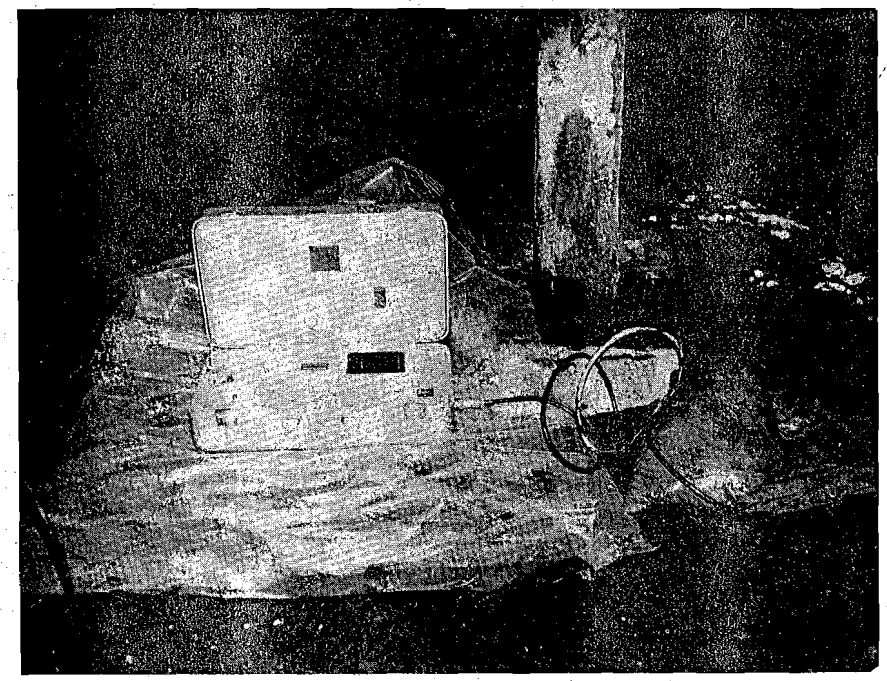

Figure 16. Model VS-1600, W. F. Sprengnether Engineering Seismograph placed for recording vibrations on the mine floor.

Table 2. Blast Hole Information - First Phase

Hole Identity	Depth (ft.)	Charge Weight (lbs.)	Stemming (ft.)	Firing Sequence
A	48	51	42	1st Round
B	48.5	51	42.5	1st Round
C	60	101	48	3rd Round
E	50	51	44	2nd Round
F	52	51	46	2nd Round
G	45	101	23	3rd Round
H	62	51	52	2nd Round
I	57	101	45	3rd Round
J	45	51	39	2nd Round
K	45	101	33	3rd Round

Note: 1. Each round was fired simultaneously i.e. no delays.
2. See Figure 14 for pattern layout.
3. Hole D was used for vertical borehole seismometer installation.

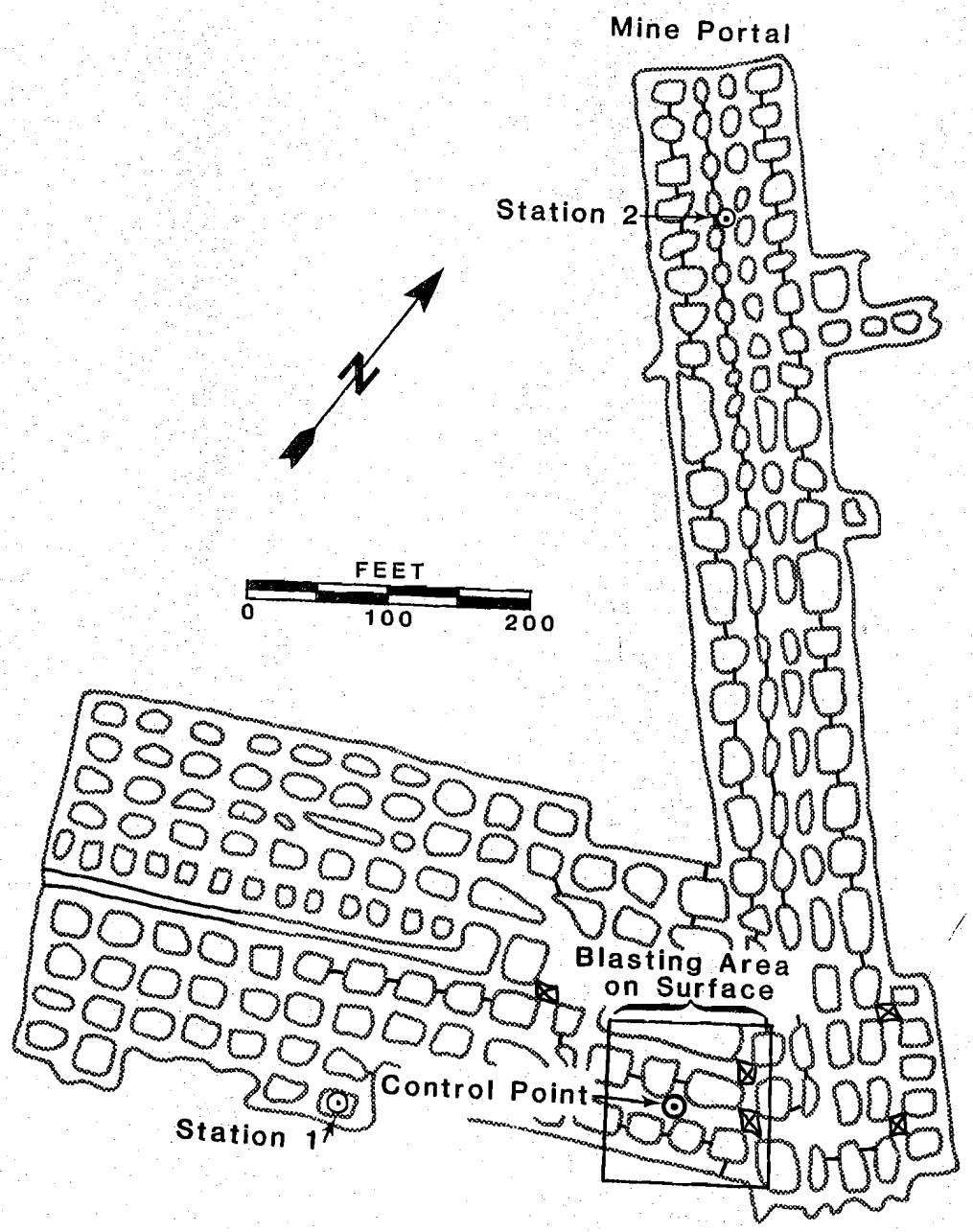

Figure 17. Location of surface instruments in relation to blasting area.

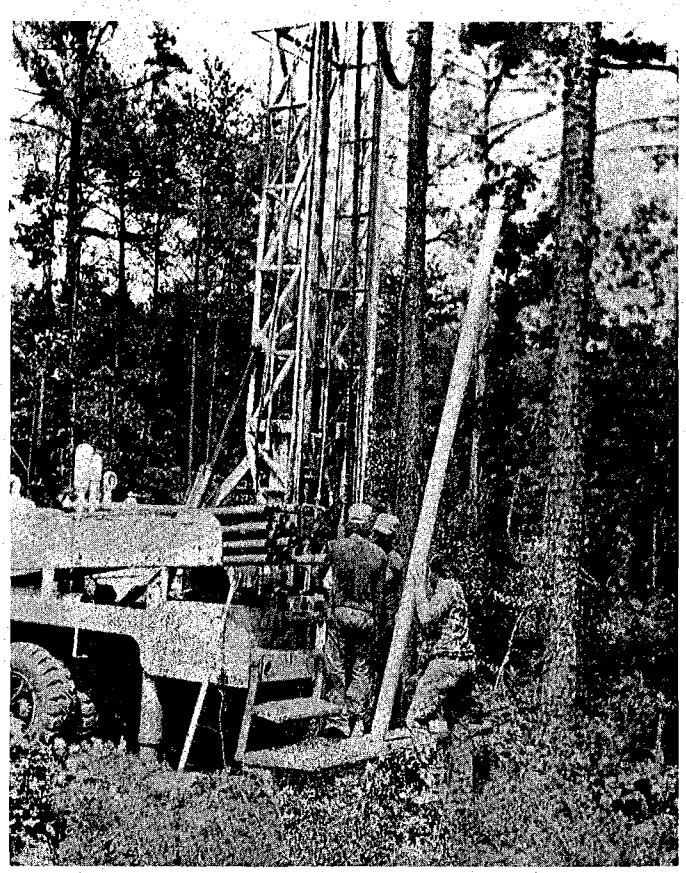

Figure 18. Emplacement of 4-inch diameter PVC casing in borehole prior to installation of vertical borehole seismometers and two-way telephone line.

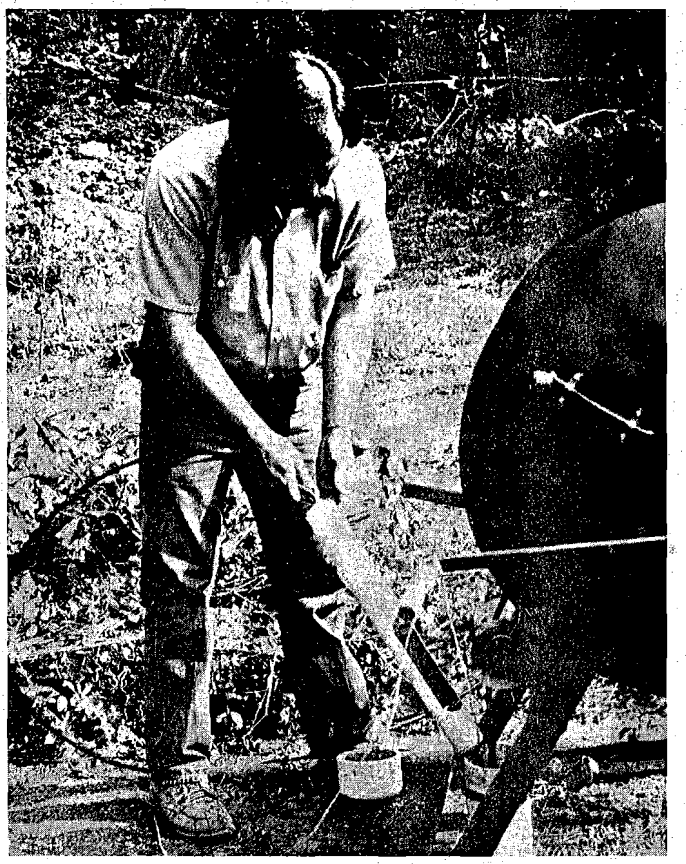

Figure 19. Installing a Model 1462, Bison Instrument, vertical borehole meter in the 4-inch diameter open borehole.

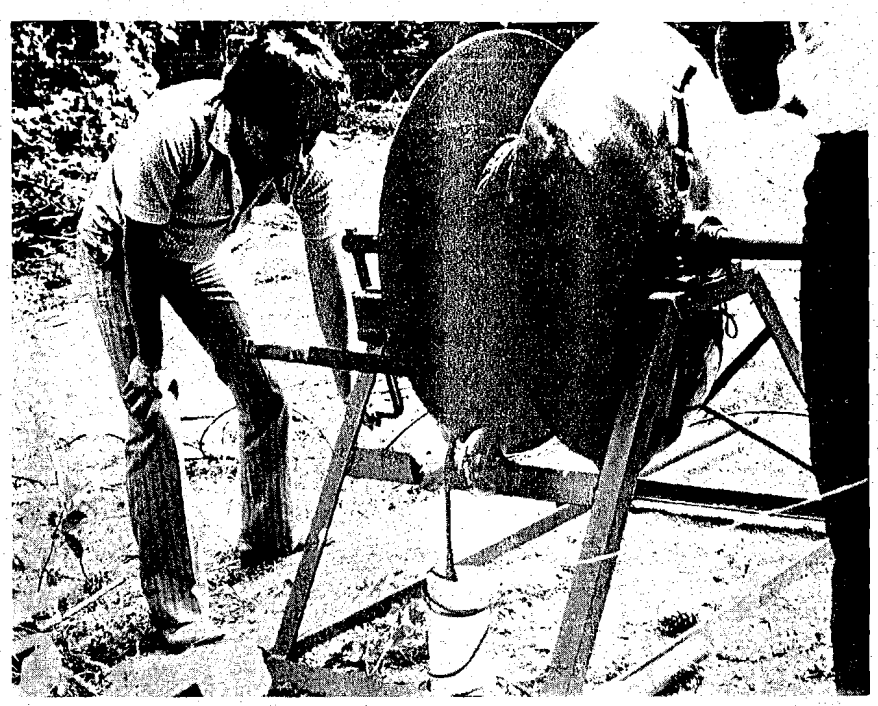

Figure 20. Lowering the Mark Engineering Borehole Seismometer into position for recording.

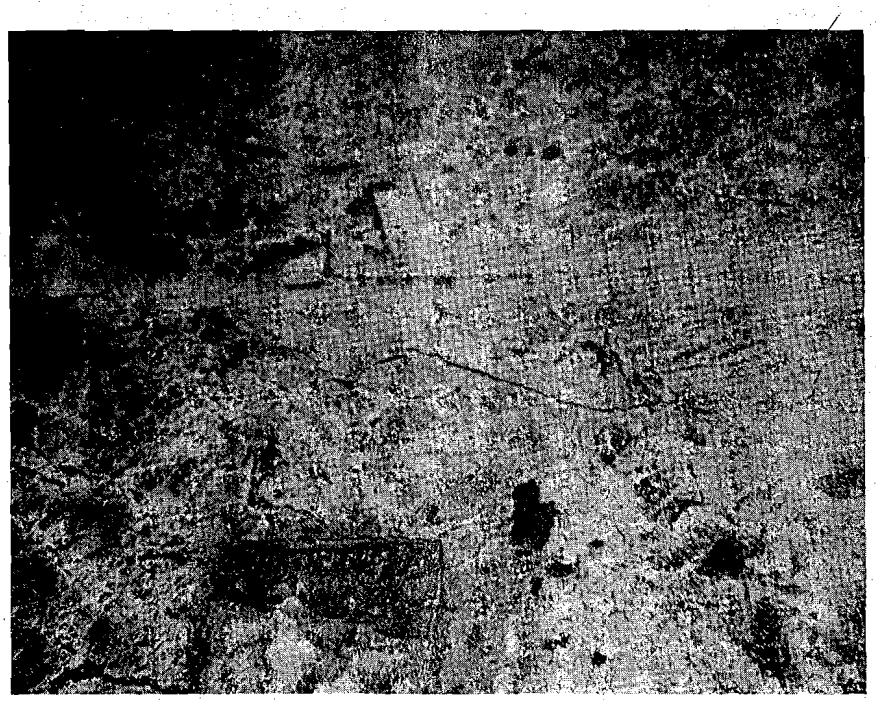

Figure 21. Cracks in mine roof prior to blasting.

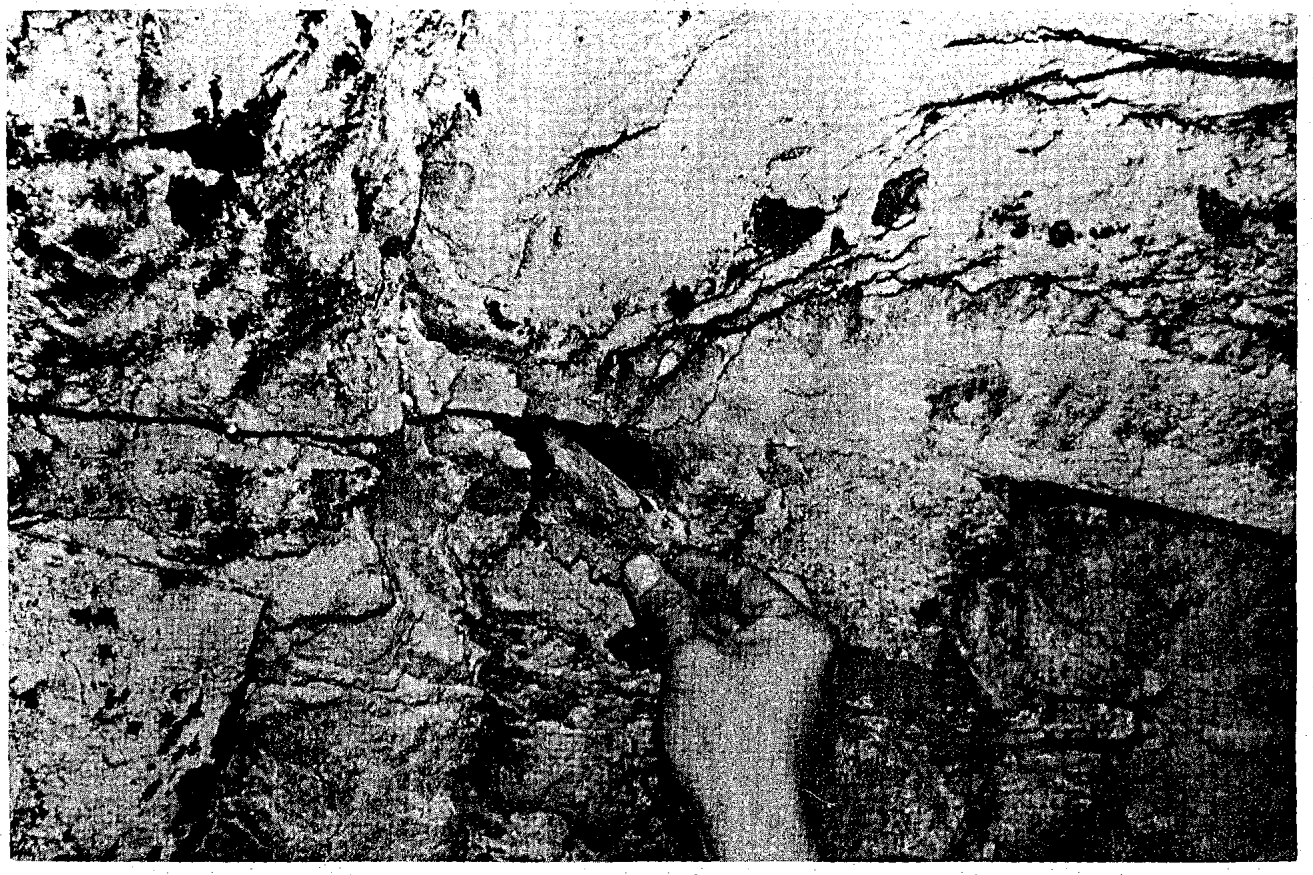

Figure 22. Post-blast photograph showing scaling and pre-existing fractures in mine roof.

Figure 23. Typical surface effects around borehole after blasting.

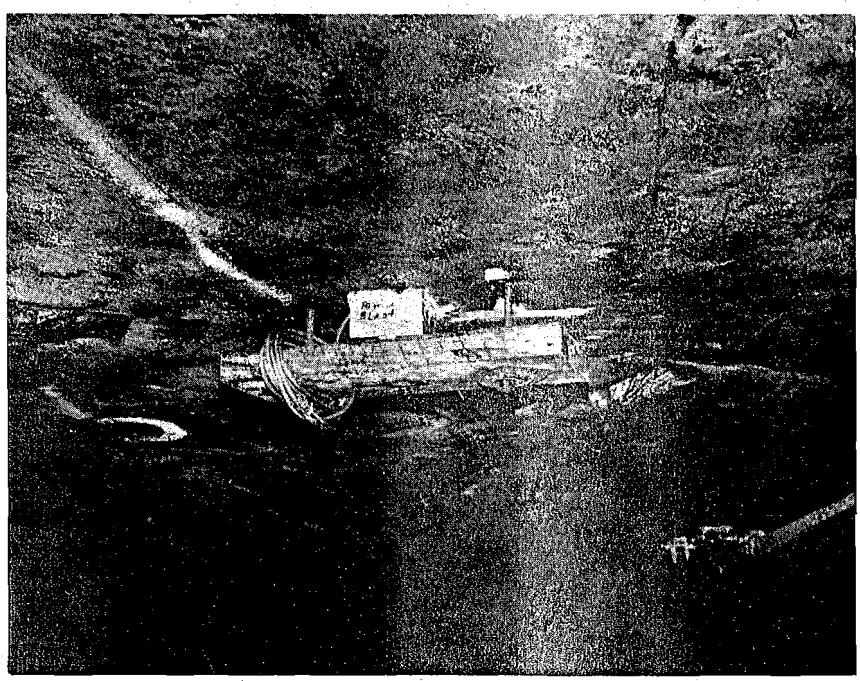

Figure 24. Seismometer (transducer) installed on mine roof.

instrumentation, a decision must be made as to the method of data collection and the type of information desired from the data. Selection of instruments requires careful thought as to program needs as well as compatibility with the overall project. Considerations include: quantity to be measured, degree of accuracy required, range of measurements expected, local environment anticipated, reliability over the life of the program, ease of access for installation and reading, and costs. Also to be considered in choosing underground instruments are the varieties of environmental factors encountered, such as particulate matter, shocks, high humidity, varying temperatures, high pressure, corrosive surroundings, large deformations, loss of accessibility, erratic power supplies, and vandalism.

Vibration data can be collected by recording wave peak readings or by capturing the entire waveform from a seismograph which can be installed in the field. External force created by blasting and the induced stress created in a mine roof can be measured by a strain gage transducer yielding information on the behavior of the rock.

Instrumentation Recording and Blasting Program - First Phase

The instrumental recording program for this part of the study was designed to monitor underground and surface vibrations, changes in the mine roof height, if measurable, and underground stresses and deformations resulting from surface blasting. Background vibrations from other sources were also monitored. To assess and appraise accuracy, repeatability, and sensitivity of selected instruments, the program was divided into two phases, first and final. The instrumentation necessary for the pre- and post-blast survey of the underground mine for the first phase of the study was installed according to the plan shown in Figure 14.

The sensors for recording underground vibrations were installed on the roof and floor of the mine opening (Figures 24 and 25). From the viewpoint of potential damage to the underground mine, the roof vibration level was the critical parameter monitored. Vibrations on the mine floor were monitored to investigate the use of floor measurements as a means to correlate roof vibration levels and potential damage.

The surface monitoring program included measuring vibrations with portable seismographs and seismometers. Surface vibrations were measured for comparison with the existing data base to identify any anomalous local site conditions. Because measurements of vibrations at the surface may be more easily obtained, their use as predictors for roof vibrations was investigated as part of this research project. Also, a vertical vibration attenuation versus depth was monitored by use of a borehole seismometer (gage). The location of the borehole seismometer is shown in Figure 14.

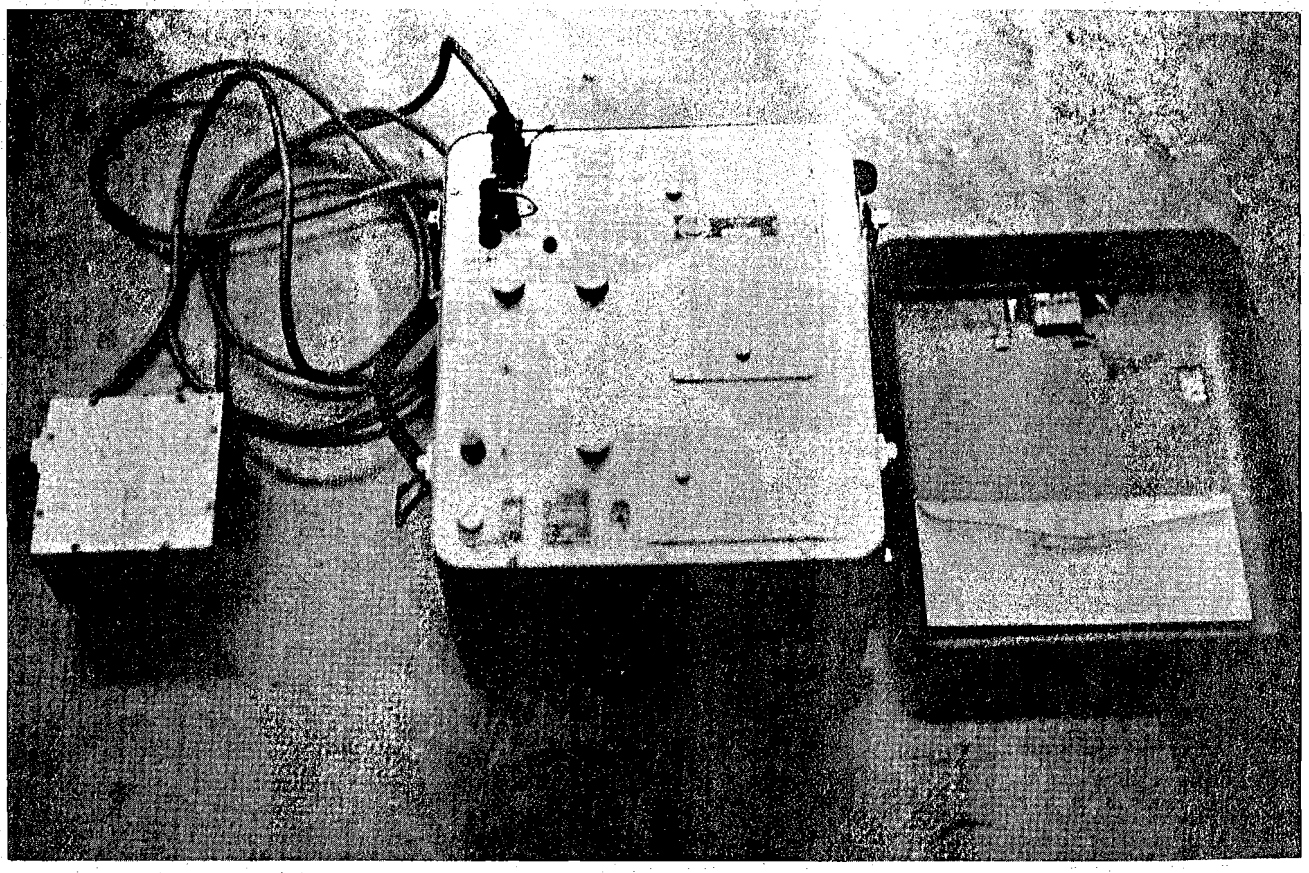

Figure 25. Sprengnether Engineering Seismograph, VS-1200, with S-1400 Seismometer (transducer) on left.

The stability of the underground mine opening was monitored by two types of instruments -- a load cell to measure the deformations or strains (consequently stress) and a continuously recording drum-type convergence meter to monitor short-term changes in roof-floor height resulting from blasting or removal of overburden.

Recording Vibrations Underground in the Mine

Three portable Sprengnether engineering seismographs, model VS-1200, with three-component S-1400 seismometers were attached to the roof in the underground mine to monitor roof vibration (Figures 14, 24, and 25). The seismometers were secured to the roof with expansion bolts supporting a T-board base. Irregular spaces between the surface of the seismometer and rock roof were filled with plaster of paris.

Each S-1400 seismometer contains three suspended coil transducer units, which are accurately aligned along orthogonal axes in a 5x5x4-inch cast aluminum box. The box weighs 7.5 pounds and is designed to represent about 100 to 150 pounds per cubic foot to match the density of the surrounding material and to provide a secure coupling. The seismometer has a natural frequency of 2 Hertz and a seismic mass of 0.5 kilogram (kg). Leveling is accomplished by a bullseye level mounted on the bottom surface of the seismometer. The emplaced seismometer was connected by an appropriate cable to the recording module of the VS-1200 seismograph.

There are two switches on the control panel, a mode selector and a gain-control switch. The trace can be recorded directly in terms of ground displacement, velocity, or acceleration, according to the mode selected. These were designed to record the velocity mode only. Only one response mode can be used at a time. Corresponding to the mode selection, sensitivities for gain switch settings are given in Table 3 and examples of the velocity sensitivity curves are shown in Figure 26.

The traces are produced by the VS-1200 with a constant-speed camera on direct-write linograph paper. One of the traces is normally reserved for event marking or air blast monitoring and was not used in this initial application. The other traces are radial, vertical, and transverse components of respective modes. An example of a three-component underground velocity response from surface blasting is shown in Figure 27.

One portable seismic triggered seismograph, model ST-4 by Dallas Instruments, Inc., was emplaced on the floor of the underground mine to monitor floor vibrations (Figure 28). The ST-4 seismograph is designed for automatic, unattached field recording of three channels of seismic data and one channel of air-overpressure signals on a magnetic compact cassette tape. It has a seismic frequency response of 1 to 200 Hz or more. The entire seismograph is housed in a 20-1/2" x 10" x 7" formica covered wooden case and weighs about 30 pounds. The basic seismic pickup types have three velocity sensors, one vertical and two horizontal, and these are mounted orthogonally in a single box with a power interlock connector. The sensor will operate regardless of the power switch setting.

Table 3. Sensitivities for Gain Switch Settings

Gain Setting	Velocity in/in/sec
1	1
2	5
3	20
4	100
5	500
6	2,000

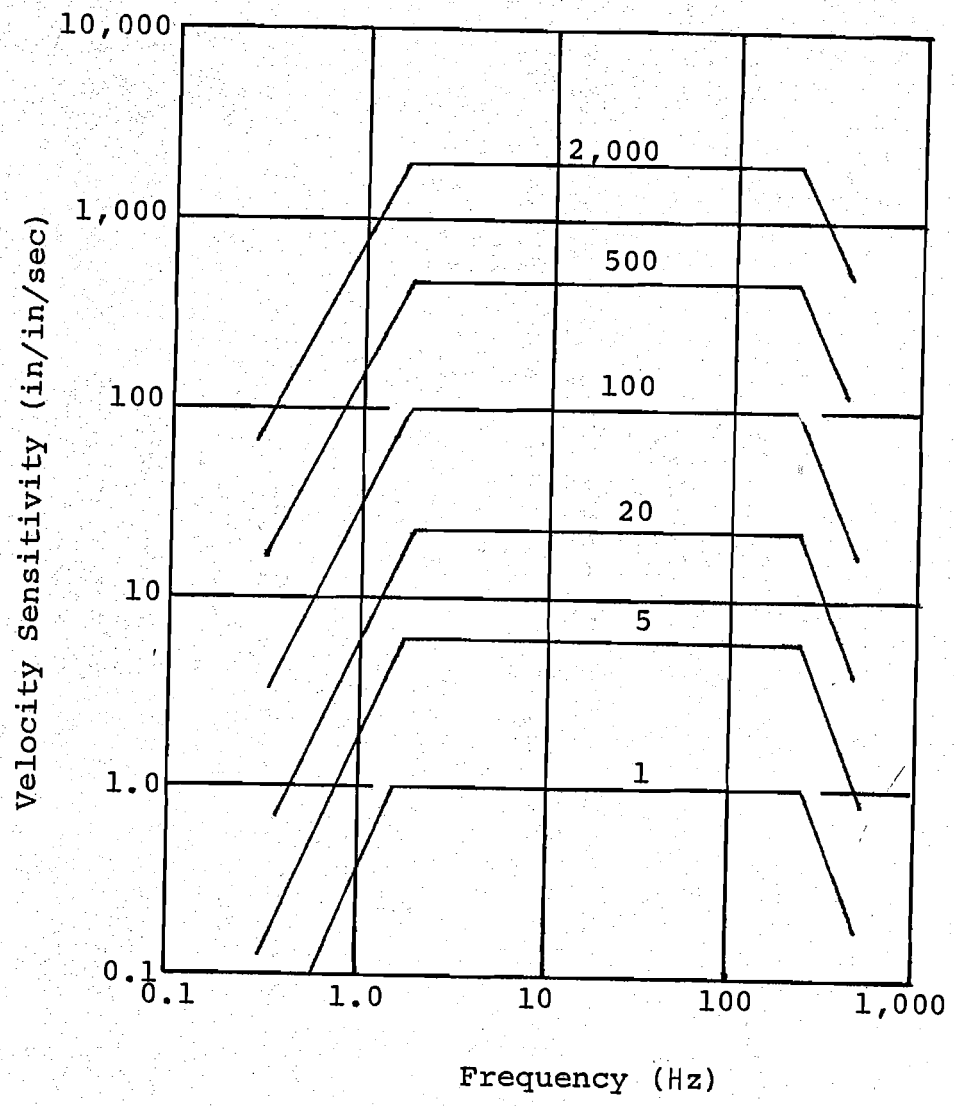

Figure 26. Velocity sensitivity curves for the VS-1200 seismograph.

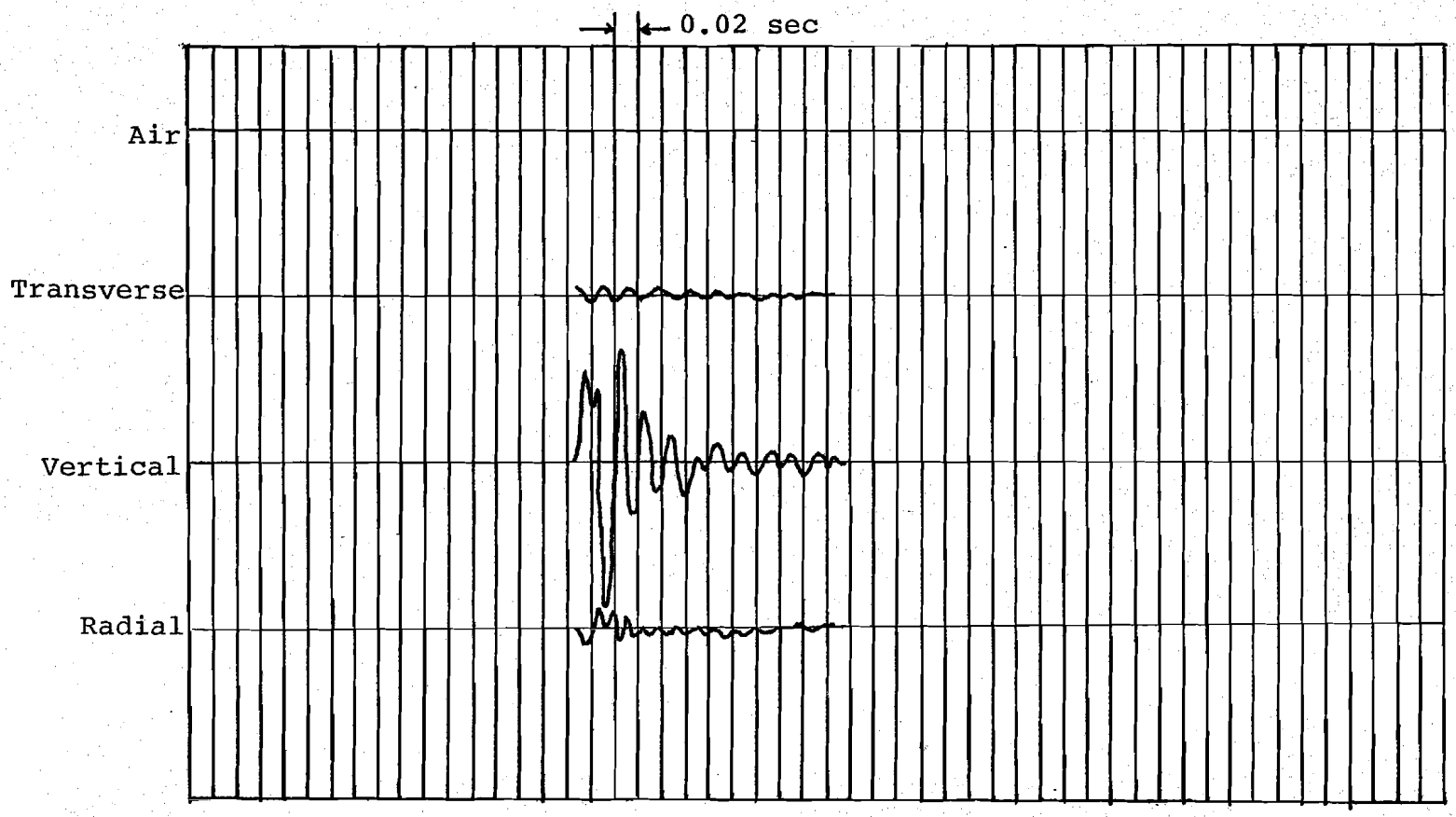

Figure 27. Tracing of underground velocity record.

Figure 28. Seismic triggered seismograph, Model ST-4, Dallas Instruments, Inc., installed on mine floor.

Recording Vibrations at the Surface

One portable Sprengnether engineering seismograph, model VS-1600, was placed on the surface for monitoring ground surface vibrations. The entire system, including the three-component seismometer and the fourth-trace air-wave detector, is housed in a 13" x 21" x 6-1/2" case for portability and weighs about 30 pounds. The seismograph has a flat response to particle velocity sensitivity of 6 decibels and a frequency range between 4.0 and 200 Hz.

The three-component seismometer, model S-4500, utilizes orthogonal 4.5 Hz digital grade long-travel geophones allowing for an 0.3-inch peak-to-peak motion. During operation, the sensor is removed from the case and placed on the ground oriented toward the approximate center of the blast. The seismometer was coupled with ground surface. The unit is designed to match a soil with an average density of about 1.6 grams per cubic centimeter.

The ground motion is recorded photographically with all three traces appearing on a single strip of either standard or direct-write photographic paper, 2.75 inches (70 mm) wide. The recording light spots are visible to the operator, just as they appear on the seismograph, through a frosted view screen. Timing lines are impressed on the seismograph at intervals of 0.02 second (2 mm spacing) and printed on the upper edge of the recording paper. Each 0.1 second line is accented by a slightly heavier line of double height. A vibration response of velocity on the surface is shown in Figure 29.

Other Vibration Recording Instruments

A portable Mark engineering borehole seismometer, model L-10-3D-SWC, was placed at a depth of 20 feet below the surface to monitor vibration attenuation versus depth. The instrument is a sidewall clamped geophone for installation in small circular, dry and/or fluid-filled boreholes. The digital grade sub-miniature geophone provides three-direction sensitivity, with one unit mounted vertically, and two units mounted horizontally at a 90-degree orientation. The borehole seismometer, as shown in Figure 30, is about 2 inches in diameter (expands to 3-1/2 inches), 34 inches long, and weighs about 10-1/2 pounds. Clamping used for coupling the seismometer on the side of the borehole is accomplished by the release of a heavy-duty spring upon contact of the unit assembly with the hole bottom. The standard test hole diameter is 2-3/4 to 3 inches, and an expander clamp is available for test holes up to 6 inches in diameter. The geophone has a 10-degree maximum vertical deviation and a frequency of 8 Hz or greater.

The L-10-3D-SWC borehole seismometer is normally connected to a Sprengnether engineering VS-1100 seismograph recording module, similar to that of a VS-1200 model. An illustration of sensitivity curves for the Sprengnether VS-1100 seismograph is shown in Figure 31.

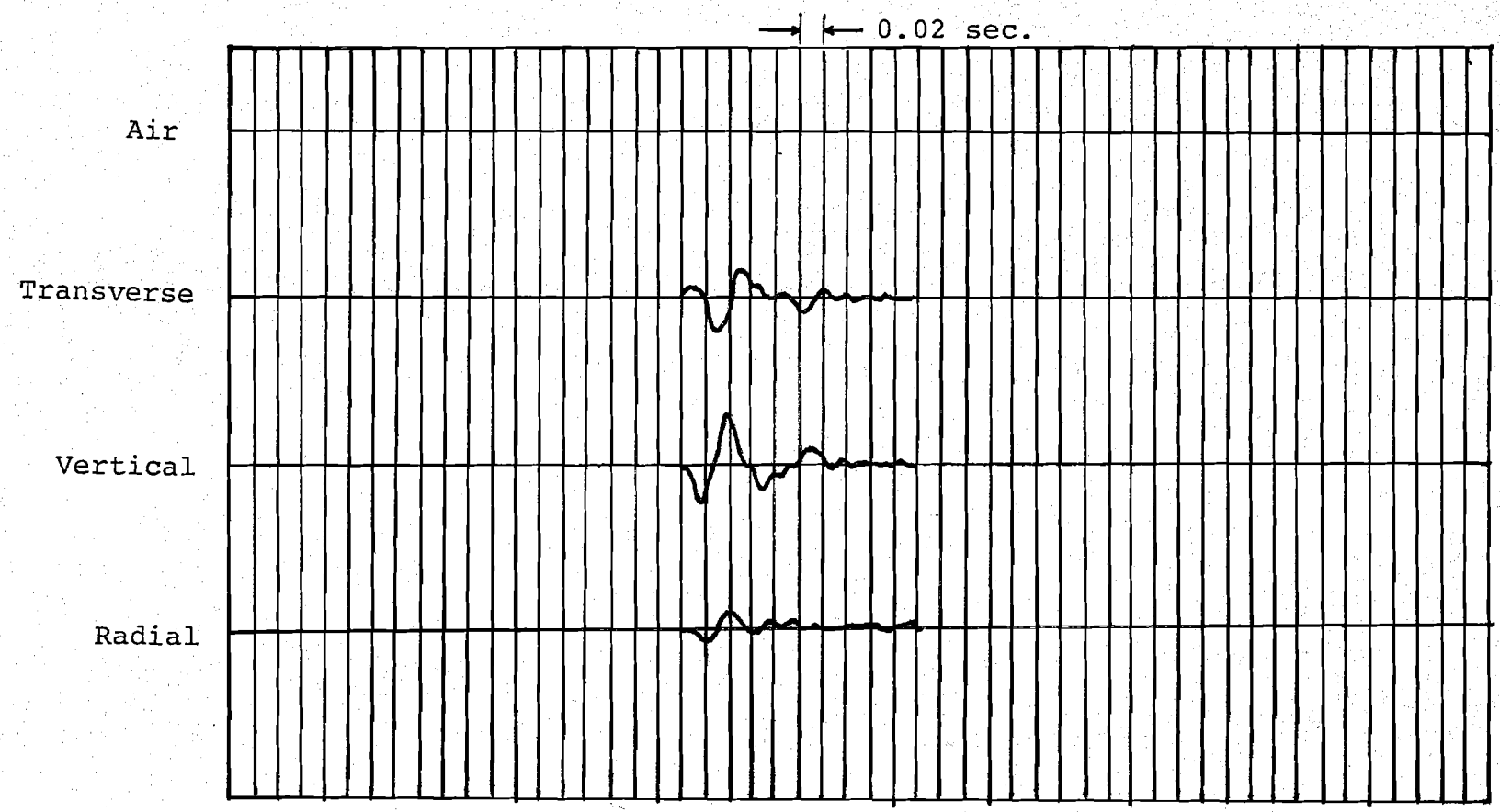

Figure 29. Typical tracing of surface velocity record.

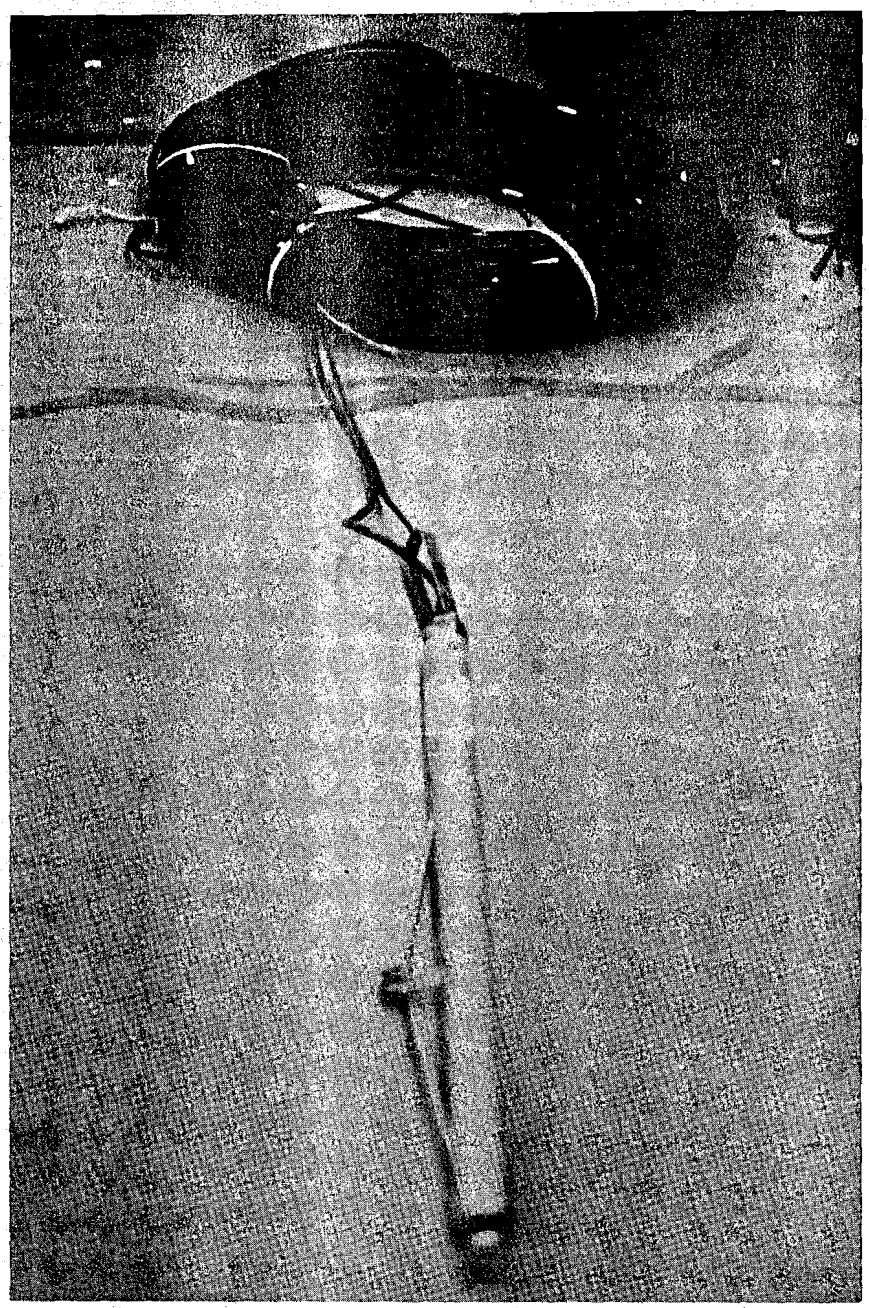

Figure 30. Mark Borehole Seismometer, Model L-10-3D SWC.

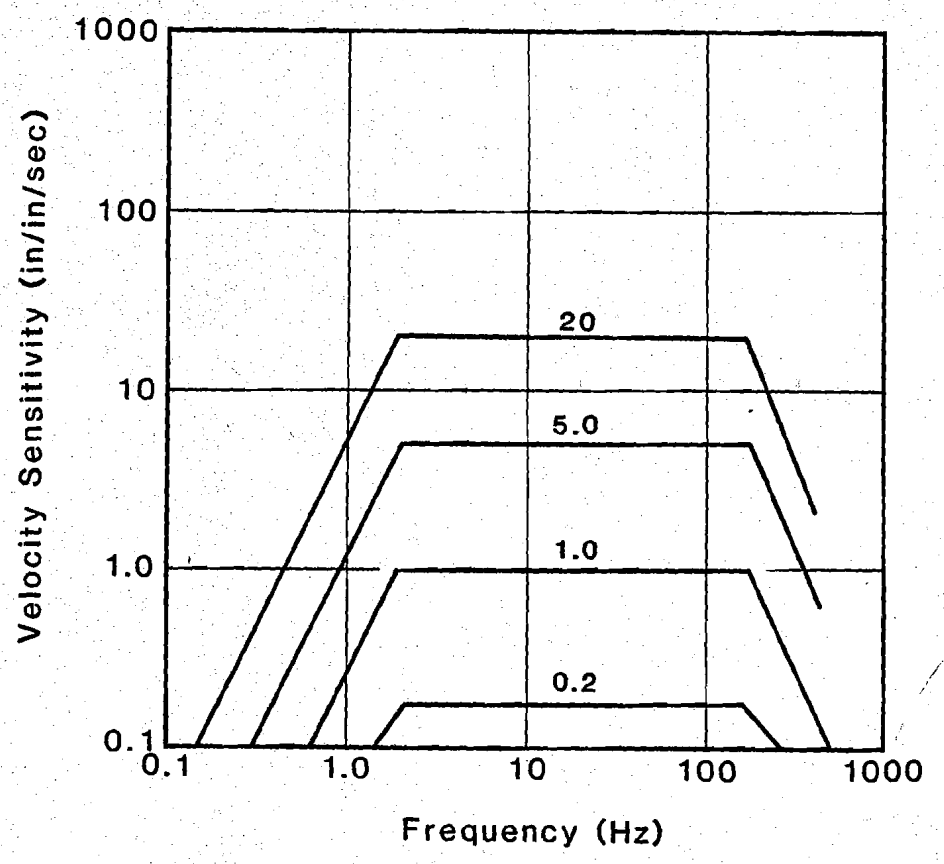

Figure 31. Velocity sensitivity curves for the VS-1100 seismograph.

Convergence Recording Instruments

Two Irad Gage direct recording convergence meters, model DCM-2, were installed in the underground mine. The Irad Gage convergence meter has been developed primarily as a low-cost means of continuously recording roof/floor converaence in mines working stratified deposits where ready access to the measurement site is possible. This instrument consists basically of a clock-work driver, a chart paper drum, and a spring-loaded scriber arm attached firmly to a 1-1/4-inch diameter inner steel tube, which is telescoped inside a 1-3/8-inch diameter tube. The tubes are connected and coupled between two pins located on expandable anchors set into a borehole drilled in the roof and floor. The tube must be located in the same vertical plane. When the roof and floor converge, the inner tube is pushed downward causing the scriber arm to trace a path over the pressure sensitive paper mounted on the slowly rotating drum. Therefore, the convergence is recorded with time on the rotating chart which can be set to revolve once in seven days. The direct plots of convergence versus time are obtained over a range of up to 5 inches (125 mm) to a resolution of 0.025 inch (0.5 mm) from the chart. The mechanisms are totally enclosed in a plexiglass housing to keep out dust and moisture while permitting inspection of the convergence trace (Figure 32).

Strain and Stress Recording Instruments

Six Irad Gage bonded strain gage load cells, model H-300, were attached to the roof with 1/2 inch in diameter and 2-foot long expansion roof bolts, tightened to 200-foot pound torque on the mine roof. The H-300 load cell is designed to measure tensile loads in rock bolts and tiebacks as well as compressive loads in steel supports. The basic load cell is rated to a maximum load of 300,000 pounds (136,000 kilograms).

The readings from the load cell are transmitted to a Vishay P-350A readout box. The P-350A digital strain indicator is designed primarily for use with resistance-type strain gages or strain gage devices to determine numerically the strain (and thus stress) in a structure or the output of a transducer. Figure 33 shows the complete system. Installation of a load cell is shown in Figure 34, and a view of an operating P-350A strain indicator is shown in Figure 35.

Summary of First Phase

The objective of this phase of the study was to assure successful application of the instruments and to evaluate the monitoring program used in the field for observing the surface blasting effects on the underground coal mine openings. Included in this program was the choosing of the instrument installation areas, the type of instruments to be used, and the type of information needed. Specifically stated, the most cost-effective and useful instrumentation that would best reflect the nature of vibrations and underground behavior was needed.

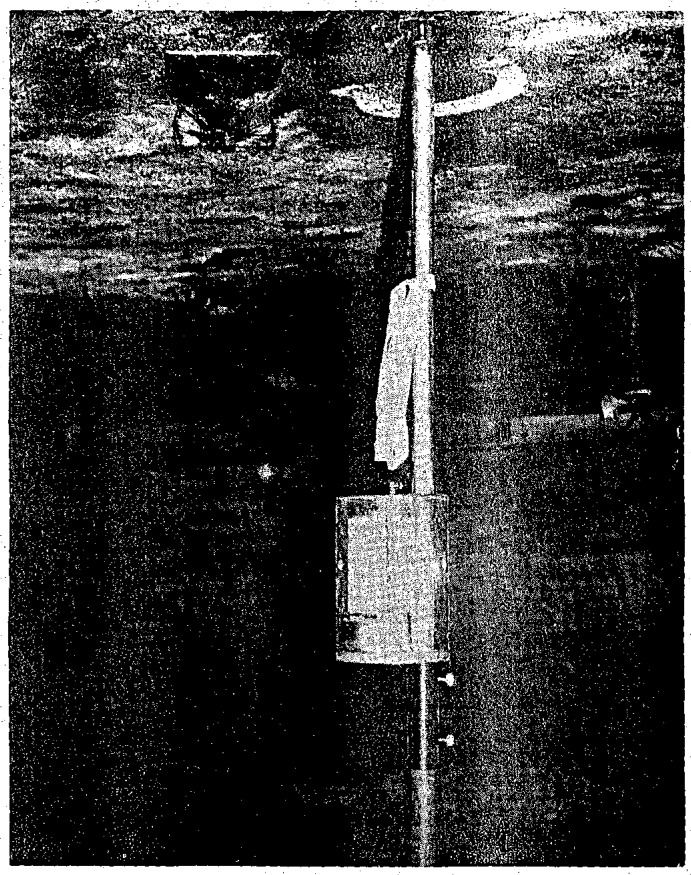

Figure 32. Irad gage direct recording convergence meter, DMC-2, with time chart installed in mine.

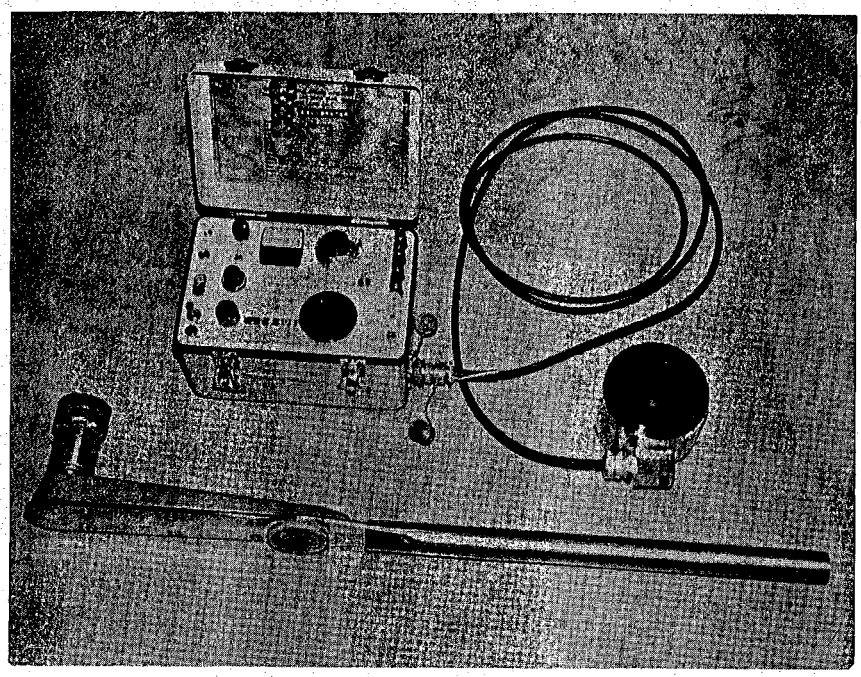

Figure 33. Irad gage H-300 load cell, P-350 strain indicator and torque wrench.

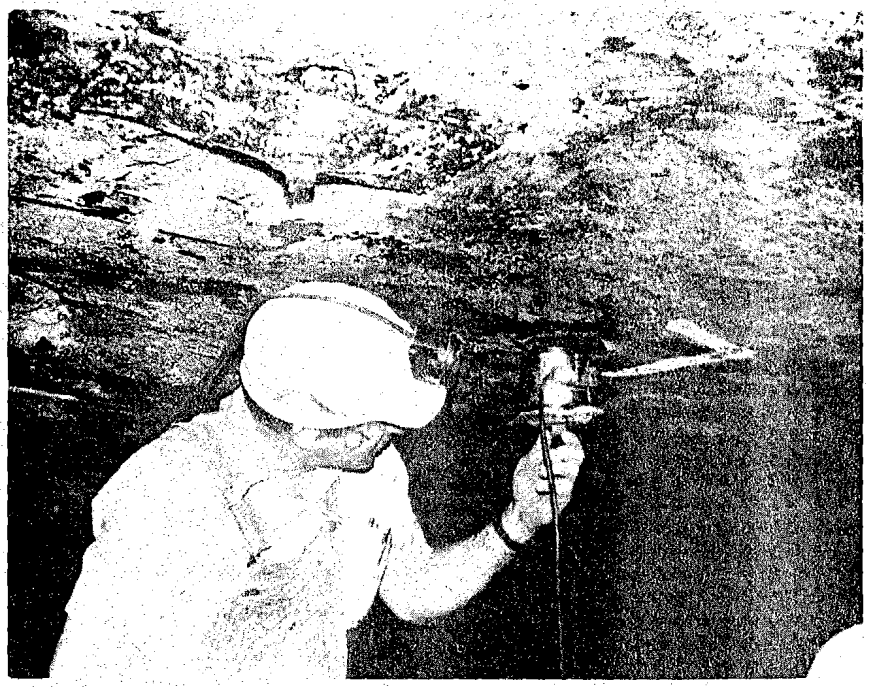

Figure 34. Load cell installation on mine roof.

Figure 35. Operating the Vishay P-350A strain indicator.

All of the portable velocity seismographs used in this study measured all three components of motion: vertical, radial, and transverse. Waveforms of the recordings of all three ground vibration components generated by a blast are recommended for the peak amplitude measurements; however, frequency may vary among the three traces. Peak or vector sum readings are adequate if only amplitude levels are desired, and it was found that the highest amplitude of vibration occurred at the center of the intersection of the underground opening.

The types of vibration recording instruments recommended are influenced by the frequencies generated by the blasting. Usually the observed frequencies ranged from less than 2 up to 150 Hz for surface blasting. The velocity seismographs used in this study have a flat response of frequency ranges from 2 to 200 Hz and would be adequate for most blasts monitored.

When researchers select a monitoring seismograph, documentation on the linearity of the frequency band should be requested, since small vibrations in frequency response can change output levels considerably. The vibration channels on the seismograph should be able to record a complete time history from which a peak measurement can be determined.

Two convergence meters were used in this study to measure the roof and floor movement and strata separation. The convergence meters were installed at the intersection of the underground mine to offer the least interference with underground mine operations and to obtain the expected maximum convergence. The drum recorders provided very little information helpful to this study. One of the convergence meters malfunctioned and the recording ability was destroyed by the humid condition on the mechanism during its operation. The other indicated that the magnitude of convergence measured prior to and after the blast was insignificant in the height of the mine opening.

Strain measurements made at three points in the mine roof from the load cells were transmitted to a strain gage. The static stresses were calculated from the strains multiplied by the elastic moduli of the load cells. The strain measurements were recorded prior to blasting, during blasting, and after blasting. None of the load cells provided conclusive readings during this phase of the study.

The instrumentation and monitoring technique developed in this phase of the study provided a means to establish more rational and effective monitoring programs for both short- and long-term effects of surface blasting.

Instrumentation Recording and Blasting Program - Final Phase

For the final phase of instrumentation and blasting the preparation of the site and the drilling of the blast holes was done in the same manner as in the first phase. Seventeen 6 3/4- inch diameter blast holes were drilled well into the bedrock. The drill hole pattern is shown in Figure 36 and the blasting sequence and data are presented in Table 4. Hole 4 was destroyed when hole 6 and 1 were shot. Hole 9 was a misfire and holes 14, 10 and 17 were not used. In contrast to the first phase blasting rounds, each round for the final phase blasting sequence consisted of one hole and each hole was fired individually.

The recording instruments used for the final phase consisted of seven portable Sprengnether seismographs (three model VS-1600's, two model VS-1100's) and two downhole meters (Bison and Mark Products). A schematic diagram showing the locations of the recording instruments installed for the final phase of the study are shown in Figure 37.

The response traces are produced by the seismograph by a light beam reflected on the moving strip light-sensitive paper in terms of transverse, vertical, and radial direction of measurement. Three vertically orthogonal time-synchronized components print the particle velocity. One of the traces is normally reserved for event marking or air blast monitoring. This fourth line was used to mark the arrival time of the propagation of blasting wave from the surface to the underground instrument and also to record the pressure in the coal pillar. A typical tracing of the recorded arrival time is shown in Figure 38.

Three tube-mounted strain gages, like the one shown in Figure 39, was specially designed and fabricated for the measurement of pressures in the coal pillar and installed at three different horizontal depths of 2 and 4 feet within the pillar. These were coupled and connected with strain indicators and recording module of the VS-1200 seismographs. This is shown in Figure 40. The responses were recorded on the event marking trace as shown in Figure 41 as well as recording of peak particle velocity from one of the three seismometers installed on the coal mine roof.

Three seismometers installed on the roof to record the ground vibrations were connected with three tube-mounted stress detectors that recorded the strain changes in terms of a dynamic stress. Figures 42 and 43 shows the installation of tube-mounted stress detector in the pillar and Figure 44 shows the instrument set-up for this part of the monitoring program.

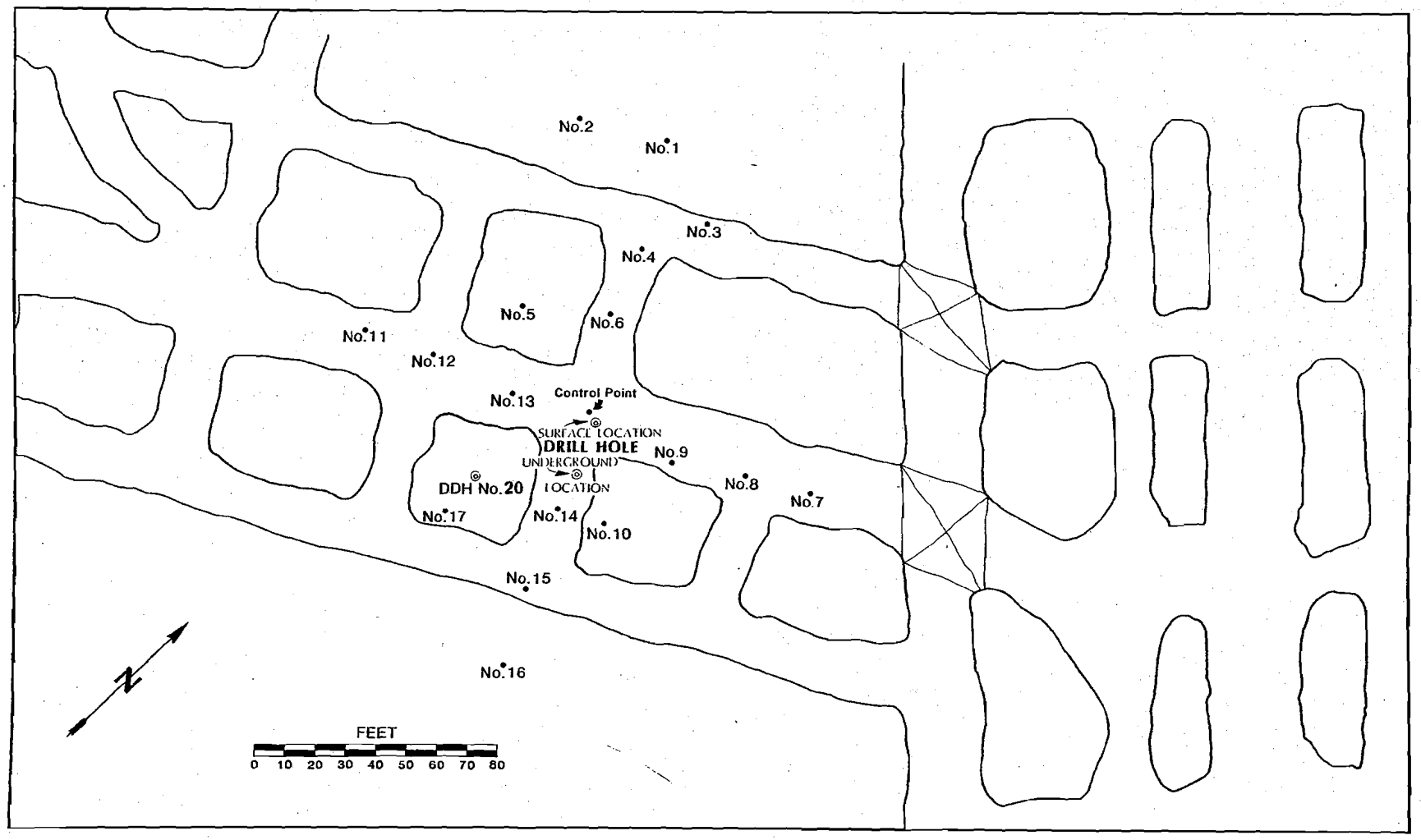

Figure 36. Diagram showing pattern of drillholes for Final Phase blasting.

Table 4. Data for Final Phase Blasting Sequence

Shot Number	Hole Number	Weight of Explosive (lbs)	Depth of Blasting Hole (ft)	Stemming Depth (ft)
1	6	204	43.0	31.5
2	1	305	45.5	22.0
3	6[a]	60	19.0	11.5
4	2	402	43.0	18.0
5	3	350	37.0	16.0
6	5	302	39.0	19.0
7[b]	9	203	52.0	33.0
8	7	305	52.0	18.0
9	8	431	52.0	28.0
10	12	203	25.0	15.0
11	11	153	42.0	28.0
12	13	207	46.0	22.0
13	15	121	48.0	34.0
14	16	272	48.0	30.0

a This hole reloaded and shot a second time.
b Misfired shot.

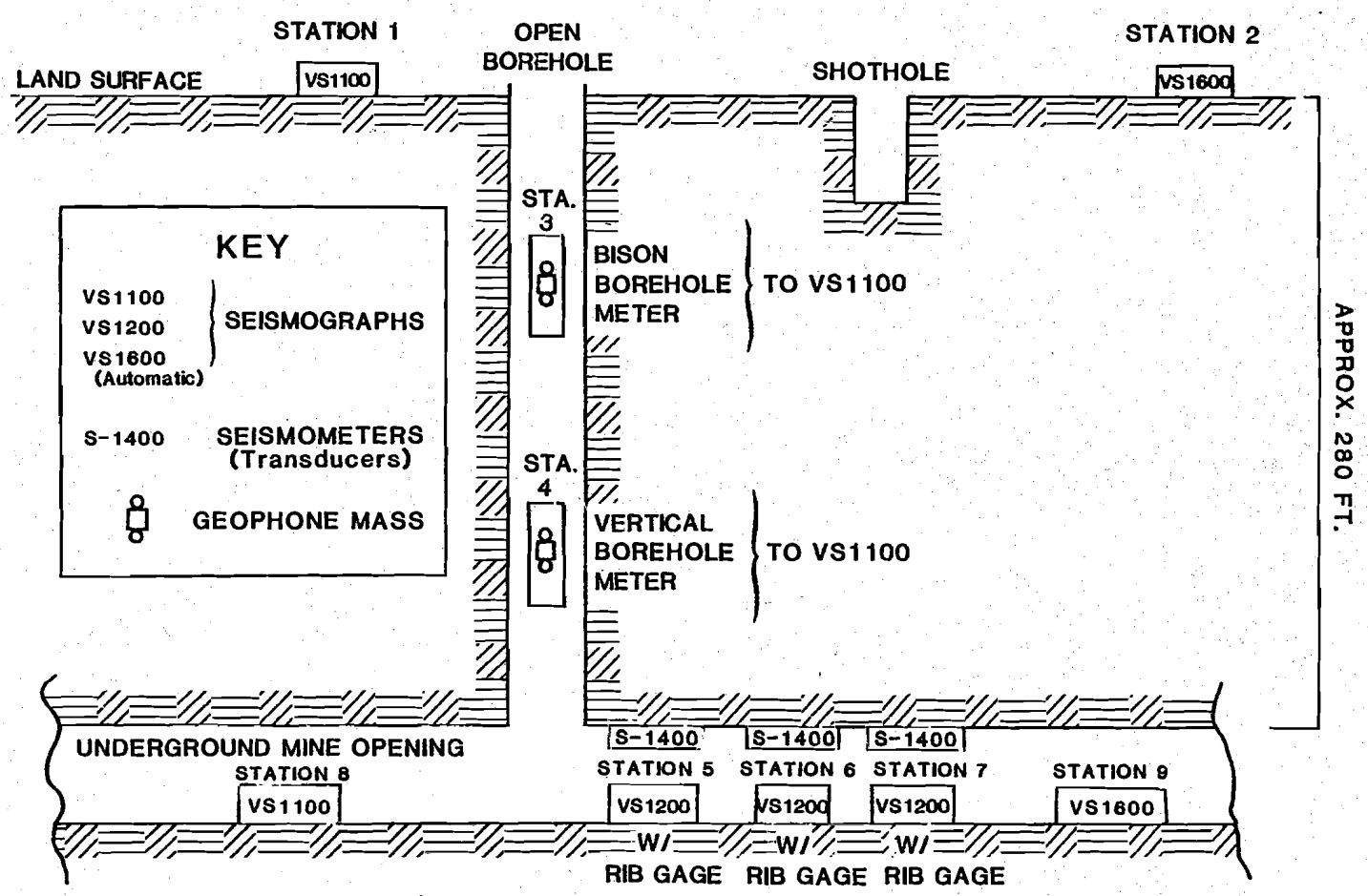

NOT TO SCALE

Figure 37. Schematic diagram showing instrumentation for final phase blasting sequence.

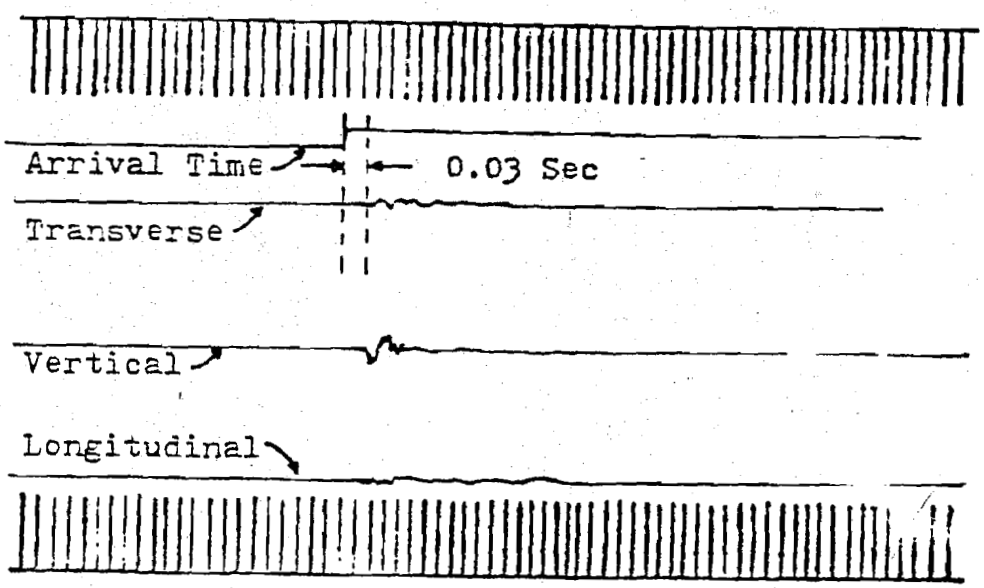

Figure 38. Recording of arrival time and peak particle velocity at station 2, shot 5.

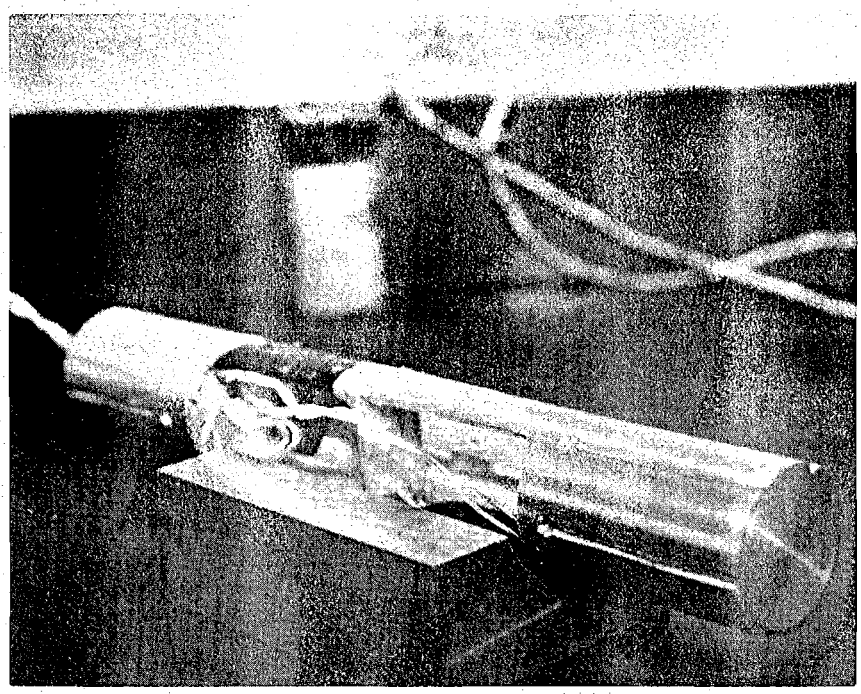

Figure 39. Tube mounted strain gage for measurement of pressures in coal pillar.

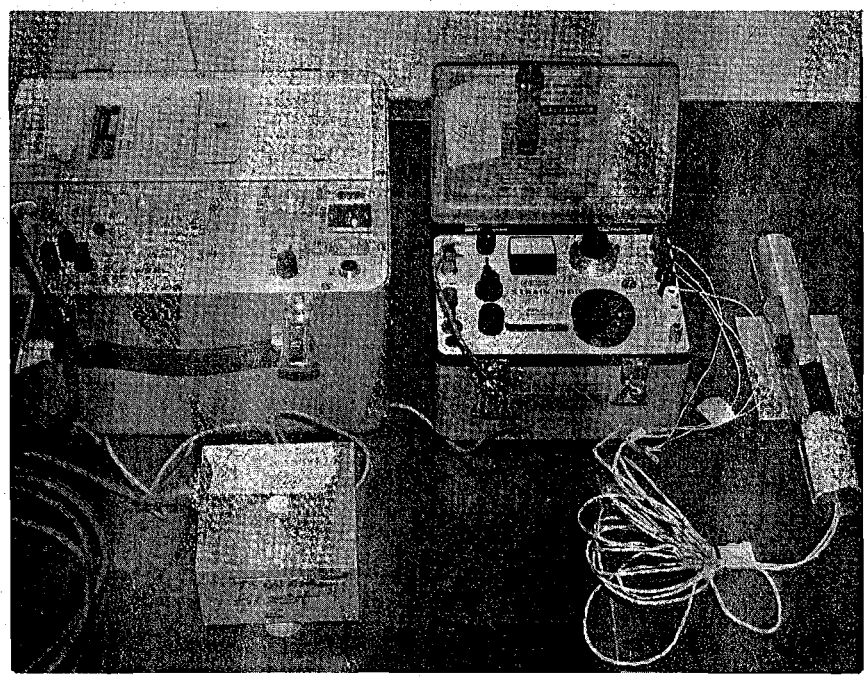

Figure 40. Complete set of instruments for combined recording of pressure and peak particle velocity.

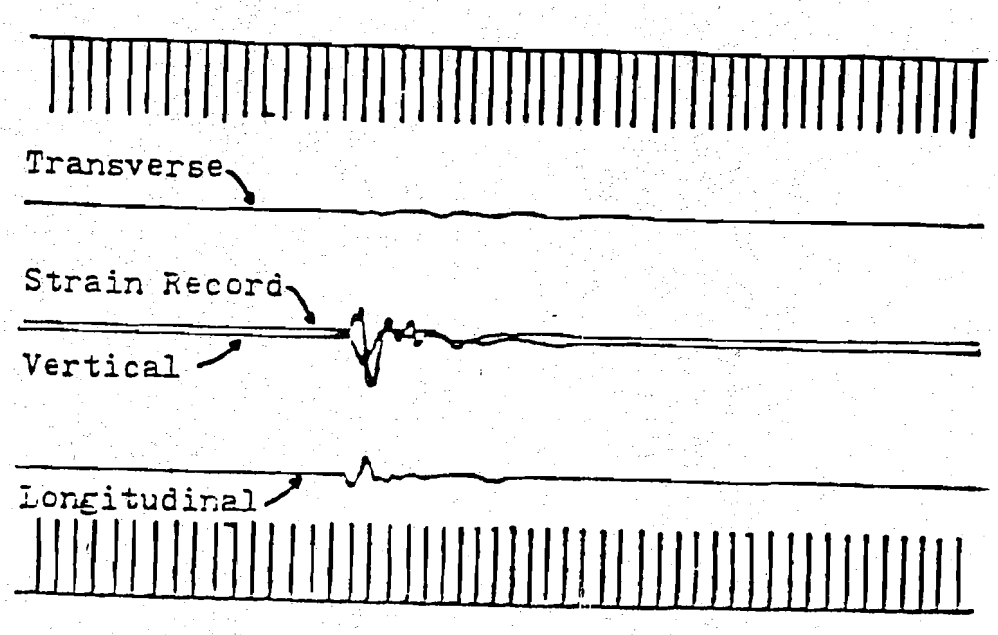

Figure 41. Recording of strain and peak particle velocity at station 6, shot 5.

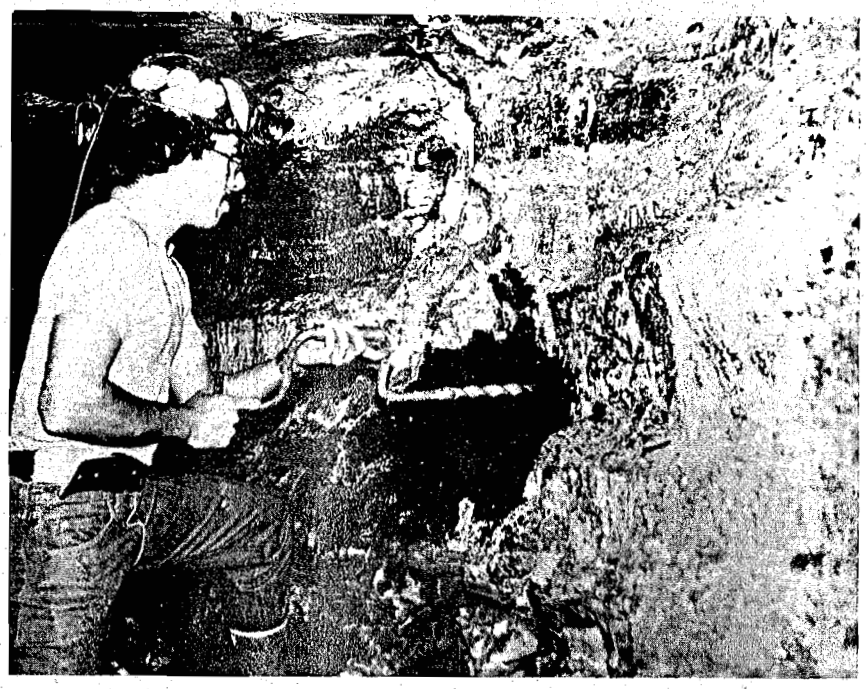

Figure 42. Drilling hole in pillar to install tube-mounted stress detector.

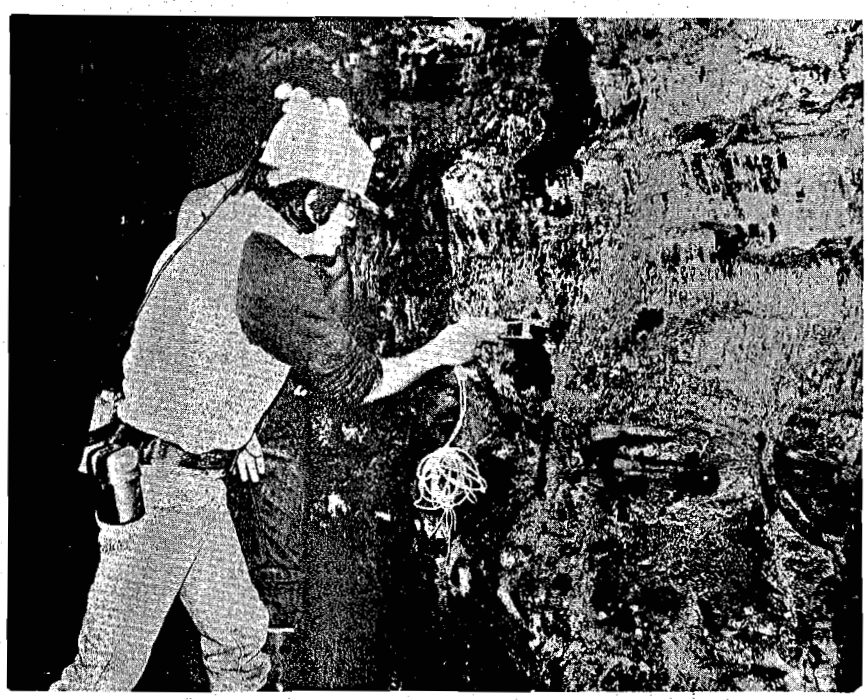

Figure 43. Inserting stress detector in pillar.

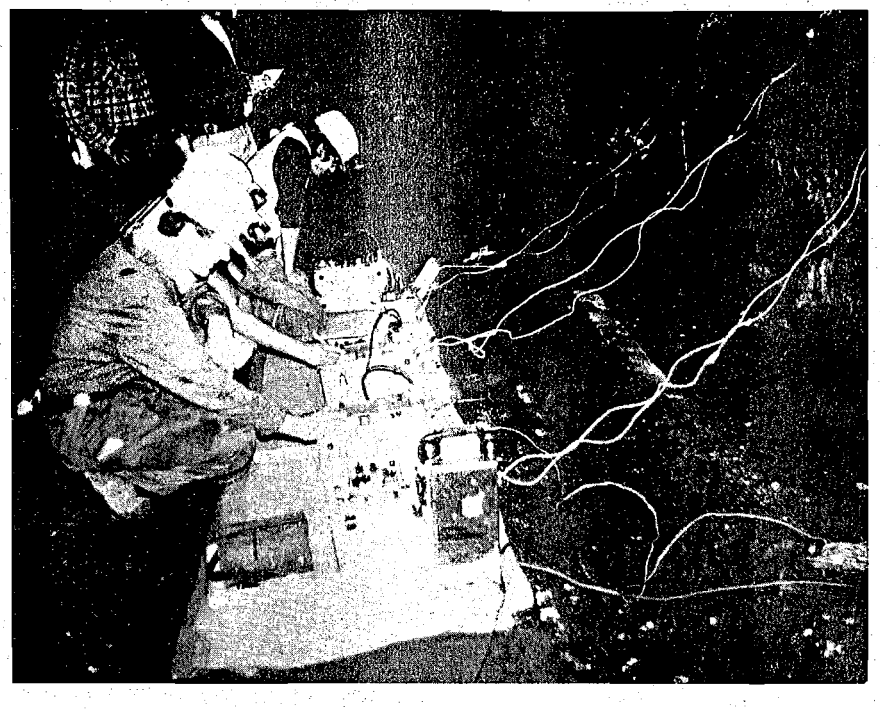

Figure 44. Instrument array for recording stress and vibration measurements in mine pillar.

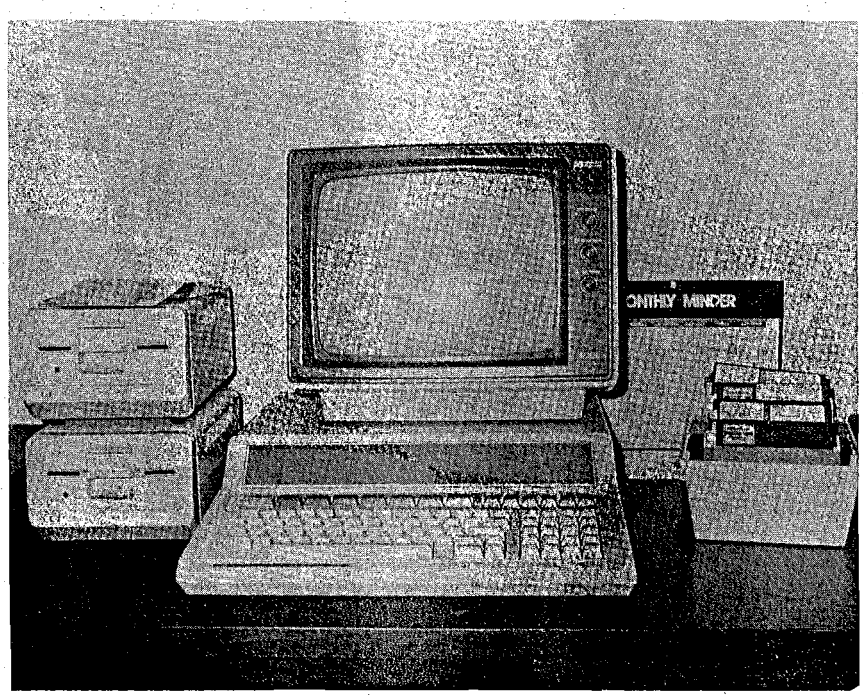

Figure 45. HP-86 computer system with two flexible disc drives used in analyzing vibration data.

DATA REDUCTION AND PROCESSING

The vibration data from the field responses were processed for the following purposes:

Maximum Response Spectrum Analysis
Fast Fourier Transform Analysis
Energy Spectral Density Analysis
Statistical Analysis for Scaled Distance Curve

The majority of the work involved with reduction and processing of data were done by a Hewlett-Packard HP-86 computer system with two flexible disc drives, a graphics plotter, a printer, and a digitizer, (Figure 45). To correlate the results, a UNIVAC 1100 digital computer along with a TEKTRONIX 4050 graphic system were used for digitizing the seismograms, the drawing of the response spectrum and other graphs, and calculating the Fourier transforms. All of the processed data are included in Appendices I and II in the latter parts of the report. These are:

APPENDIX I-A	Time History for Velocity, Acceleration and Displacement Frequency Spectrum (Magnitude) Frequency Spectrum (Phase) Energy Density Spectrum
APPENDIX I-B	Compiled Maximum Response Compiled Blasting and Vibration Data Scaled Distance Curve
APPENDIX I-C	Max-Max Response Spectrum
APPENDIX I-D	Time History and Maximum Response
APPENDIX I-E	Time Domain Data for Stresses in the Mine Roof

The programmed data are all presented in Appendix II for computer applications.

Data Presentation and Analysis

Maximum response spectrum is defined as the maximum response of a system for a prescribed ground vibration which is plotted against the natural frequency or period for various fractions of critical damping. It was assumed in this study that the subsurface rocks are elastic, homogeneous, and isotropic, and the maximum-maximum response spectrum was used for this analysis.

Fourier transform has been used to answer many questions relating to the nature of the data and has been useful in exhibiting the frequency content of the functions analyzed. The Fourier transform allows a periodic function to be expressed as an integral sum over a continuous range of frequencies. In order to reduce the time involved in computation, the Fast Fourier transform was used to determine the Fourier transform of blasting vibration waveforms by means of digital analysis techniques.

The instantaneous energy occurring in a given signal is usually taken as the square of the signal amplitude. The Energy Spectrum or Energy-density spectrum was provided for this analysis.

The calculation of structural response and Fourier spectrum depend upon the accuracy of the ground velocity measurement. The response spectrum curves involve the same basic type of response calculations that enter into the computation of a dynamic response of all types, and can thus logically form a systematic basis for an evaluation of the overall "effective" accuracy of the input ground motion.

The digitized data obtained from the study was considered as "uncorrected" in the sense that no corrections or adjustments were made during the digitization process. Recording and digitizing errors in the uncorrected seismograms fall into two general groups. The first group includes the errors occurring in the random variation. The second group contains flaws caused by instrumental operation. The corrections were made for the justification of ground velocity record only within this group.

Errors involved in group one are:

a) Errors caused by the imperfections in seismometer design
b) Errors resulting from indistinct tracing lines
c) Random errors occurring during the digitization process

These errors are more difficult to correct or cannot be corrected because they require extensive computational procedures not suitable for routine data processing:

Errors involved in group two are:

a) Errors due to the transverse play of the recording paper in the driving mechanism

b) Systematic errors generated by imperfect mechanical transverse mechanisms of the digitizing system

The first error in group two is corrected by using the digitized data of the time marks. The other errors may be corrected by using the instrument adjustment.

The peak particle velocities determined from uncorrected data are reduced according to the formula

$$\text{Peak particle velocity} = \frac{\text{Trace amplitude}}{\text{Gain x Factor Calibration}} \quad (1+0.0001 \times \text{Cable length})$$

Trace amplitude is the amplitude of particle velocity which has been digitized. The gain switch indicates the gain factor markings on different types of seismographs and was set at different types of positions during the recording and playback. Calibration factors were given by the manufacturer's specifications. The values of this factor for the downhole geophone (Bison) at Station 3 was 0.28, the borehole meter (Mark Products) at Station 4 was 0.16, the VS-1200 was 0.19, and the VS-1100 was 1.0. The signal reduced by the resistance of the cable was ignored because it was considered too small.

For a seismometer, the natural frequency is low compared to the vibration frequency to be measured. The ratio of these two frequencies approaches a large number and the relative displacement approaches the displacement of the motion of the ground. Therefore, the mass designed in the seismometer remains stationary while the supporting mechanism moves with the vibrating body. This means that the measured particle velocity is close to that of the particle velocity of the ground, and the responses of ground vibrations approximate the real particle velocity. Therefore, it is not necessary to make any instrumental adjustment on the vibration records.

The peak particle velocities with some of the corrections are shown in tables 5, 6, and 7. Some shot data are missing in these tables because of indistinguishable vibration responses.

Statistical Analysis

Whenever a safety level of ground vibrations from blasting is considered it is necessary to predict the vibration levels for a given blasting operation. This involves several parameters such as the distance from shot to the monitoring station, charge weight, and geological conditions at the site. It is reasonable to expect, however, the vibration level will be raised with increasing charge size and diminish with increasing distance from the blast. A generally accepted form associated with these parameters are as follow:

$$V = H\left(\frac{D}{W^{\alpha}}\right)^{\beta}$$

Table 5. Vibration Data - Surface

Hole Number	Shot Number	Charge Weight (lb.)	Station	Slant Distance[a] (ft.)	Scaled Distance $ft/lb^{1/2}$	Scaled Distance $ft/lb^{1/3}$	Peak Particle Velocity, (in/sec.) T	V	L
6	1	204.0	1	801.02	56.08	136.07	.080	.079	.042
			2	146.45	10.25	24.88	.990	.380	1.920
1	2	305.0	1	825.90	47.29	122.70	.040	.079	.038
2	4	402.0	2	199.08	9.97	27.07	2.540	2.880	3.940
3	5	350.0	2	186.81	9.99	26.51	2.080	3.420	3.540
5	6	302.0	1	1200.80	69.10	178.98	.045	.135	.083
			2	137.24	7.90	20.46	3.830	4.570	5.900
7	8	305.0	1	1250.84	71.98	186.44	.046	.068	.038
8	9	431.0	1	1250.87	60.25	165.60	.073	.128	.106
			2	147.00	7.08	19.46	1.110	4.420	6.970
12	10	203.0	1	1338.74	93.96	227.79	.046	.068	.038
			2	60.91	4.28	10.36	4.520	6.410	6.540
14	11	153.0	1	1313.70	106.21	245.62	.015	.020	.090
			2	73.00	5.90	13.65	.350	1.060	1.800
13	12	207.0	1	1231.93	85.63	208.26	.025	.084	.065
			2	125.00	8.69	21.13	1.980	2.350	5.010
15	13	121.0	2	122.10	11.09	24.67	1.540	2.340	3.530
16	14	272.0	1	1231.85	74.65	190.12	.035	.117	.077
			2	127.30	7.72	19.65	3.150	2.010	3.060

a. Distance between the shot point and control station.

Table 6. Vibration Data- Underground Mine Roof

Hole Number	Shot Number	Charge Weight (lb.)	Station	Slant Distance[a] (ft.)	Scaled Distance ft/lb$^{1/2}$	Scaled Distance ft/lb$^{1/3}$	Peak Particle Velocity, (in/sec.) T	V	L
6	1	204.0	5	257.80	18.05	43.79	.318	1.320	.326
			6	259.08	18.14	44.01	.550	1.880	.200
1	2	305.0	5	250.26	14.33	37.18	.066	.122	.045
			6	251.61	14.41	37.38	.060	.094	.035
			7	235.73	14.53	37.69	.022	.173	.040
6	3	60.0	5	235.25	30.37	60.09	.014	.066	.026
			6	235.42	30.39	60.13	.007	.061	.005
			7	236.16	30.49	60.32	.004	.067	.006
2	4	402.0	5	253.32	12.68	34.32	.085	.144	.048
			6	254.22	12.68	34.35	.079	.178	.054
			7	256.65	12.80	34.77	.029	.198	.053
3	5	350.0	5	251.40	13.44	35.67	.065	.256	.036
			6	253.50	13.55	35.97	.087	.245	.024
			7	254.26	13.59	35.60	.023	.259	.024
5	6	302.0	5	238.85	13.74	35.60	.062	.308	.031
			6	241.77	13.91	36.04	.054	.251	.054
			7	239.77	13.80	35.74	.027	.248	.044

Table 6. (cont.)

Hole Number	Shot Number	Charge Weight (lb.)	Station	Slant Distance[a] (ft.)	Scaled Distance ft/lb$^{1/2}$	Scaled Distance ft/lb$^{1/3}$	Peak Particle Velocity, (in/sec.) T	V	L
7	8	305.0	5	252.96	14.48	37.58	.026	.170	.037
			6	244.99	14.03	36.40	.045	.176	.020
			7	242.57	13.89	36.04	.020	.220	.048
8	9	431.0	5	235.87	11.36	31.23	.039	.430	.047
12	10	203.0	5	249.80	17.53	42.50	.075	.133	.048
			6	248.05	17.41	42.21	.053	.117	.089
11	11	153.0	5	242.23	19.58	45.29	.014	.069	.023
			6	240.90	19.48	45.04	.025	.055	.018
			7	247.38	20.00	46.25	.031	.088	.013
13	12	207.0	5	230.56	16.03	38.98	.045	.233	.046
			6	229.58	15.96	38.81	.028	.211	.049
			7	230.40	16.01	38.95	.031	.209	.023
15	13	121.0	5	235.52	21.41	47.62	.016	.090	.010
			6	233.80	21.25	47.27	.013	.089	.020
			7	241.19	21.93	48.76	.008	.111	.019
16	14	272.0	5	244.64	14.83	37.76	.075	.147	.031
			6	242.25	14.69	37.39	.061	.126	.062
			7	244.65	14.83	37.76	.017	.204	.076

a. Distance between the shot point and control station.

Table 7. Vibration Data-Underground Mine Floor

Hole Number	Shot Number	Charge Weight (lb.)	Station	Slant Distance[a] (ft.)	Scaled Distance ft/lb$^{1/2}$	Scaled Distance ft/lb$^{1/3}$	Peak Particle Velocity, (in/sec.) T	V	L
6	1	204.0	8	241.37	16.90	41.00	.250	.900	.200
1	2	305.0	8	257.20	14.73	38.21	.200	.300	.300
2	4	402.0	9	260.25	12.98	35.26	.300	.250	.300
3	5	305.0	8	273.78	15.68	40.67	.100	.350	.070
			9	260.45	13.92	36.96	.300	.400	.250
5	6	302.0	8	277.01	15.94	41.29	.120	.470	.140
			9	244.77	14.08	36.48	.200	.350	.250
7	8	305.0	9	249.05	14.26	37.00	.150	.250	.250
8	9	431.0	8	241.22	11.62	31.93	.090	.600	.130
			9	242.2	11.67	32.07	.250	.500	.200
12	10	203.0	8	253.66	17.80	43.16	.250	.300	.150
			9	270.60	18.99	46.04	.180	.270	.070
11	11	153.0	9	265.96	21.50	49.73	.060	.160	.160
13	12	207.0	8	236.06	16.41	39.91	.150	.200	.100
15	13	121.0	8	241.05	21.91	48.74	.100	.200	.150
			9	282.72	25.70	57.16	.040	.120	.060
16	14	272.0	8	249.12	15.11	38.45	.150	.350	.200
			9	296.02	17.95	45.69	.070	.350	.140

a. Distance between the shot point and control station.

where V is the peak particle velocity, W the charge weight, D the slant distance, and H, α , and β are constants in terms of a given site or shooting procedure. The constants can be determined by linear regression analysis.

In the linear regression analysis, both square root and cube root scaling factors are used to calculate a trend line by computing the scaled distance. One of the standard assumptions made in the analysis (Draper and Smith, 1966; and Chatterjee and Price, 1977) is that the model which describes the data is to be linear.

Some suitable values were found in the literature for the scaling factors (Nichols, 1964 and Olson, et. al. 1970). These reports recommended that the cube root scaling provided the best grouping for an underground mine opening for the vibration measurements and square root scaling was suitable for surface measurements. The grouped data in terms of cube and square root are listed in Tables 8, 9, and 10. The results from the study closely match the recommendations from these reported and the surface regression line has better grouping for square root, and the underground regression line for cube root. Figures 46, 47, and 48 show the 95-percent confidence interval data for the surface, underground, mine roof, and mine floor, respectively.

Borehole Meter and Other Responses

The response from Station 3 was generally smaller than that of Station 4. It was reasonable to assume that a wave propagates as a vector-wave train. The vertical component of a vector wave depends upon the point of the wave front's spherical surface. When the wave propagates evenly through the media from a detonation point, the vectors at any point on a spherical wave-front surface have the same magnitude, with the directions perpendicular to the tangential plane at this particular point. If the location of a point is closer to the surface plane, a smaller value of the vertical component can be expected. It was assumed that the propagation media were isotropic and homogenous.

To illustrate this, a two-dimensional plane was adopted as shown in Figure 49. The figure shows the relative location of various points under consideration where S is the blasting point, B is the borehole meter at Station 3 and C is Station 5. The line BC represents the open borehole which was drilled down to the coal mine roof. The value of the vertical component at point B is directly proportional to that at point B. The relationship can be expressed as:

$$\text{Correction Factor} = \frac{\sin(\Theta_1)}{\sin(\Theta_2)}$$

The corrected results for Station 3 are presented in Table 11. The computer programs for correcting and plotting the response data are included in Appendix II. The response of shot 8 at Station 3 was chosen for programming purposes.

Table 8. Linear Regression Data for Surface

α	H	β	F (Distribution Ratio)	Percentage Variation	P (Tail of Distribution Graph)
1/2	74.19	-1.65	349.75	87.77 %	.0000
1/3	321.99	-1.64	357.01	86.65 %	.0000
1/2a	79.36	-1.66	376.89	88.94 %	.0000
1/3a	348.59	-1.64	342.22	87.48 %	.0000

a The data for Shot 1 and 3 are not included.

Table 9. Linear Regression Data for Mine Roof

α	H	β	F (Distribution Ratio)	Percentage Variation	D (Tail of Distribution Graph)
1/2	0.04	.55	1.102	3.23 %	.3014
1/3	0.01	.89	1.25	3.64 %	.2721
1/2a	40.98	-2.03	37.05	56.96 %	.0000
1/3a	24194.12	-3.26	44.63	61.45 %	.0000

a The data for Shots 1 and 3 are not included.

Table 10. Linear Regression Data for Mine Floor

α	H	β	F (Distribution Ratio)	Percentage Variation	D (Tail of Distribution Graph)
1/2	11.11	-1.46	16.49	24.08 %	.0002
1/3	442.21	-2.09	17.54	25.22 %	.0001
1/2a	12.02	-1.50	20.01	29.04 %	.0000
1/3a	450.61	-2.11	20.21	29.20 %	.0000

a The data for Shots 1 and 3 are not included.

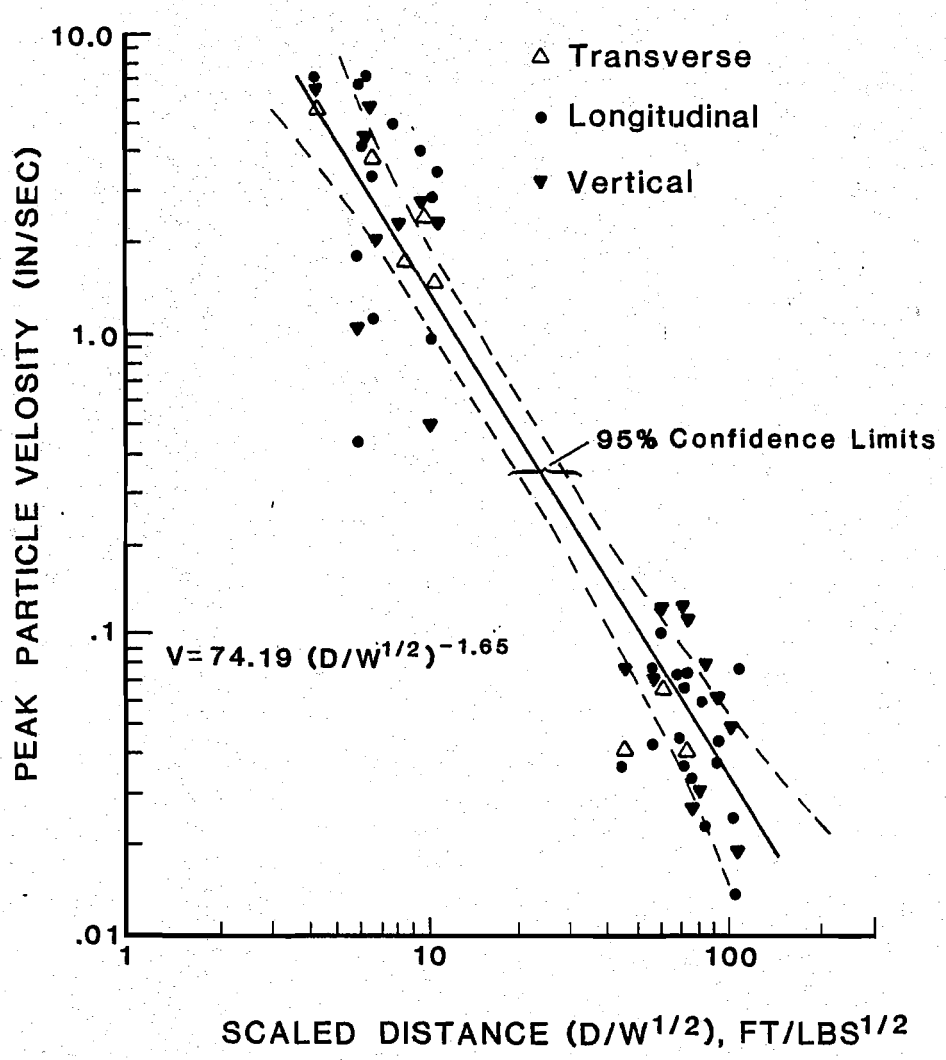

Figure 46. Linear regression curve for the surface with scaling factor of 1/2.

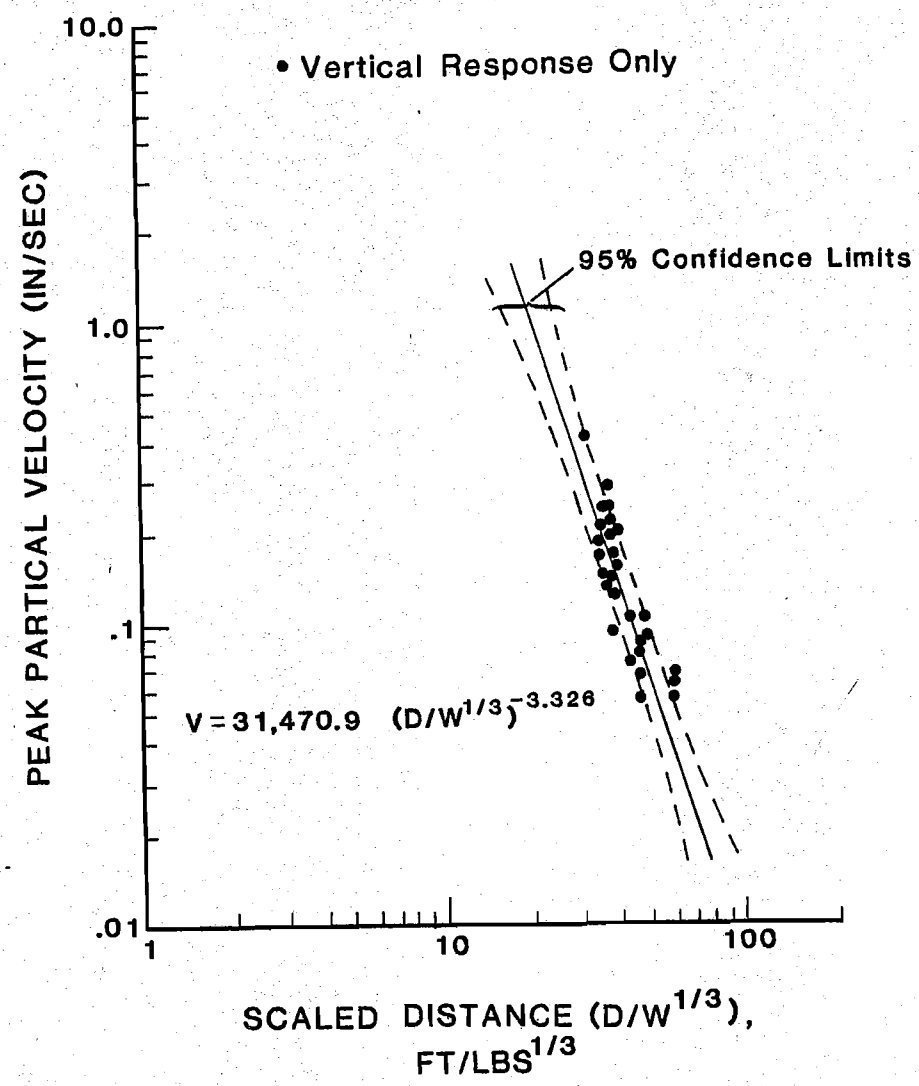

Figure 47. Linear regression curve for the underground mine roof with scaling factor of 1/3.

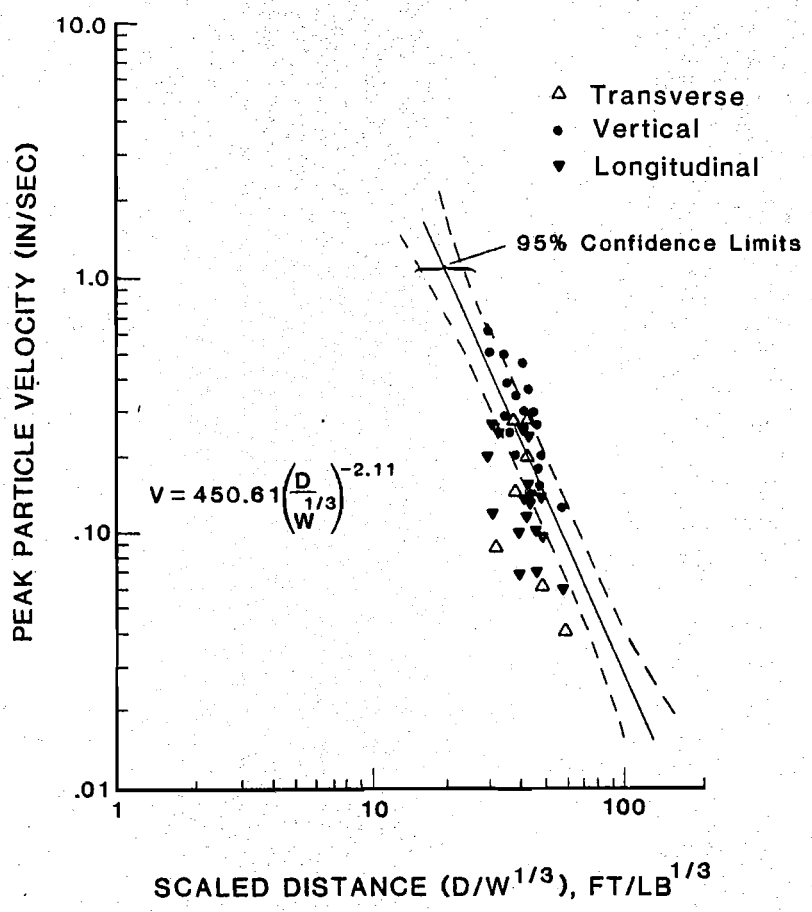

Figure 48. Linear regression curve for the underground mine floor with scaling factor of 1/3.

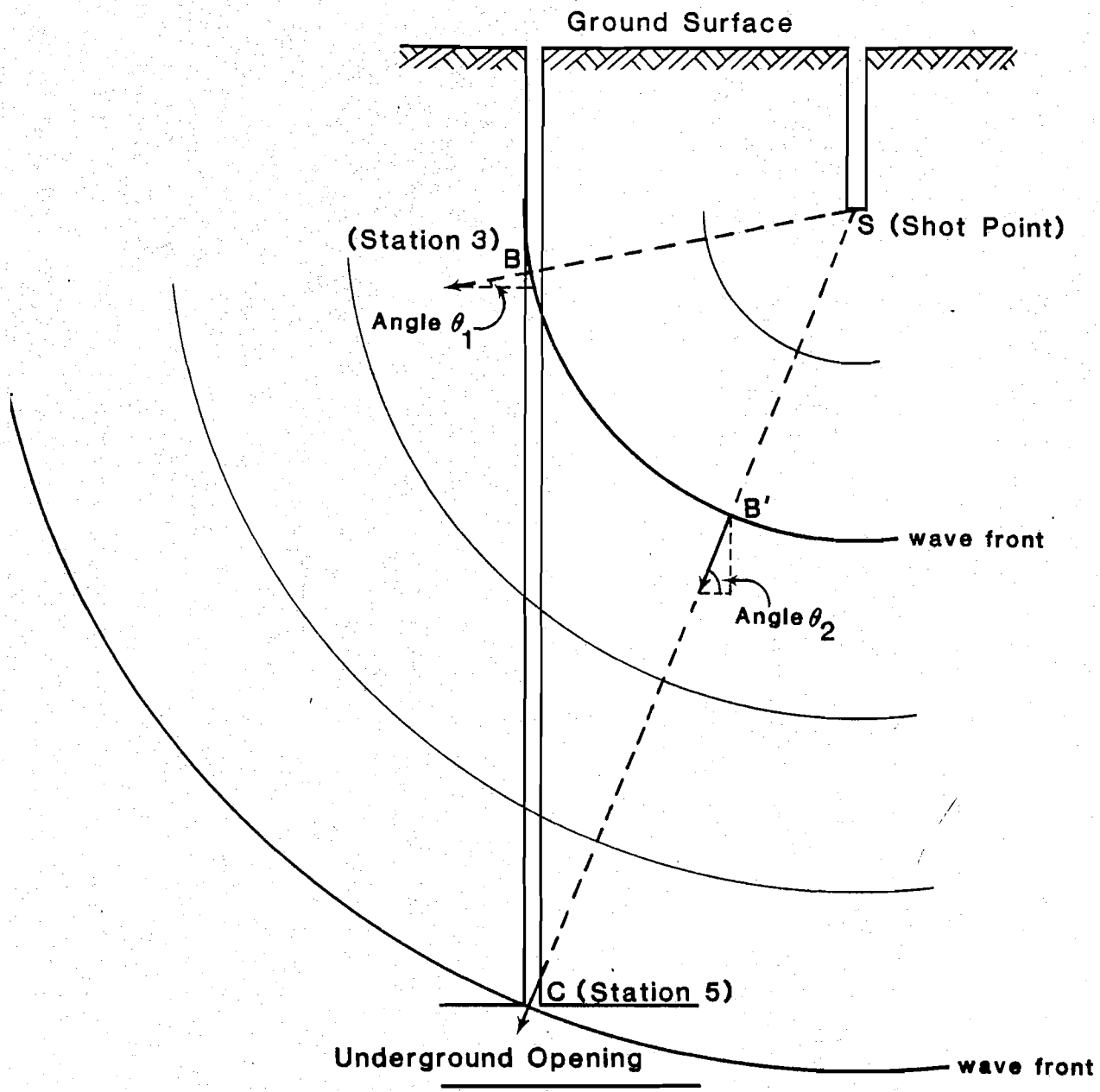

Figure 49. Two-dimensional plane view showing locations of shot point(S), Station 3 (B), and Station 5 (C).

Table 11. Vibration Data - Station 3 After Correction

Hole Number	Shot Number	Charge Weight (lb.)	Slant Distance (ft.)	Scaled Distance $ft/lb^{1/2}$	Scaled Distance $ft/lb^{1/3}$	Peak Particle Velocity, (in/sec.) Vertical
1	2	305.0	94.61	5.417	14.055	1.170
2	4	402.0	97.79	4.877	13.239	1.820
3	5	350.0	73.66	3.937	10.452	3.400
5	6	302.0	45.05	2.59	6.715	2.380
7	8	305.0	79.26	4.538	11.775	5.370
8	9	431.0	57.50	2.773	7.620	7.000
12	10	203.0	89.53	6.271	15.203	4.320
11	11	153.0	64.13	5.185	11.990	2.310
13	12	207.0	29.53	2.052	4.992	1.700
15	13	121.0	65.71	5.974	13.285	2.360
16	14	272.0	81.09	4.917	12.515	4.380

After correcting the digitized velocity data, direct integral and differential methods were performed to obtain the displacement, velocity and acceleration and an example is shown in Figure 50. The maximum values of these served as a boundary for this particular measured blasting vibration. The safety level may be determined according to the maximum quantity. This is shown in Figure 51 as the response spectrum between the defined damage level at the surface and maximum response for a given blast in an underground mine.

A result of Fast Fourier Transform (FFT) is shown in Figure 52. According to the results of FFT, the maximum amplitude occurs at a constant value of frequency. The maximum amplitude decreases with increasing distance. Figures 53 and 54 show the Fourier transforms of Shot 6 at Stations 1 and 2 on the surface respectively. Both maximum values appear at 9.8 Hz. The frequency underground was small compared to the values obtained on the surface. These are compared in Figures 53, 54, and 55. If this phenomena is true, the damage level could be defined as a maximum amplitude of the Fourier transform and its particular frequency domain. The ratios of the total energy between stations 3 and 5 for all shots are listed in Table 12. Theoretically, these values are supposed to be equal to each other, however, the total energy ratios varied from 1.75 to 4.78 indicating the nonuniformity of the different overlying rock layers.

COMPUTER SIMULATION PROGRAM FOR DYNAMIC ANALYSIS

A computer program for the study of stress and stability analysis of underground mine openings was available for adaptation to this research at The University of Alabama Seebeck Computer Center. The program on file is called DYNON (Dynamic Nonlinear Analysis) and utilizes the finite element method (Brown and Hayatdavoudi, 1980). There are a number of reports published on the finite element method, detailing the methodology and procedures (listed in references). For the computer simulation program in this study, the DYNON program was used. Rectangular-shaped elements were incorporated into a finite element mesh for this analysis and a complete scheme of this analysis is shown in Figure 56. The mesh area was discritized into 181 elements with 210 joints. The underground opening is shaded on the mesh and is not considered an element.

The geometry, size, and number of elements are arbitrary decision and depend upon the user's discretion and "feel" for the situation. In this instance it was believed that the shock wave generated by the detonation would attenuate rapidly as it penetrated and passed through the successive layers of rock in the subsurface. Therefore, 600 feet was chosen as the horizontal limiting boundary and approximately 250 feet was chosen as the limiting boundary below the detonation point.

The purpose of the program is to enable one to evaluate the stresses around the underground opening (shaded) element, particularly the contiguous elements 55, 68, and 69. To analyze the stresses in the configuration by the finite element method, joints numbered 1 through 15 were restrained in both directions, horizontally and vertically. In addition, the horizontal movement of the joints numbered 16 through 196, were also restrained. These joints are shown along the left of the finite element mesh.

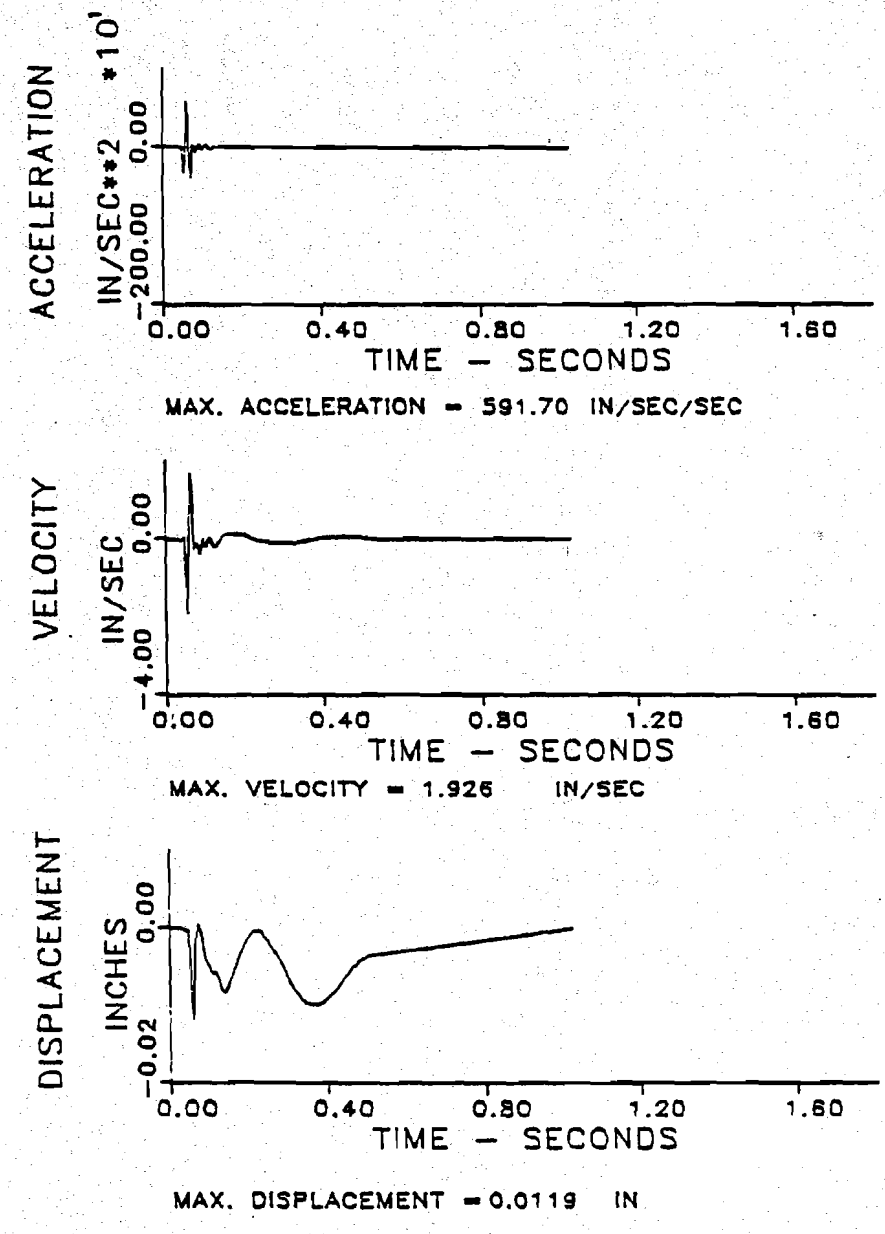

Figure 50. Corrected results of particle acceleration, velocity, and displacement for Shot 8 at Station 3 (see figure 49).

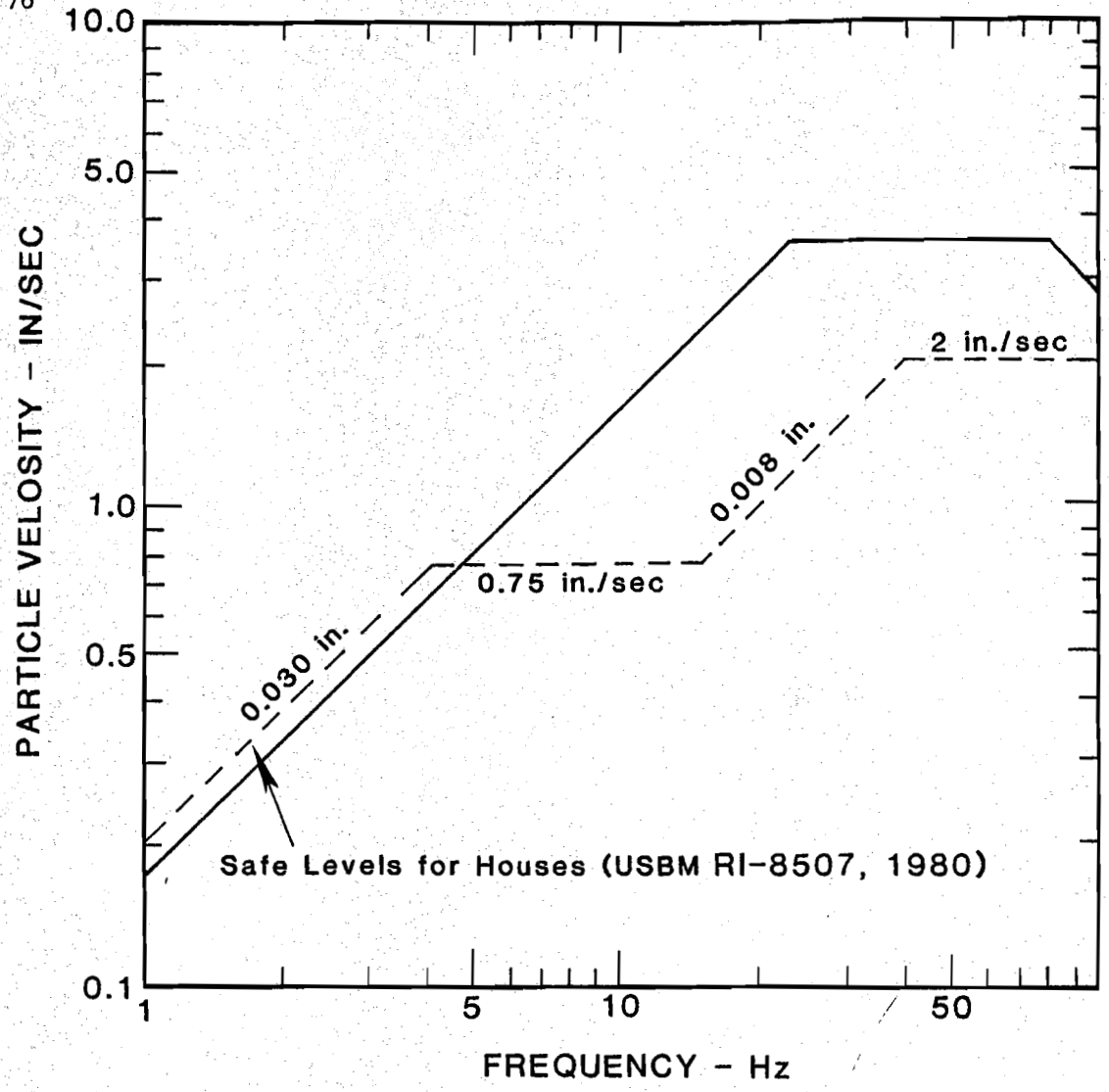

MAXIMUM DISPLACEMENT	.0224 Inches
MAXIMUM VELOCITY	3.591 In/Sec
MAXIMUM ACCELERATION	1638.5288 In/Sec/Sec

Figure 51. Maximum response spectrum for Shot 8 at Station 3 (see Figure 49).

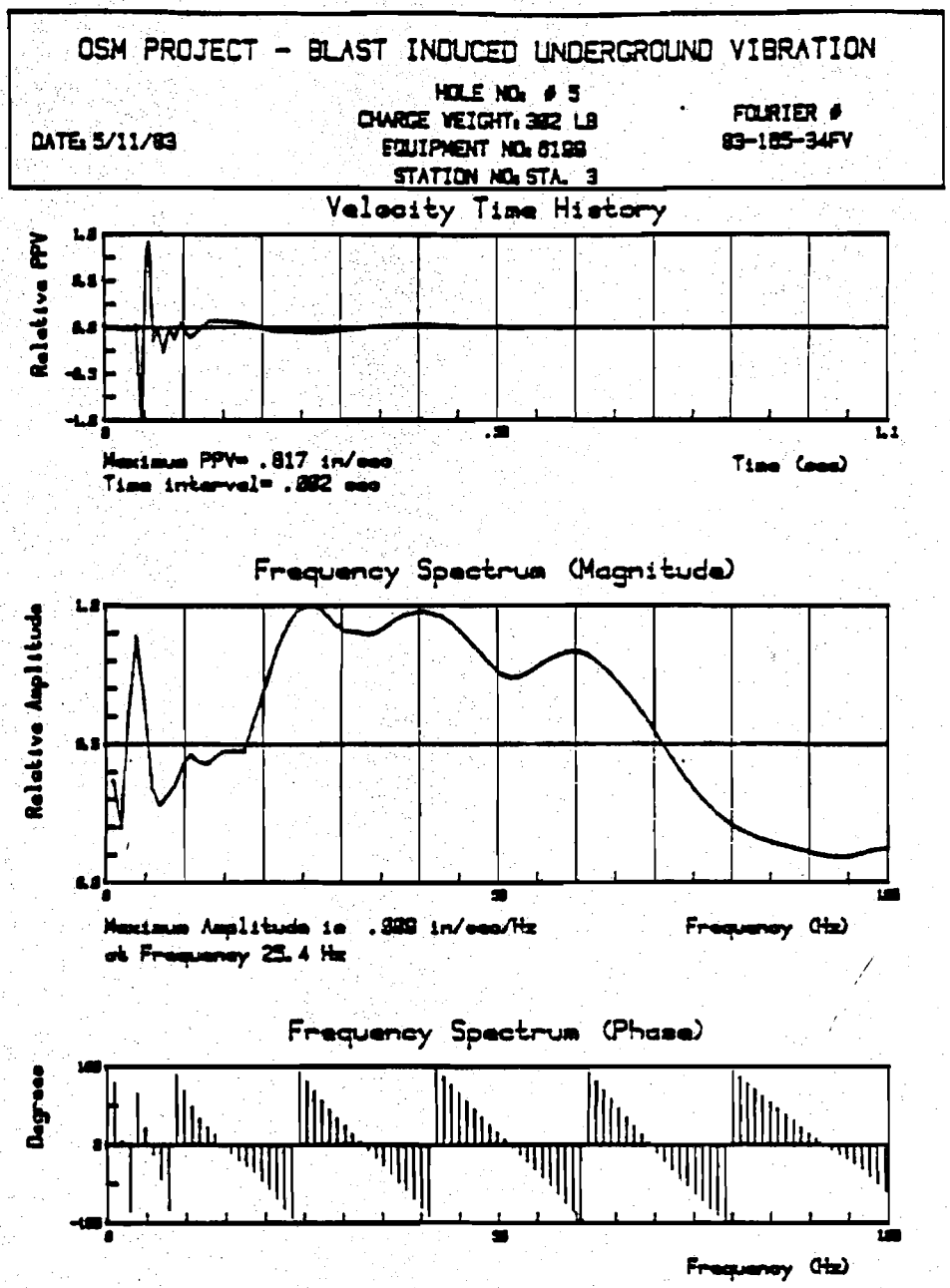

Figure 52. Fast Fourier Transform for Shot 6 at Station 3 (see Figure 49).

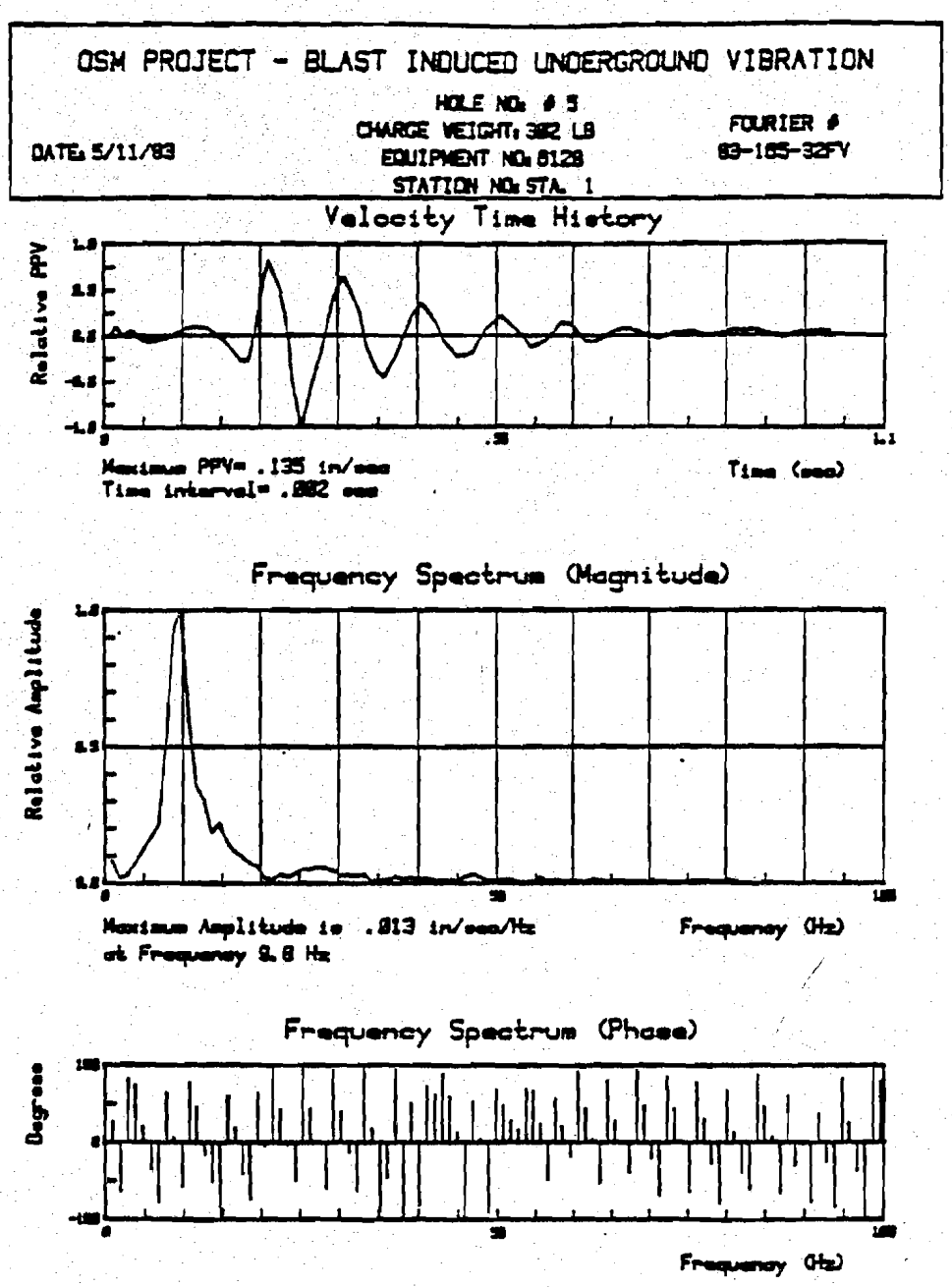

Figure 53. Fast Fourier Transform for Shot 6 at Station 1 (see Figure 49).

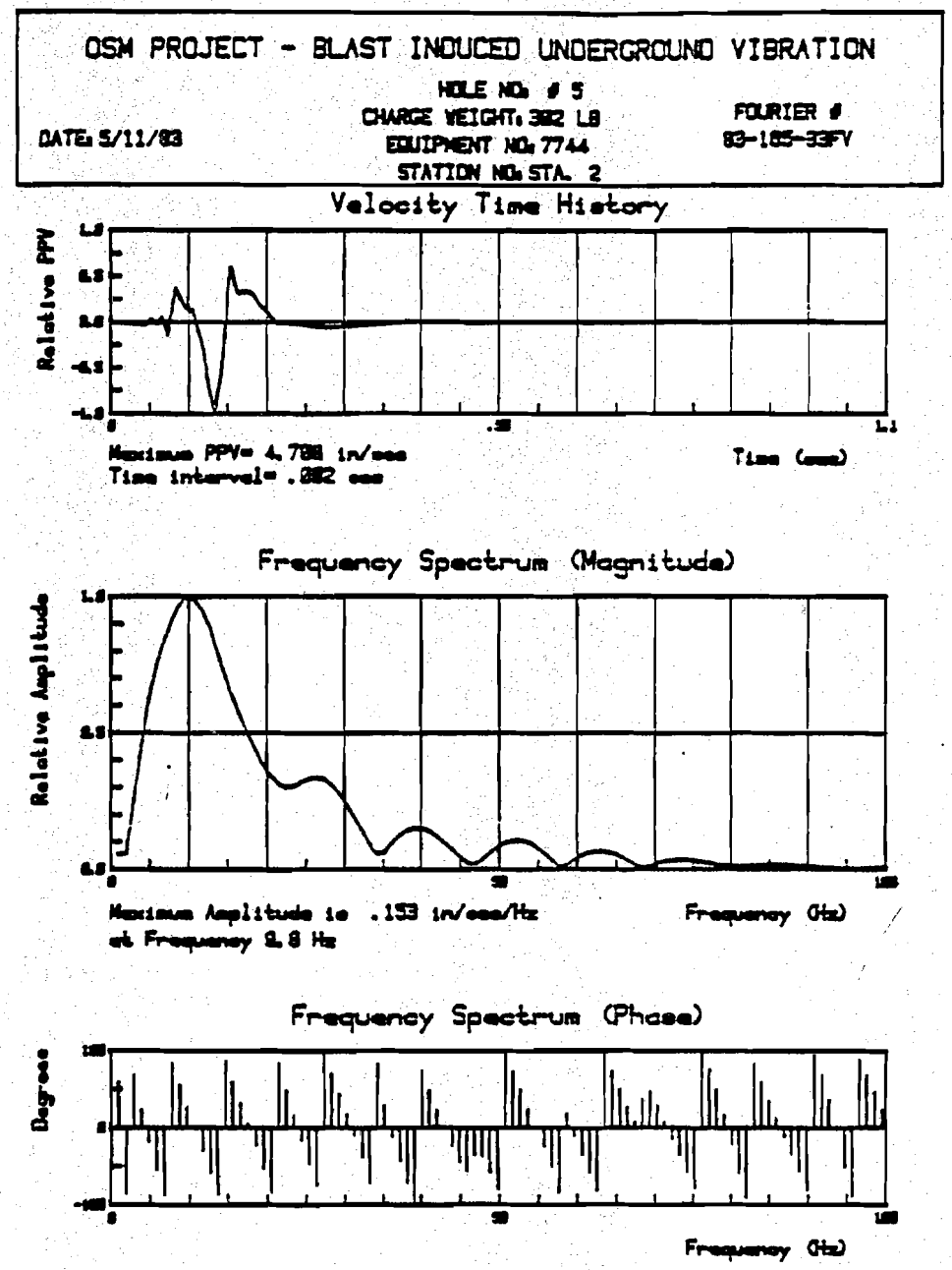

Figure 54. Fast Fourier Transform for Shot 6 at Station 2 (see Figure 49).

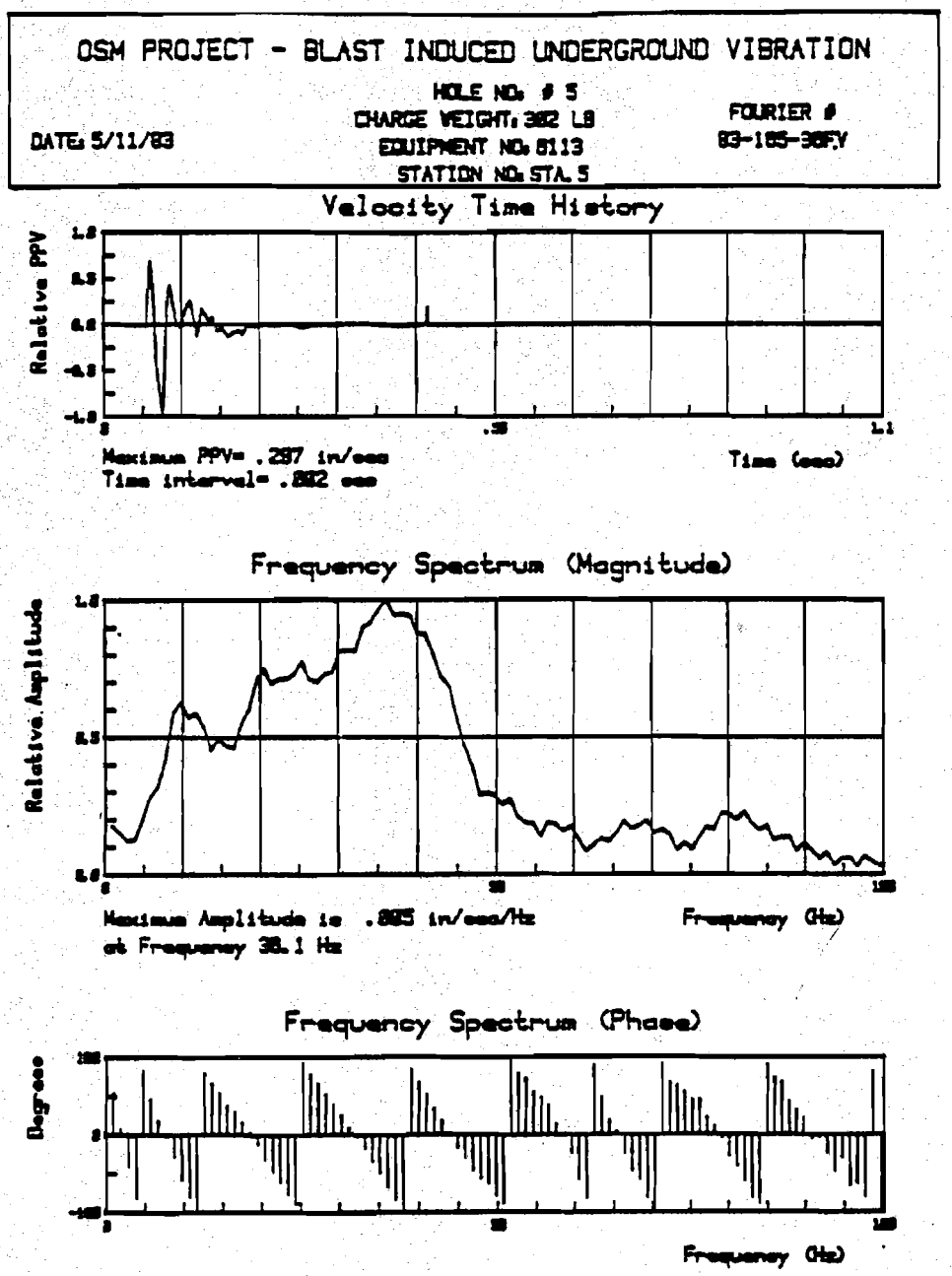

Figure 55. Fast Fourier Transform for Shot 6 at Station 5 (see Figure 49).

Table 12. Energy Ratios for Stations 3 and 5 (see Figure 49)

Shot Number	Total Enery		Energy Ratio
	Station 3	Station 5	
1	.04564	.01278	3.57
2	.04625	.00016	290.0
3	.00054	.00031	1.75
4	.02166	.00025	88.0
5	.03783	.00048	78.0
6	.02092	.00060	34.6
8	.06932	.00014	478.0
9	.13299	.00127	104.0
10	.04246	.00021	199.8
11	.01633	.00015	108.0
13	.00435	.00006	66.3
14	.04377	.00019	233.8

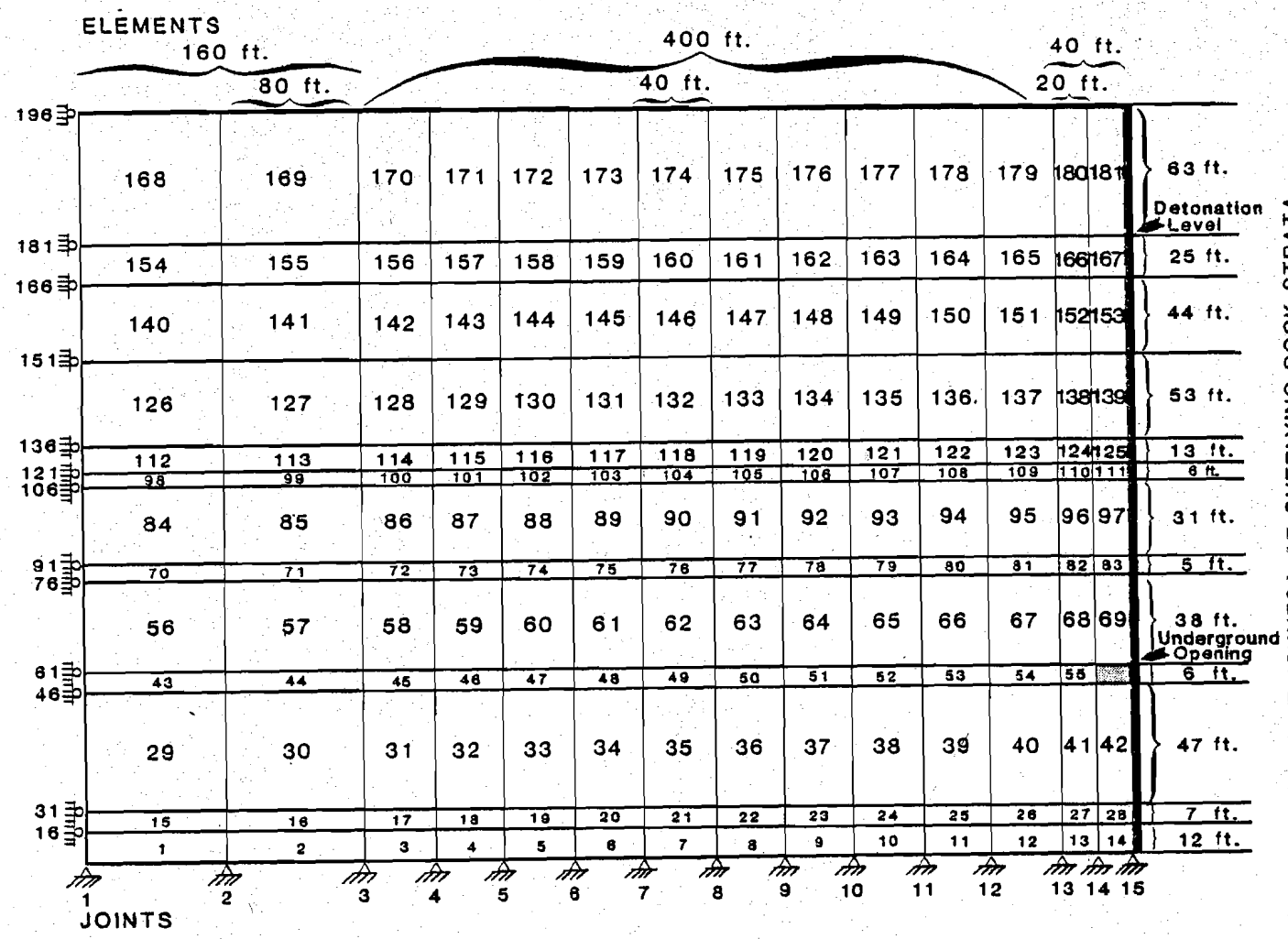

Figure 56. Finite element mesh generated for this study.

The explosive detonation was initiated at Element 167 and it progressed throughout the entire mesh as a function of time. Because of the symmetry, only half of the mesh is used in the analysis. The layers of rock and variations in their thicknesses were assumed to meet the field conditions of the site and are shown on the mesh along the right margin.

The engineering properties of the different layers of rock overlying the mine were determined from laboratory tests and are listed in Table 1. This information with the connectivity data as shown in the finite element mesh (Figure 56) was stored in the computer data file.

A trapezoidal load-time function with a minimum duration of 0.002 second as an input was assumed for the impact loading caused from the blasting. It was also assumed that the explosion will reach its maximum impacting force within 0.0005 second and this force will last for 0.001 second (Figure 57).

Because detonation of borehole pressure in the media is not perfectly known and variations occur with each explosion, the result of the linear regression analysis obtained from the field data was used as an approximation. As a reference, a maximum loading interval of about 4 to 12 million pounds was chosen, and this approximation is explained later in the report. The final outcome of the computer analysis was based on the stress as a function of depth from the detonation level with a varying load-time function. The results of these calculations are tabulated in Table 13 and plotted on Figure 58.

Vibration data collected from the roof of the mine was tabulated previously in Table 6. A regression curve of the peak particle velocity versus the scaled distance was also shown in Figure 47. From the figure the linear regression equation is given as:

$$V = 31470.9\ [D/W^{1/3}]^{-3.26}$$

From this equation the stress and strain of the surrounding rock media in the underground opening can be evaluated. An article from a VME technical report defines and describes the dynamic stress field in rock surrounding a blast as follows:

> When an explosive charge detonates in borehole the expansion of the high-pressure gaseous reaction products sets the borehole walls in motion outwards, creating a dynamic stress field in the surrounding rock. The initial effect in the nearby rock is high intensity, short duration shock wave, which quickly decays with the distance. The continued gas expansion leads to further motion and sets up an expanding stress field in rock mass. Where the free surface is close enough to the borehole the rock breaks loose. The other directions in the motion spreads further in the form of the well known ground vibration waves. These are a complicated combination of elastic waves which moves the rock in the compressive, shear, and surface wave modes. Each mode or wave type (P-, S-, and R-wave) has a characteristic propagation velocity, C, reflecting a material property of the rock mass. The particles in the rock mass move with the highest velocity equal to the peak particle velocity, V, decreasing with the distance from the charge. Damage is a result of the induced strain, ε, which for an elastic medium can be expressed by the equation $\varepsilon = V/C$ (Larsson, 1983).

$$\varepsilon = V/C$$

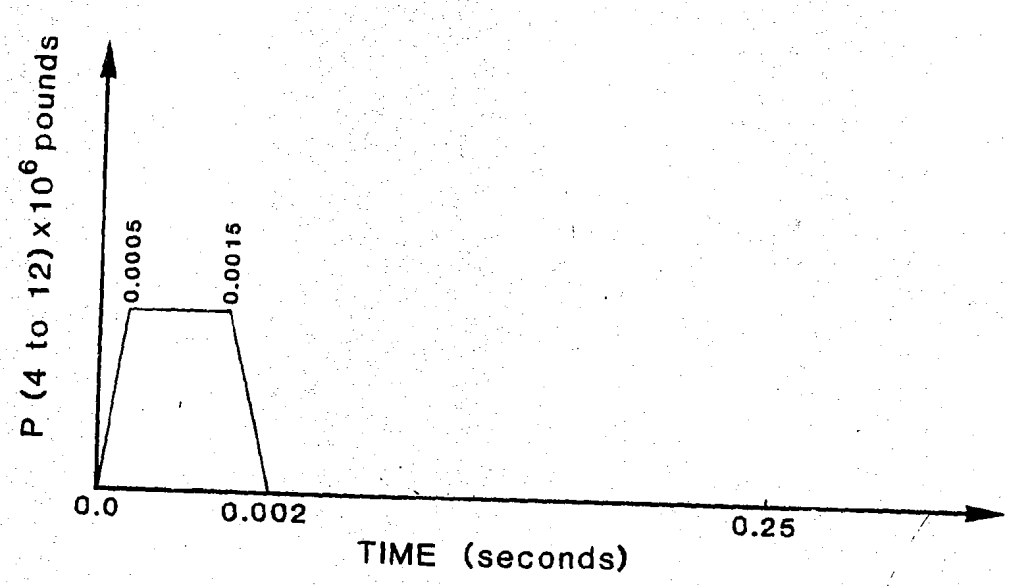

Figure 57. Input load-time function.

Table 13. Stress Versus Depth For Different Loadings

Depth[a] (ft)	σ Stress (Psi)				
	$P = 4 \times 10^6$ (lbs)	$P = 6 \times 10^6$ (lbs)	$P = 8 \times 10^6$ (lbs)	$P = 10 \times 10^6$ (lbs)	$P = 12 \times 10^6$ (lbs)
47	265.0	397.5	530.0	662.5	795.0
95.5	85.8	128.8	171.6	214.6	257.5
128.5	35.8	53.7	71.6	89.4	107.3
156.5	25.2	37.7	50.3	62.9	75.5
174.5	16.3	24.4	32.6	40.8	48.9
196.0	14.2	21.3	28.4	35.5	42.6
244.5	10.6	15.9	21.1	26.4	31.7

a) Depth from the detonation level.
b) Reference loading in the blast hole.

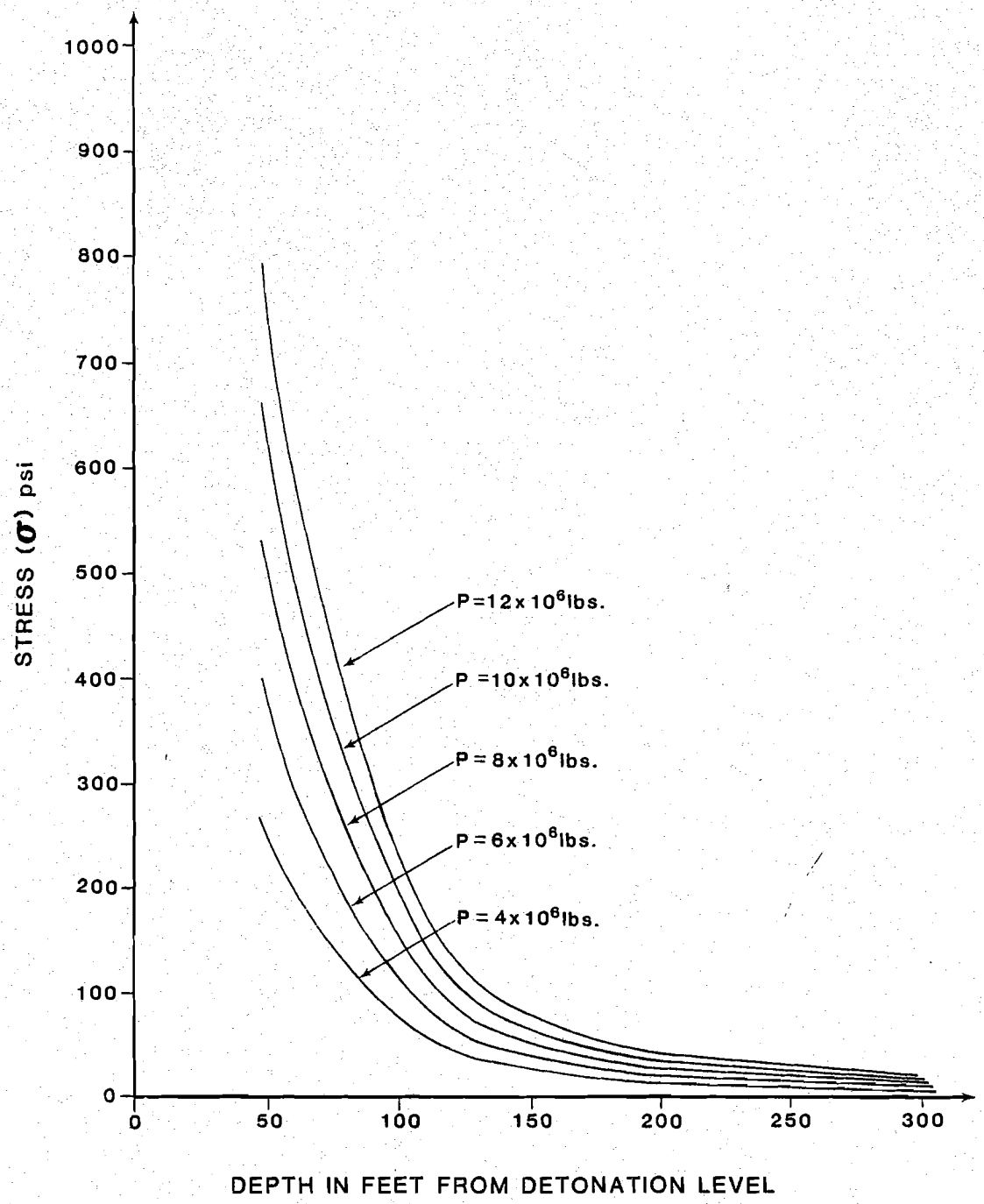

Figure 58. Stress versus depth for different loadings.

From equation (2) a stress equation for rock layers of different thicknesses and engineering properties can be developed. Using Young's modulus of elasticity of materials:

$$\sigma = \varepsilon \times E \qquad (3)$$

and substituting equation (3) in equation (2),
we get:

$$\sigma = \frac{VE}{C} = \frac{31,470.9\ E}{C[D/W^{1/3}]^{-3.326}}$$

The term C was calculated based on the arrival time of about 9,000 ft/sec which was in turn correlated with Vp (peak particle velocity) in Table 1. Based on these data it was found that

$$C = 9,000 \text{ ft/sec.}$$
and
$$E = 2,850,000 \text{ psi}$$

From this information and using the previously described calculations, the velocity, stress and strain as a function of time were calculated and the results given in Table 14. A graph of the stress versus depth from the detonation level for different charge weights are shown in Figure 59.

Comparison Between Field Results and Computer Simulations

For calculating the stress variations at different levels of rock in the subsurface using the computer simulation analysis, a range of load-time functions was used in order to correlate the force.

According to Brown and Hayatdavoudi, (1980), the maximum induced vertical force from blasting was calculated based on the detonation pressure of the explosive and this in turn was converted to borehole pressure. For purposes of this study the borehole pressure was calculated as 45 percent of the detonation pressure (Dupont, 1977). Usage today by many investigators stipulates that this force be multiplied by the area of the borehole occupied by the explosive train. For example, 400 pounds of explosive with a detonation velocity of 10,000 feet per second has a detonation pressure of about 290, 814 psi. This is based on the following empirical formula:

$$P_D = 216 \times 10^{-4} \times W_1 V_d^2 \, [0.45/(1+0.0128\ W_1)]$$

where P_D = detonation pressure (psi)
W_1 = charge weight density (pcf)
V_d = detonation velocity (ft/sec)

Therefore, the borehole pressure is:

$$P_B = 0.45 \times 290,814 = 130,866.3 \text{ psi}$$

The maximum vertical force generated in a 6.5-inch diameter borehole will be approximately:

$$F = \frac{\pi D^2}{4} (P_B) = 4,340,344 \text{ lbs.}$$

Because borehole pressure is imperfectly understood and not an easily measurable entity, a number of formulae have been devised to calculate the detonation pressure and borehole pressure. These are all chiefly based on the charge weight and the detonation velocity. A number of other investigators have made calculations using empirical formulae and these are listed in Table 15.

Table 14. Data for Linear Regression Equation

Shot Number	Hole Number	Charge Weight (lbs)	Station 3 Data D_B (ft.)	V_B (in/sec.)	ε_B (in/in.)	σ_B (Psi)	Station 5 Data D_R (ft.)	V_R (in./sec)	ε_R (in./in.)	σ_R (psi)
1	6	204	36.04	75.96	7.03×10^{-4}	2004.67	242.29	.134	1.24×10^{-6}	3.54
2	1	305	94.61	4.79	4.43×10^{5}	126.35	258.31	.169	1.57×10^{-6}	4.47
3	6[a]	60	51.67	5.90	5.46×10^{-5}	155.75	266.10	.025	2.34×10^{-7}	.668
4	2	402	97.79	5.83	5.39×10^{-5}	153.74	260.56	.224	2.07×10^{-6}	5.91
5	3	350	73.66	12.82	1.19×10^{-4}	338.37	249.76	.221	2.04×10^{-6}	5.83
6	5	302	45.05	55.87	5.17×10^{-4}	1474.38	245.71	.198	1.83×10^{-6}	5.23
8	7	305	79.26	8.63	7.98×10^{-5}	227.66	250.16	.189	1.75×10^{-6}	4.98
9	8	431	57.50	36.81	3.41×10^{-4}	971.39	243.20	.304	2.81×10^{-6}	8.02
10	12	203	89.35	3.69	3.41×10^{-5}	97.32	254.78	.113	1.05×10^{-6}	2.78
11	11	153	64.12	8.13	7.52×10^{-5}	214.45	247.87	.091	8.38×10^{-7}	2.39
12	13	207	29.53	149.77	1.38×10^{-3}	3952.26	237.01	.147	1.36×10^{-6}	3.88
13	15	121	65.71	5.77	5.35×10^{-5}	152.37	262.56	.0576	5.33×10^{-7}	1.52
14	16	272	81.09	7.04	6.52×10^{-4}	185.86	257.84	.150	1.39×10^{-6}	3.96

a. Hole loaded and shot twice
D_B: Distance from Shot to Station 3
V_B: Peak Velocity at Station 3
ε_B: Strain Measured at Station 3
σ_B: Stress Measured at Station 3

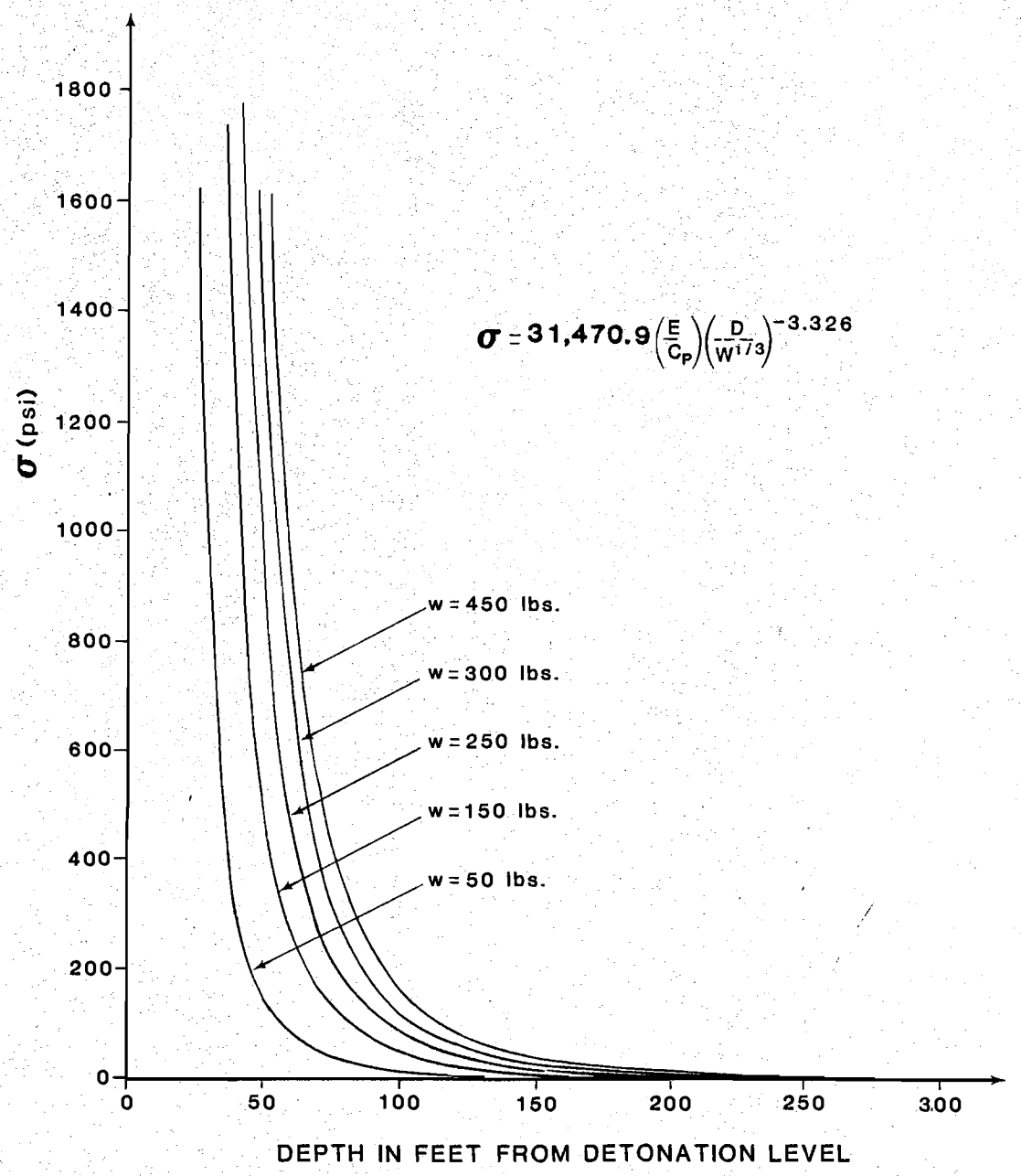

Figure 59. Stresses on underground mine roof versus depth for different charge weights.

Table 15. Calculated Pressures/Forces by Different Workers

Worker (a)	P_D (psi)	P_B (psi)	F (lbs)
Jones	122,440	361.627	12.9×10^6
Cook III	694,389	205,417	7.3×10^6
Cook II	645,621	190,990	6.8×10^6
Paterson	613,202	181,400	6.5×10^6
Cook IV	592,458	134,185	6.3×10^6
Roth	453,596	134,185	4.8×10^6
Y. Kumagai	417,929	123,634	4.4×10^6
Derkopf	417,760	123,584	4.4×10^6

(a) All workers listed are reported in Hino (1959)
P_D = Detonation pressure
P_B = Borehole pressure
F = Force

Proceeding with this background and referring to Tables 12, and 15 using Shot 2 as an example, the stress and distance to Station 3 are:

$$\alpha_B = 126.35 \text{ psi and } D_B = 94.61 \text{ ft.}$$

Using these two values and referring to Figure 58, a load of about 5 million lbs can be interpolated from the graph. According to this loading a stress of about 10 to 15 psi for the roof of the mine can then be picked from the graph. In Figure 59, a stress value of approximately 12 psi compares closely with Shot 2 and Hole 1 loaded with a 305-lb charge weight.

The data for this comparison is given as follows:

For Shot 2 - W (charge weight) = 305 lbs
H (depth of borehole) = 45.5 ft
V_d (detonation velocity = 13,000 ft/sec
W_1 (charge weight density) = 1.1 gm/cm
A (area of borehole) = 35.78 in^2
g (gravity) = 980 cm/sec

Inserting these data in the formulae discussed previously, the calculations fit relatively close within some of the values calculated by the investigators listed in Table 15.

This calculation of the estimated vertical force by linear regression method and computer simulation fall within the range calculated by Roth and Cook IV (Table 14). This, however, cannot be generalized for all of the shot data because there are many variables involved in the detonation process with explosives.

STRESSES CALCULATED AT THE MINE ROOF

Three experimental strain gages were fabricated to measure the stress on the mine roof induced by the explosive detonation at the surface. The gage and the emplacement of one of the gages in the coal pillar are shown in Figures 39, 42, and 43.

The principal component of the gages was an aluminum plate mounted within the aluminum tube and these three plates were 1/4-, 1/8-, and 1/16-inch in thickness. Strain gages were mounted on the plates and connected to a strain indicator and this was in turn connected with a seismograph. The instrument installation is shown in Figure 43.

All of the gages were calibrated prior to installation. Stress measurements from the blast were recorded by only one of the installed gages owing to damage during installation to the other two gages. The results of the measurements obtained from the installation and the procedures used to calculate the stresses are presented in the following discussion.

The stress in the roof of the mine is equal to the ratio of Young's modulii for aluminum and the roof rock multiplied by the stress in the aluminum i.e.;

$$\sigma_{\text{Roof Rock}} = (E_{\text{Rock}}/E_{\text{Aluminum}}) \times \sigma_{\text{Aluminum}}$$

where $E_{\text{Aluminum}} = 5.5 \times 10^{-6}$ and $E_{\text{Rock}} =$ 9.6×10^{-5} as determined from laboratory tests.

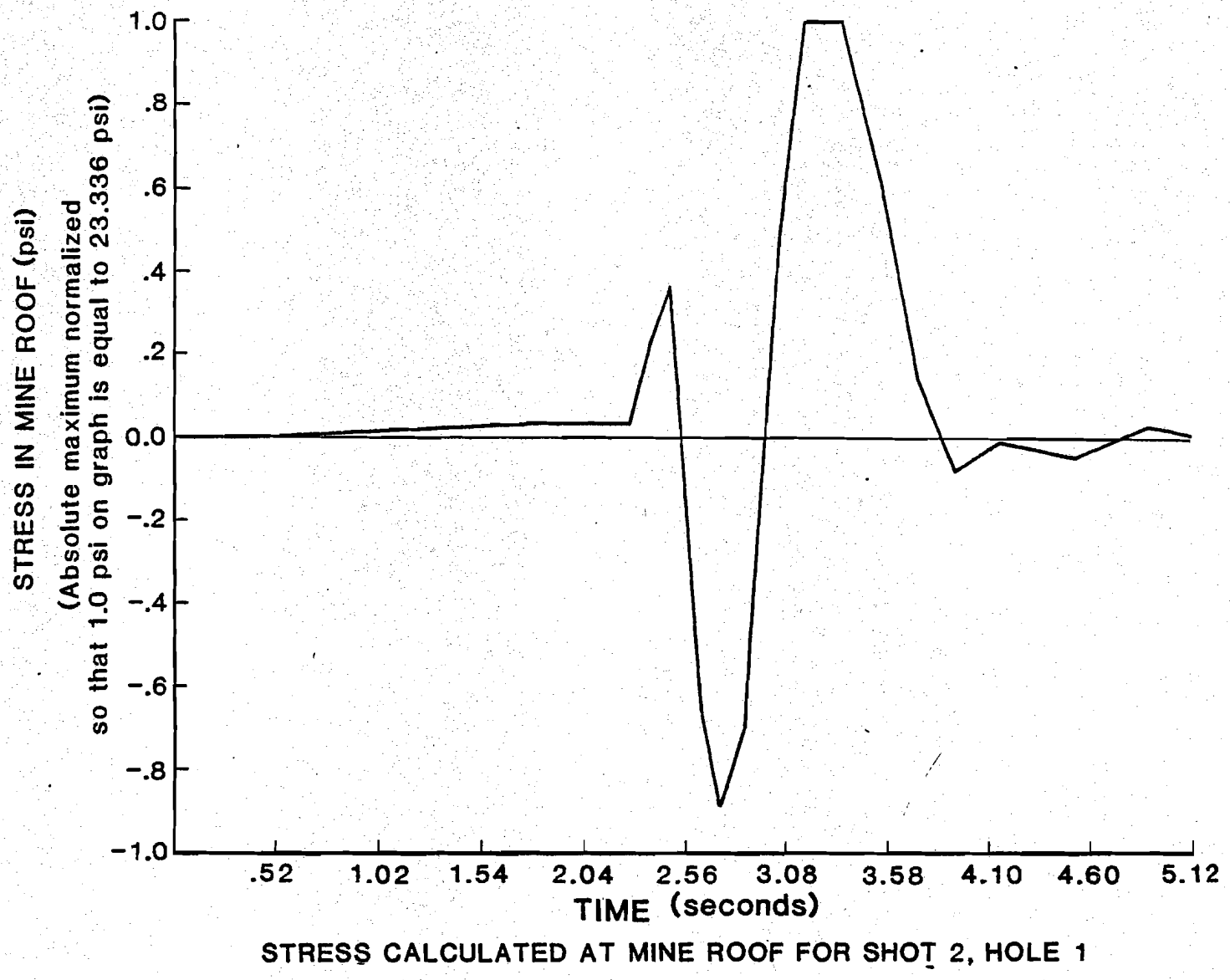

Figure 60. Stress-time domain curve (see Appendix IE for other shots).

One of the corresponding mine roof stress-time domain curves as based on field data from blasting is shown in Figure 60. The other stress-time domain data can be found in Appendix I-E, pages 350 through 354.

The observed field stresses calculated values at the roof level of the mine with different shots are tabulated in Table 16. Note that the stresses at the mine roof did not exceed 38 psi which was measured from the detonation of 431 lbs of explosives.

Referring to Table 16, it can be seen that the stresses within the lower and upper boundary limits of Figure 47 vary within fairly narrow limits. Also, the revised stresses calculated for the aluminum strain gage approach the calculated stress in the rock of the mine roof within what should be acceptable limits. In the column labeled (psi) revised stress in aluminum, shots 1, 3, 6 and 12 were too close to the detonation level to be properly recorded and should not be considered.

Factors to consider in the calculation of stress under the situation encountered in this study and future work along these lines, would include but not be limited to, charge weight, distance from shot point, as well as, amount of stemming, degree of coupling between the charge and borehole, proper response to detonation, and the placement and position of primer in the explosive train. There may be others not quite so apparent.

SUMMARY: OBSERVATIONS AND CONCLUSIONS

The major observations and conclusions derived from this study are summarized as follows:

The types of vibration recordng instruments recommended are influenced by the frequencies generated by the blasting. Usually the observed frequencies ranged from less than 2 up to 150 Hertz for surface blasting. The velocity seismographs used in this study had a flat response of frequency ranges from 2 to 200 Hertz and would be adequate for most blasts monitored.

Documentation on the linearity of the frequency band is especially important in a monitoring seismograph, since small vibrations in frequency response can change output levels considerably. The vibration channels on the seismograph should be able to record a complete time history from which a peak measurement can be determined.

Waveforms of the recordings of all three ground vibration components generated by a blast are recommended for the peak amplitude measurements; however, frequency may vary among three components of motion--vertical, radical and transverse. Peak or vector sum readings are adequate if only amplitude levels are desired. Empirically, the largest component of ground motion is usually the radial component at the surface and the vertical component in the subsurface.

Loose surface placement of the seismometer package should be avoided if high frequency motion is to be expected. Slippage can occur at this level and the seismometer package should be anchored. The seismometer package should be buried with the soil compacted around it, or if burial is not possible, it should be very firmly anchored or bolted to the roof if mine roof measurements are needed. To ensure proper coupling when buried, the density of the seismometer package should be close to the average density of the soil around it.

Table 16. Summary of Observed and Calculated Stresses in the Mine Roof

Shot No.	Hole No.	Charge Wt. (lbs)	Al Gage Stress (psi) Field Reading	Al Gage Stress (psi) Computer Simulation	Roof Rock Stress (psi) Experimental	Observed Stress (psi) Lower Boundary (refer to Figure 47)	Observed Stress (psi) Upper Boundary (refer to Figure 47)
1	6	204	148	b	25.83	3.54	3.67
2	1	305	116	11	20.35	4.47	4.53
3	6[a]	60	40	b	7.02	8.68	0.73
4	2	402	144	17	25.26	5.91	5.96
5	3	350	136	23	23.86	5.83	6.02
6	5	302	136	b	23.86	5.23	5.34
7[c]	-	-	-	-	-	-	-
8	7	305	116	16	20.35	4.98	5.67
9	8	431	148	38	25.96	8.02	8.45
10	12	203	84	9	14.74	2.98	3.13
11	11	153	56	12	9.82	2.39	2.55
12	13	207	84	b	14.74	3.88	4.01
13	15	121	56	5	9.82	1.52	1.66
14	16	272	100	12	17.54	3.96	4.00

a. Hole loaded and shot twice
b. Too close to detonation point for realistic recording.
c. Misfired shot, no data

Blasting results are significantly affected by the site geology both at the surface and in the subsurface. A thorough knowledge of the geology particularly the rock type, stratigraphic sequence, and structural conditions are essential. The hydrological conditions are also of prime concern. All of these parameters affect the type of shock or seismic wave generated and propagated within the media.

It was observed that the value of the vertical components of vibration data were relatively higher than that of the other components. This implies that in evaluating the effects on an underground opening caused by surface blasting, the vertical direction of vibration is the most important one to be considered.

The statistical analysis indicated that using the square-root scaling provided a better result for the surface measurements and the underground measurements are best grouped by using cube-root scaling.

Shots 1 and 3 were fired separately in the same borehole at different depths and amounts of stemming. The records indicated that these shots produced higher particle velocities than other shots. This may be caused by the resonance of the rock media or there possibly was a focusing effect in the subsurface layers. The statistical analysis also showed that these points do not properly fit the linear regression equation.

The vibration curves using the Fourier Transform approach showed that the frequency of the maximum amplitude remained as a constant for blasting, even though the responses were recorded from different locations. Therefore, a safety level of blasting could be determined by Fast Fourier Transform using the maximum amplitude and the frequency. Vibration levels measured on the mine floor were generally lower than those measured at the mine roof.

The energy spectrum can be used as the total energy transmitted by the vibration and is considered as equivalent to a superposition of radial waves of various frequencies carrying only a part of the total energy. Therefore, the percentage of attenuation between two points at different distances from the vibration source may be determined by using the proportion of the total energy at these points.

The Fourier Transform can be useful to study the safety criterion utilizing various frequencies. The vibrations containing higher amplitudes at a certain frequency range may or could cause damage to the underground mine openings. The vibration records should be analyzed by using the fast Fourier Transform procedure and these may provide an optimal conclusion for a safety criterion.

The research indicated the adaptability and useability of computer simulation to measure stresses impacted to an underground mine roof from blasting on the surface. In particular, a finite element analysis approach seems to provide a path to follow in similar studies of this kind. Certainly refinements in the techniques and procedures performed in conducting this work can be undertaken by other investigators interested in research related to blasting effects on underground mine roofs.

This study, as others in the past like it, have had to conclude that data gained at a particular mine are limited to a site selective basis regardless of how many parameters can be produced in the simulation model. The stratigraphic succession of overlying rock units, the localized structural disruptions at each mine, and the lithologic changes encountered in the vertical as well as horizontal sequences over relatively short distances, are too numerous and frequent to correlate from one coal basin to another with any degree of confidence.

Nevertheless, the instrumentation and procedures for collection, analysis of the field data, and the computer programs were effective in analyzing the effects of surface blasting on underground mine roofs.

RECOMMENDATIONS

The kind of seismic waves generated by surface blasting and the vibration levels surrounding underground mine openings were the major subjects of this study. Further work needed in the subjects concern the nature and geometry of the wave path. Moreover, detonation pressure and borehole pressure need closer examination. Both researchers and explosive manufacturers would like to learn more about these phenonema.

Another area of potential research is the type of waveform generated as the wave propogates through a media. The exact nature of the source effect and its resultant radiation pattern are presently unclear. The degree of attenuation or damping effects as the wave train passes through various media is not well known or even measurable in the field at this time.

The wide range and variety of seismographs and the sophistication of machines available today has developed rapidly so that investigators have a good choice available for their own particular need. It would appear that the work done on this research might well open areas for additional instrumentation particularly with regard to a more refined measurement of stress impacted to a mine roof.

The following manuals were consulted, and the descriptive material concerning instruments described in these manuals was referred to and used in the preparation of this report.

Dallas Instrument, Inc., Instruction Manual, Dallas, Texas.

Irad Gage Geotechnical Intrumentation Company, Inc., Instruction Manual, Lebanon, New Hamphire.

Mark Production Company, Instruction Manual, Houston, Texas.

Sprengnether Instrument Company, Inc., Instruction Manual, St. Louis, Missouri.

User Guide, Seebeck Computer Center, The Uhiversity of Alabama, Preliminary Ed., Sept. 1981.

Vishay Intertechnology, Inc., Instruction Manual, Raleigh, North Carolina.

REFERENCES

Benioff, H., 1934, "The Physical Evaluation of Seismic Destructiveness," Bull. Seismological Soc. Amer. Vol. 24, pp. 398-403.

Beus, Michael J. and Chan, Samuel M., 1980, "Shaft Design in the Coeur d'alene Mining District, Idaho--Results of In-Situ Stress and Physical Property Measurements," U. S. Bur. Mines, R.I.-8435, pp 39.

Biot, M. A., 1941, "A Mechanical Analyzer for the Prediction of Earthquake Stress," Bull. Seismological Soc. Amer., Vol. 31, No. 2, April., pp. 175-189.

Brigham, E. Oran, 1974, "The Fast Fourier Transform," Prentice-Hall Inc., Englewood Cliffs, New Jersey.

Brown, Robert C. and Hayatdavoudi, Asodollah, 1980, "Stability Analysis of Underground Chambers Subject to Dynamic Loading," Bur. of Engineering Research, The University of Alabama, Jan.

Bycroft, G. N., 1957, "The Magnification Caused by Partial Resonance of the Foundation of a Ground Vibration Detector," Trans. Am. Geophys. Union, 38, No. 6, December, pp. 928-831.

Campbell, R. B. and Dodd, J. S., 1968, "Estimated Rock Stresses at Morrow Point Underground Power Plant from Earthquakes and Underground Nuclear Blasts," Proceedings of the Ninth Symposium on Rock Mechanics, Soc. Min. Engineers, Amer. Inst. of Min., Metall. and Pet. Engineers, Port City Press, Baltimore, Maryland, pp. 84-114.

Champeney, D. C., 1975, "Fourier Transforms and Their Physical Applications," Academic Press Inc. (London), LTD. Third Print.

Chatterjee, Samprit and Bertram Price, 1977, "Regression Analysis by Example," John Wiley & Sons, Inc..

Cook, Melvin G., 1958, "The Science of High Explosives," Van Nostrand Reinhold Co, Reprint 1971, Robert E. Kreiger Publishing Co., Inc., Huntington, N.Y., 440 pp.

Crandall, F. J., 1949, "Ground Vibration Due to Blasting and Its Effect Upon Structures," J. Boston Soc. Civil Eng., pp. 222-245.

Draper, N. R. and H. Smith, 1966, "Applied Regression Analysis," John Wiley & Sons, Inc..

Duval, W. I., 1961, "Design Criteria for Portable Seismographs," U.S. Bur. of Mines, 5707, 6 pp.

Duval, W. I. and Fogelson, D. E., 1962, "Review of Criteria for Estimating Damage to Residence from Blasting Vibrations," U.S. Bur. of Mines, R.I. 5968, 19 pp.

Duval, W. I., 1964, "Design Requiremets for Instrumentation to Record Vibrations Produced by Blasting," Bur. of Mines R.I.-6487, pp 7.

Fogelson, D. E. and Johnson, C. F., 1962, "Calibration Studies of Three Portable Seismographs," U.S. Bur. of Mines, R.I. 6009, pp 21.

Gutowski, T. G., Whitting, L. E. and Dym, C.C., 1978, "Some Aspects of the Ground Vibration Problem," Noise Control Eng. Vol. 10, No. 3, May - June, pp. 94-100.

Hayatdavoudi, A. and Brown, R. C., 1979, "Surface Coal Mine Blasting Effects on Underground Coal Mine Stability," Final Report of Investigation, Vol. I & II, School of Mines and Energy Development, The University of Alabama, August.

Hendron, A, Jr. J., and L. L. Oriard, 1972, "Specifications for Controlled Blasting in Civil Engineering Projects," 1st North American Rapid Excavaton and Tunneling Conference, Chicago, Illinois, pp. 5-7.

Hino, Kumao, 1959, "Theory and Practice of Blasting," Nippon Kayaku Co. Ltd, First Ed., 189 pp.

Hudson, D. E., 1956, "Response Spectrum Techniques in Engineering Seismology," Proc. World Conference on Earthquake Research Institute and the University Cal., Berkely, pp. 4-1, 4-12.

Hudson, D. E. and A. G. Brady, 1972, "Analyses of Strong Morion Earthquake Accelerograms," Vol. III, Response Spectra, part A., EERL-72-80 Pasadena Cal..

Hudson, D. E. and A. G. Brady, 1971, "Strong-motion Earthquake Acceleragrams Digitized and Plotted Data," Vol. II, Corrected Accelerograms and Integrated Ground Velocity and Displacement Curves, EERL 71-50, Pasadena, California.

Huntsberger, David V., D. James Croft, and Patrick Billingsley, 1980, "Statistal Inference for Management and Economics," Allyn and Bacon, Inc..

Jensen, Dennis E. and Munson, Robert D., 1979, "Underground Vibrations from Surface Blasting at Jenny Mine, Kentucky," contract research final report, Woodward-Clyde Consultants, Orange, California, November.

Johnson, C. F., 1962, "Coupling Small Vibration Gages to Soil," Earthquake Notes, Vol. 33, September, pp. 40-48.

Langefors, U., Kihlstrom, B., and Westerberg, H., 1958, "Ground Vibrations in Blasting," Water Power, Vol. 10, February, pp. 335-338, 390-395, 421-424.

Larsson, Bernt, 1983, "Protection of the Wells When Blasting in Halite," VME In-House Technical Report, Reg. No. 1983-04-C, May.

Lucole, S. W. and Dowding, C. H., 1979, "Statistical Analysis of Blast Emission Records frm Quarrying, Mining, and Construction Operations in the State of Illinois," report to Illinois Institute of Natural Resources, Doc. No. 79102, Proj. 30.0113, January, 200 pp.

Merrill, Robert H., 1967, "Three-Component Borehole Deformation Gage for Determining the Stress in Rock," U.S. Bur. of Mines R.I. 7015, 38 pp.

Merrill, Robert H. and Peterson, Jon R., "Deformation of a Borehold in Rock," Bur. of Mines R.I.-5581, 32 pp.

Meyer, A. V. C. and Duvall, W. I., 1962, "Calibration Study of a Peak Reading Accelerograph," U.S. Bur. of Mines R.I.-6026, 6 pp.

Newmark, Nathan M. and Emilio Rosenblueth, 1971, "Fundamentals of Earthquake Engineering," Prentice Hall, Inc., N.J..

Nicholls, H. R. 1964, "Case Study of Validity of Scaling Laws for Explosion-Generated Motions," U.S. Bur. of Mines R.I.-6472, pp. 1-14.

Nicholls, H. R., Johnson, C. F., and Duvall, W. I., 1971, "Blasting Vibrations and Their Effects on Structures," U.S. Bur. of Mines Bull. 656, 106. pp.

Obert, Leonard, Merrill, Robert H., and Morgan, Thomas A., 1972, "Borehole Deformation Gage for Determining the Stress in Mine Rock," U.S. Bur. of Mines R.I.-5978, 11 pp.

Olson, J. J., D. E. Dick, D. E. Fogelson, and L. R. Fletcher, 1970, "Mine Roof Vibrations from Production Blast, Shullsburg Mine," Shullsburg, Wisconsin," U.S. Bur. of Mines R.I.-7462, pp. 1-35.

Papoulis, Athansios, 1962, "The Fourier Integral and Its Applications," McGraw-Hill Book Company, Inc..

Reed, John and Mann, David C., 1961, "St. Joe Builds Practical Rock Mechanics Tools," Eng. and Min. J., Vol. 162, March, pp. 100-106.

Rockwell, E. H., 1927, "Vibrations Caused by Quarry Blasting and Their Effects on Structures," Rock Products, Vol. 30, pp. 51-61.

Siskind, D. E., Stagg, M. S., Kopp, J. W., and Dowding, C. H., 1980, Structure Response and Damage Produced by Ground Vibration from Surface Mine Blasting," U.S. Bur. of Mines, R.I.-8507, 74 pp.

Siskind, D. E., Snodgrass, James J. Dick, Richard A. and Quiring, John N., 1973, "Mine Roof Vibrations From Underground Blasting," U.S. Bur. of Mines, R.I.-7764, 17 pp.

Skipp, B. O., 1977, "Ground Vibration Instrumentation--A General View, Instrumentation for Ground Vibration and Earthquakes," Proceedings from Conference for Earthquakes and Civil Engineering Dynamics, Keele University, Staffordshire, England, Paper 2, July, pp. 11-34.

Stagg, M. S. and Engler, A. J., 1980, "Measurement of Blast-Induced Ground Vibrations and Seismograph Calibrations," U.S. Bur. of Mines R.I.-8506, 62 pp.

Theonen, J. R. and Windes, S. L., 1942, "Seismic Effects of Quarry Blasting," U.S. Bur. of Mines Bull, 442, 83 pp.

Thomson, W. T., 1981, "Theory of Vibration With Applications," Prentice-Hall Inc., Englewood Cliffs, New Jersey.

Timoshenko, S., Young, D. H. and Weaver, W. Jr., 1974, "Vibration Problems in Engineering," John Wiley & Sons, Inc..

Tincelin, E., and Sinou, P., 1964, "Control of Weak Rock Strata in the Iron Ore Mines of Lorraine,"Internat. J. Rock Mech. and Min. Sci., Vol. 1, No. 1, pp. 341-383.

Waddell, Galen G., 1965, "Instrumentation for Rock Mechanics as Used in a Mine and Its Possible Application to Other Engineering Problems," Proceedings of the Third Annual Eng. Geol. and Soils Eng. Symp., Boise, Idaho, April, pp. 91-117.

Wall, J. R., Jr., 1967, "Seismic Induced Architectural Damage of Masonary Structures at Mercury, Nevada," Bull, Seismolog. Soc. Soc. American, Volume 57, No. 5, October, pp. 991-1007.

Washburn, H. and Wiley, H., 1941, "The Effect of the Placement of a Seismometer on Its Response Characteristics," Geophysics, Vol. 6, pp. 116-131.